Backman, J., Duncan, R. A., et al., 1988
Proceedings of the Ocean Drilling Program, Initial Reports, Vol. 115

11. SITE 714[1]

Shipboard Scientific Party[2]

HOLE 714A

Date occupied: 0850 L, 23 June 1987

Date departed: 0215 L, 24 June 1987

Time on hole: 17 hr, 25 min

Position: 05°03.6′N, 73°47.2′E

Water depth (sea level; corrected m, echo-sounding): 2038.3

Water depth (rig floor; corrected m, echo-sounding): 2048.8

Bottom felt (m, drill pipe): 2042.0

Penetration (m): 233.0

Number of cores: 25

Total length of cored section (m): 233.0

Total core recovered (m): 194.6

Core recovery (%): 83.5

Oldest sediment cored:
Depth (mbsf): 233.0
Nature: foraminifer-bearing nannofossil chalk
Age: late Oligocene
Measured velocity (km/s): 1.779

HOLE 714B

Date occupied: 0435 L, 24 June 1987

Date departed: 1115 L, 24 June 1987

Time on hole: 6 hr, 40 min

Position: 05°03.6′N, 73°47.2′E

Water depth (sea level; corrected m, echo-sounding): 2038.3

Water depth (rig floor; corrected m, echo-sounding): 2048.8

Bottom felt (m, drill pipe): 2042.0

Penetration (m): 122.6

Number of cores: 13

Total length of cored section (m): 122.6

Total core recovered (m): 114.9

Core recovery (%): 93.7

Oldest sediment cored:
Depth (mbsf): 122.6
Nature: foraminifer-bearing nannofossil ooze
Age: middle Miocene
Measured velocity (km/s): 1.529

Principal results: Site 714 is located in the northern equatorial Indian Ocean at 5°03.6′N and 73°47.2′E in water depths of 2031.5 m. The site lies on the eastern shoulder of the Maldives Ridge, which forms part of the aseismic ridge extending northward from the Chagos Bank to the Laccadive Islands (Fig. 1). Seismic profiles across the Maldives Ridge area reveal massive accumulations from 1 to 1.5 km of sediments and sedimentary rocks on top of the presumed volcanic basement (see "Seismic Stratigraphy" section, this chapter). Our main purpose was to retrieve a complete late Neogene sequence of soft aragonite-bearing (periplatform) oozes.

Originally, we planned to drill the target for Site 714 at a water depth of about 1500 m on a narrow ridge separated from the main bank complex. The occurrence of strong reflectors virtually at the sediment/water interface, presumed (and later confirmed) to be submerged reef limestone, forced us to move the site to a greater water depth (2031.5 m). This locality showed about 0.24 s (two-way traveltime) of transparent reflective layers in the upper part of the sediment sequence, and thus promised to yield a stratigraphic record of at least 200 m of suitable softer oozes. Our primary goal was to study the causal mechanism(s) for the observed connection between climatic changes and periplatform aragonite content.

We cored two holes continuously at Site 714. Hole 714A terminated in foraminifer-nannofossil chalk of late Oligocene age (about 28 Ma) at 233.0 mbsf, whereas Hole 714B ended in foraminifer-bearing nannofossil ooze at 122.6 mbsf of middle Miocene age. The depositional history contains a single major hiatus, spanning the time interval from 0.5 to about 8.0 Ma (late Pleistocene through late Miocene). Otherwise, the sequence is characterized by continuous sediment accumulation. In fact, this sequence is both more expanded and more complete than any other lower upper Miocene through lower Miocene sequence recovered during Leg 115.

The excellent preservation of foraminifers and calcareous nannofossils in this Miocene section may thus contribute substantially to our understanding of their low-latitude intercorrelation during Miocene times. The middle Miocene also contains moderately well-preserved siliceous faunas and floras, which again emphasizes the potential importance of this tropical Indian Ocean sequence for Miocene biostratigraphy and paleoceanography. To some extent, this balances the disappointing fact that we retrieved only one tenth (0–0.5 Ma) of the anticipated recovery of aragonite-bearing periplatform oozes.

We took 25 cores from Hole 714A, 13 of which were retrieved with the advanced hydraulic piston corer (APC) and the remaining 12 with the extended core barrel (XCB). The total recovery was 83.5% (97.3% APC and 69.3% XCB). From Hole 714B, we retrieved 13 APC cores, with a recovery of 93.7%.

The sequence is comprised of two lithostratigraphic units (see "Lithostratigraphy" section, this chapter), one of which is divided into two subunits.

Unit I (0–19.55 mbsf) consists of late Pleistocene (0–0.5 Ma), dark greenish gray, clay-bearing, foraminifer-bearing nannofossil ooze, grading downcore to a foraminifer-bearing, clayey nannofossil ooze. The average carbonate content is 76%, but the extremes vary from 60% to 84%.

Unit II (19.55–233.0 mbsf) is divided into two subunits. Subunit IIA (19.55–120.0 mbsf) consists of very light greenish gray, lower upper Miocene through middle Miocene (8.2–15 Ma), clay-bearing, foraminifer-bearing nannofossil ooze. The carbonate content shows a generally progressive increase from lows of about 81%–82% at 9 Ma to peak values of about 89% at 15 Ma, as estimated from mean values in 1-m.y. time increments. The carbonate values range from 61% to 95%.

Subunit IIB (120.0–233.0 mbsf) is similar in composition to Subunit IIA, but they are distinguished on the basis of the degree of lithification. The ooze of the latter grades into the clay-bearing, foraminifer-nannofossil chalk characterizing Subunit IIB. Burrow mottles (moderate) occur throughout Unit II. The carbonate content of Subunit IIB displays more subtle variations than those observed in

---

[1] Backman, J., Duncan, R. A., et al., 1988. *Proc. ODP, Init. Repts.*, 115: College Station, TX (Ocean Drilling Program).

[2] Shipboard Scientific Party is as given in the list of Participants preceding the contents with the addition of Isabella Premoli Silva, Dipartimento di Scienze della Terra, Universitá di Milano, Via Mangiagalli 34, I-20129 Milano, Italy.

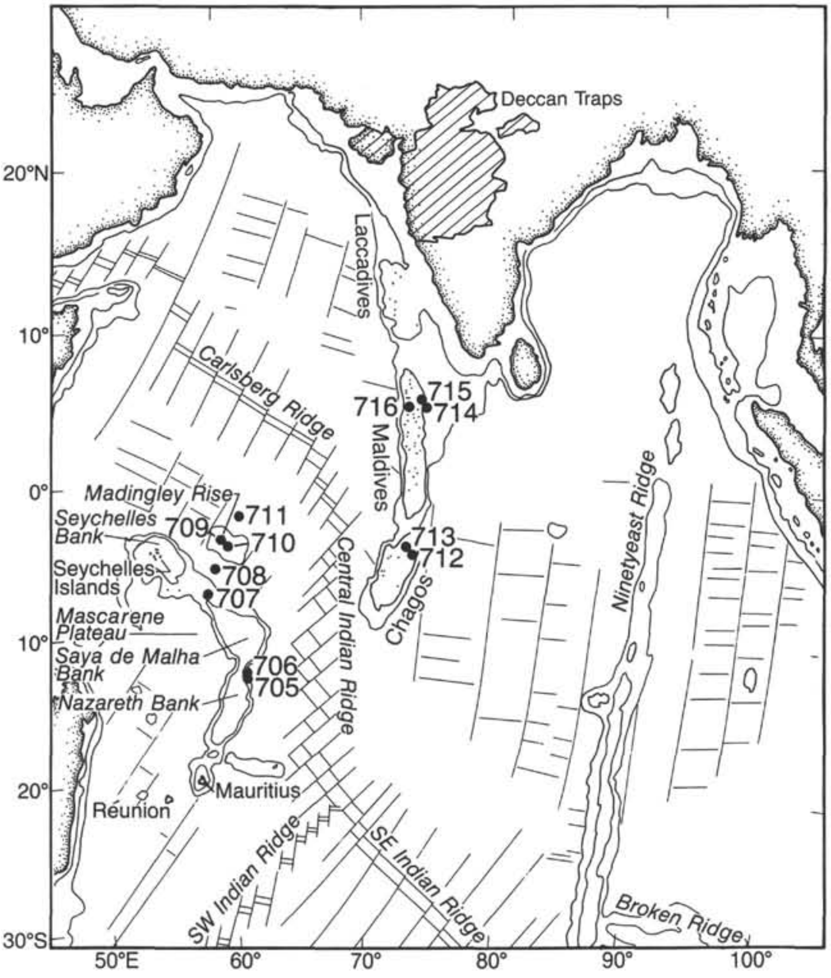

Figure 1. Bathymetric map of the central Indian Ocean showing the location of Site 714.

Subunit IIA, and we discerned no obvious trends. Apart from a single extreme value of 61%, all carbonate contents are in the range between 77% and 93%, with an average of 87%. A 10-point running mean, however, suggests that the carbonate content changes throughout Unit II as if influenced by a quasicyclical, low-frequency component (~0.5 m.y.?). Figure 2 summarizes the cored stratigraphic sequence.

Summary of Interpretation

Considering the well-preserved microfossil assemblages, the stratigraphic continuity, and the reasonably high sedimentation rates (10–20 m/m.y.) throughout the Miocene sequence of Site 714, it is clearly disappointing that the intensities of natural remanent magnetization (NRM) are too low to yield a magnetostratigraphic record. We have to rely, therefore, on the calcareous nannofossil correlation to magnetostratigraphy from Site 710 and apply those results to the material recovered from Site 714. This approach, together with the use of well-calibrated planktonic foraminifer datum events from Atlantic and Pacific low-latitude regions (Site 710 was located below the foraminifer lysocline during Miocene times), should, however, provide the necessary means for the reconstruction of a highly resolved chronology at Site 714.

Preliminary attempts to calculate mass accumulation rates of bulk and carbonate sediment are shown in Figure 3. The Pleistocene bulk accumulation rate is approximately twice that of the average of the pre-Pleistocene rates. Nevertheless, the Miocene rates are consistently higher than 1 g/cm^2/1000 yr between 8.2 and 19 Ma, and slightly below that value throughout most of the earliest Miocene and late Oligocene. The accumulation rate of the noncarbonate fraction by and large mimics the changes in bulk and carbonate accumulation, with the highest Miocene values around the middle/late and early/middle Miocene boundaries and slightly lower rates during the middle and early Miocene.

At a water depth of 2031.5 m, we assume that carbonate dissolution has had a minor effect on the carbonate accumulation. Moreover, taking into account the consistently high bulk sediment percentage of nannofossils (see "Lithostratigraphy" section, this chapter), we may assume that winnowing has had only a marginal effect on the presented mass accumulation rates. Provided the age-depth model (see "Sedimentation Rates" section, this chapter) for Site 714 is accurate, it follows that the mass accumulation rates illustrated in Figure 3 should reflect the true time-dependent variability in input of carbonate. Clues as to the cause(s) for this variability will emerge as the result of shore-based analyses.

BACKGROUND AND OBJECTIVES

Hard parts of foraminifers and coccolithophorids are formed of calcite, which represents the chief source material for deep-sea carbonates. Aragonite also contributes to the formation of oceanic carbonate sediments, mainly because the pelagic pteropods construct tests of this mineral. Aragonite is less stable than calcite, implying that the former mineral dissolves more easily than the latter. This results in an aragonite-compensation depth which is considerably shallower than that of calcite. Accordingly, the sedimentary lysocline is also shallower for aragonite than for calcite.

Periplatform oozes represent a third source of oceanic carbonate sediment formed within a unique environmental setting.

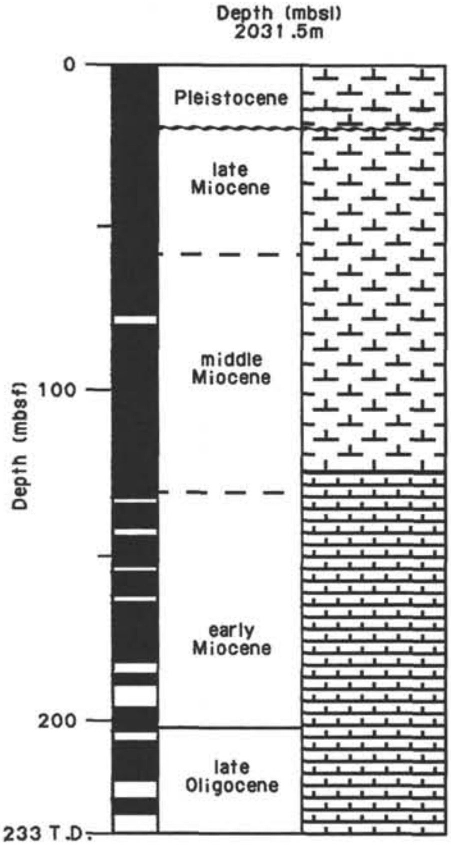

Figure 2. Stratigraphic summary, Site 714. Black column represents recovered section.

Such oozes are composed of a mixture of the common pelagic input (foraminifers, coccolithophorids, and pteropods) and banktop-precipitated aragonite, and are exclusively deposited in the close vicinity of shallow carbonate banks such as the Bahamas. Aragonite produced on the banks, mostly by benthic algae or by inorganic precipitation, is partly swept away and exported to deeper periplatform areas, where the aragonite becomes preserved if the sites of redeposition are located above the aragonite-compensation depth.

Analyses of the mineralogic composition of periplatform oozes from the Bahama Bank region have established that the aragonite content of the sediments coincides with the late Pleistocene glacial/interglacial cycles (Kier and Pilkey, 1971; Droxler et al., 1983; Boardman et al., 1986). Increased relative abundance of aragonite is linked with interglacial stages and *vice versa*. The causal mechanism for this connection between climate and periplatform aragonite content, however, has been the subject of debate (e.g., Boardman and Neumann, 1986; Droxler, 1986). One line of reasoning favors the argument that bank-derived sediment is deposited during times of high sea-level stands (e.g., interglacial times) when banktops are flooded and export of banktop-produced aragonite occurs. In this case, the observed variability in aragonite content essentially reflects the primary input signal.

The opposing model argues that, to a major extent, the phase relationship between aragonite content and climatic cycles reflects differences in preservational states of aragonite during glacial and interglacial times. This argument is based on the observation that time-dependent changes in the degree of aragonite preservation are directly linked to changes in ocean chemistry, because the saturation values of different minerals and relative positions of lysoclines or compensation depths are, in turn, coupled to climatic changes. Thus, the phase relationship between climate and aragonite concentration could represent aragonite dissolution cycles overprinting the primary input signal.

The number of locations producing periplatform oozes is limited. The Maldives Archipelago in the equatorial Indian Ocean is one such area. Our primary objective at Site 714 was to recover a complete sequence of periplatform ooze of Neogene age. This would allow us (1) to derive a highly resolved stable isotope stratigraphy for the Neogene utilizing the high sediment accumulation rates expected in the periplatform sediments; (2) to determine the interaction between sea-level fluctuations and carbonate off-bank transport; (3) to determine the effects of monsoonal circulation in the northern Indian Ocean on carbonate production and preservation as well as on periplatform oozes in general; and (4) to locate and decipher the possible diagenetic imprint on the primary input signal as well as to determine the fate of the metastable shallow-water-derived components (aragonite and magnesian calcite) through burial diagenesis.

OPERATIONS

Maldives to Site MLD-2

All who came aboard at Male except for the two Maldivian observers were put ashore. At 1515 hr, 22 June 1987, the ship was under way for Site MLD-2. The presite survey at MLD-2 did not look promising to the Co-Chiefs. Surveying continued, therefore, until an alternate site was found approximately 6 nmi south of MLD-2. The Maldivian government had already given its clearance to drill anywhere within a 10-nmi radius of the proposed sites.

We dropped a beacon at 0230 hr, 23 June, to establish Site 714. Because of gusting winds to 70 kt, we temporarily lost the beacon as it descended to the bottom. After approximately 1 hr, the ship was positioned over the beacon and was in its dynamic positioning (DP) mode at 0355 hr.

Hole 714A

We established the mud line at 2031.5 m and commenced APC coring. The hole was advanced to 2149.9 m (118.4 mbsf), with 115.2 m of core recovered for a recovery rate of 97.3%. The pull-out force on Core 115-714A-13H was 35,000 lb, so the decision was made to go to the XCB system. The hole was further advanced to 2264.5 m (233 mbsf), with 12 XCB-coring runs recovering 114.6 m of core for a recovery rate of 69.3%. Although the XCB shoe seals were worn badly by this point in the leg, they were still used. Total penetration was 233 mbsf to 2264.5 m, with 194.6 m of core recovered for a total recovery rate of 83.5% (Table 1).

Hole 714B

The mud line was established at 2031.5 m and APC coring commenced. The objective of this hole was to double APC-core the middle/late Miocene sediments. After 13 APC coring runs with 122.6 m of penetration, we met our objective and abandoned the hole. Total penetration was 122.6 mbsf to 2154.1 m with 114.9 m of core recovered for a recovery rate of 93.7% (Table 1).

LITHOSTRATIGRAPHY

The sedimentary sequence at Site 714 is dominated by a thick interval of light greenish gray nannofossil ooze and chalk with variable amounts of three secondary components: foraminifers, clay, and, to a lesser extent, biogenic silica. A thin, darker interval of more clay-rich nannofossil ooze overlies this thick interval. The distinctive color change between these two intervals marks an approximately 8-m.y. hiatus separating Pleistocene sediment above from late Miocene to late Oligocene sediment

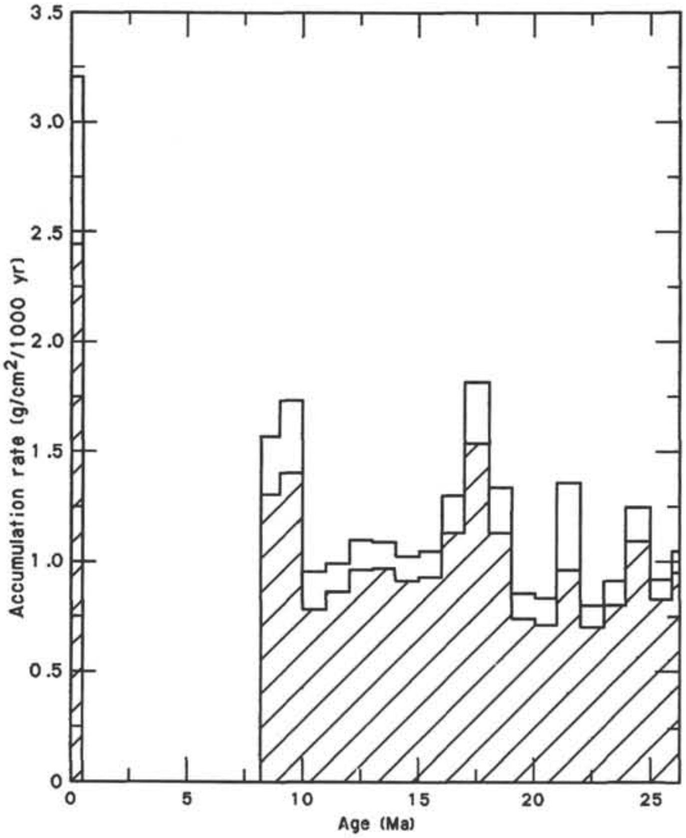

Figure 3. Mass accumulation rates of bulk sediment (unfilled area) and biogenic calcium carbonate (diagonal lines) plotted vs. estimated age at Hole 714A. The gap from 0.5 Ma to 8.2 Ma represents a hiatus. The data represent mean values within 1-m.y. time increments.

Core no.	Date (June 1987)	Time (UTC)	Depth (mbsf)	Length cored (m)	Length recovered (m)	Recovery (%)
115-714A-						
1H	23	0900	0–2.8	2.8	2.80	100.0
2H	23	0930	2.8–12.4	9.6	9.78	102.0
3H	23	1000	12.4–22.0	9.6	9.47	98.6
4H	23	1030	22.0–31.7	9.7	9.61	99.1
5H	23	1100	31.7–41.4	9.7	9.64	99.4
6H	23	1130	41.4–51.0	9.6	9.75	101.0
7H	23	1200	51.0–60.6	9.6	9.81	102.0
8H	23	1230	60.6–70.2	9.6	9.98	104.0
9H	23	1300	70.2–79.8	9.6	5.13	53.4
10H	23	1330	79.8–89.5	9.7	9.98	103.0
11H	23	1400	89.5–99.1	9.6	9.55	99.5
12H	23	1445	99.1–108.7	9.6	9.80	102.0
13H	23	1515	108.7–118.4	9.7	9.94	102.0
14X	23	1600	118.4–126.8	8.4	9.09	108.0
15X	23	1645	126.8–136.4	9.6	8.00	83.3
16X	23	1715	136.4–146.1	9.7	7.37	76.0
17X	23	1745	146.1–155.7	9.6	6.81	70.9
18X	23	1830	155.7–165.3	9.6	8.28	86.3
19X	23	1900	165.3–175.0	9.7	9.40	96.9
20X	23	2000	175.0–184.7	9.7	7.18	74.0
21X	23	2115	184.7–194.4	9.7	1.00	10.3
22X	23	2215	194.4–204.1	9.7	7.04	72.6
23X	23	2345	204.1–213.8	9.7	9.77	101.0
24X	24	0100	213.8–223.3	9.5	2.03	21.3
25X	24	0230	223.3–233.0	9.7	3.42	35.2
115-714B-						
1H	24	0500	0–6.8	6.8	9.51	140.0
2H	24	0530	6.8–16.4	9.6	0	0
3H	24	0600	16.4–26.0	9.6	8.72	90.8
4H	24	0645	26.0–35.7	9.7	9.66	99.6
5H	24	0715	35.7–45.4	9.7	9.08	93.6
6H	24	0745	45.4–55.0	9.6	9.94	103.0
7H	24	0815	55.0–64.6	9.6	9.76	101.0
8H	24	0845	64.6–74.3	9.7	9.67	99.7
9H	24	0915	74.3–83.9	9.6	9.70	101.0
10H	24	0945	83.9–93.6	9.7	9.81	101.0
11H	24	1015	93.6–103.2	9.6	9.64	100.0
12H	24	1045	103.2–112.9	9.7	9.78	101.0
13H	24	1115	112.9–122.6	9.7	9.66	99.6

below. The color change forms the basis for dividing the sediment into two units (Units I and II). Unit II, the older unit, is further subdivided into two subunits (Subunits IIA and IIB) by the transition from ooze to chalk, which coincides very closely with an increase in foraminifer content. The stratigraphic distribution of the units and subunits is summarized in Figure 4, and each is discussed in detail below.

Unit I: Core 115-714A-1H to Section 115-714A-3H-5, 115 cm (0–19.55 mbsf) and Core 115-714B-1H to Section 115-714B-3H-1, 135 cm (0–17.75 mbsf); Age: Pleistocene.

Unit I in both holes consists of foraminifer-bearing, clay-bearing nannofossil ooze alternating with foraminifer-bearing, clayey nannofossil ooze. Color systematically alternates between dark gray and gray (5Y 4/1, 5/1) and greenish gray (5GY 5/1, 6/1). Most of the color changes exhibit gradational boundaries. Smear slide analyses reveal a nannofossil content which is consistently between 50% and 70%, and a foraminifer content between 12% and 25%. An additional carbonate component is aragonite needles which occur in minor (up to 5%) to trace amounts. Also, minor to trace amounts of biogenic silica, quartz, and volcanic glass are found scattered throughout Unit I.

The lowest carbonate content at Site 714 (analyses from Hole 714A) are found in Unit I, averaging about 75% and dropping to about 60%. There seems to be a general trend toward increasing carbonate content with depth in Unit I. Superimposed upon this general trend are smaller amplitude, higher frequency fluctuations which seem to roughly correlate with the observed color cycles in the sequence. Carbonate content in the darker intervals (dark gray and gray) averages below 75%, while in the lighter intervals (greenish gray) carbonate content averages almost 80%. Thus, the cyclic color changes are related possibly to changes in carbonate production and preservation (and/or detrital input).

We identified a single turbidite 50 cm above the 8-m.y. hiatus in both holes, suggesting only minor disturbance in Unit I. The turbidite seems to be a good lithostratigraphic datum in Unit I. This, along with the matching magnetic susceptibility peaks in the upper part of Unit I (see "Paleomagnetism" section, this chapter), demonstrates the good physical correlation between Holes 714A and 714B within the Pleistocene.

Unit II: Section 115-714A-3H-5, 115 cm, through Core 115-714A-25X (19.55–233.00 mbsf) and Section 115-714B-3H-1, 135 cm, through Core 115-714B-13H (17.75–120.9 mbsf); Age: late Miocene to late Oligocene.

All the sediment cored below the hiatus has been grouped into lithologic Unit II. It is composed primarily of greenish gray nannofossil ooze and chalk with higher amounts of foraminifers than Unit I. As would be expected, chalk content increases with depth. Carbonate content is consistently between 80% and 90%, averaging about 86%, with less than 10% of the analyses falling outside the 80%–90% range (see Fig. 11) As previously mentioned, the ooze/chalk transition, accompanied by an apparent increase in foraminifer content, divides Unit II into two subunits (see Fig. 4).

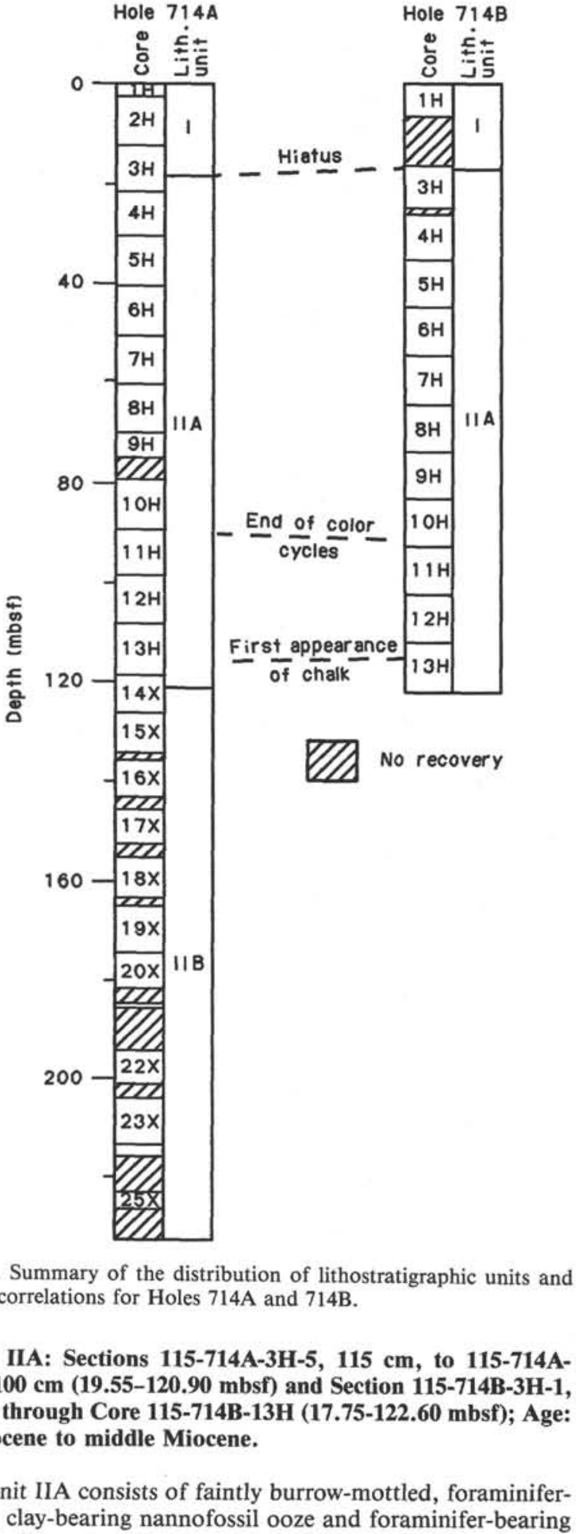

Figure 4. Summary of the distribution of lithostratigraphic units and physical correlations for Holes 714A and 714B.

Subunit IIA: Sections 115-714A-3H-5, 115 cm, to 115-714A-14X-2, 100 cm (19.55-120.90 mbsf) and Section 115-714B-3H-1, 135 cm, through Core 115-714B-13H (17.75-122.60 mbsf); Age: late Miocene to middle Miocene.

Subunit IIA consists of faintly burrow-mottled, foraminifer-bearing, clay-bearing nannofossil ooze and foraminifer-bearing nannofossil ooze with faint, but distinct, alternating color changes from light greenish gray (5GY 7/1) to light gray (5Y 7/1) observed in all but the lowest part of the subunit. The amount of clay-bearing ooze is greatly reduced in the lower 60% of Subunit IIA. Ooze firmness gradually increases with depth.

Examination of the average carbonate content of cores (within Hole 714A) in Subunit IIA reveals a slight decrease in carbonate content (from around 84% to 81%) with depth at the top of the subunit, followed by a steady increase to around 90% near the base of the subunit. The most carbonate-rich intervals at Site 714 occur within the lower part of this subunit (around 80-110 mbsf; lower part of the middle Miocene). Visual core descriptions reveal no distinguishing characteristic for this interval.

Biogenic silica seems to dominate the noncarbonate component (greater than 15% estimated relative abundance in smear slide analyses) within the middle third of Subunit IIA (approximately 60-90 mbsf). This, along with the increasing carbonate content with depth in this interval, suggests a low clay content. The apparent biogenic silica peak seems to be superimposed upon an interval of rising carbonate content. This indicates, perhaps, that carbonate variations in Subunit IIA are complicated by influxes of biogenic silica, as well as clay, and can be evaluated better when cast in terms of absolute accumulation (see introductory discussion to this chapter).

A minor to trace component in Subunit IIA is pyrite, which is sparsely disseminated in scattered intervals, and also occurs in pyritic burrows and as pyrite staining in thin horizontal bands and vertical streaks. The presence of minor amounts of pyrite, the distinctive greenish gray color, and the odor of hydrogen sulfide gas released during core splitting indicate sulfate-reduced (low oxygen) conditions in Subunit IIA. Other minor to trace components in Subunit IIA include possible aragonite needles near the top and scattered occurrences of volcanic glass, mica, quartz, and dolomite.

Subunit IIB: Section 115-714A-14X-2, 100 cm, through Core 115-714A-25X (120.90-233.00 mbsf); Age: middle Miocene to late Oligocene.

The top of Subunit IIB is marked by the transition from firm nannofossil ooze (with a few scattered chalk nodules) to abundant nannofossil chalk. This transition is clear in Hole 714A (see Fig. 4). Hole 714B terminates just before the transition. Subunit IIB is composed of clay-bearing, foraminifer-bearing nannofossil chalk which grades into foraminifer nannofossil chalk below. Ooze occurs primarily as a minor component throughout the subunit thinly distributed between and around chalk nodules, biscuits, and layers, and is most likely an artifact of drilling (drilling paste). Another indication of drilling disturbance is the relatively common fracturing observed in the chalk throughout the sequence.

The upper part of Subunit IIB (down to 169 mbsf) is uniformly a very light greenish gray (5G 8/1) and exhibits only faint burrow mottling in scattered intervals. The uniform color is interrupted by an interval of very abundant faint to distinct light greenish gray (5G 7/1) laminae occurring in clusters (169-180 mbsf). Within and below this interval, burrow mottling is much more common. Particularly conspicuous are scattered large *Zoophycus* burrows among other more common and fainter light gray (10YR 7/2) horizontal to subhorizontal burrows.

The average carbonate content for cores in Subunit IIB exhibits a slight decrease from around 88% at the top of the subunit to a low of 83% by 146.1 mbsf (Core 115-714A-16X). Below this level values return to near 89% and remain at this level for the rest of the hole. Only a few analyses fall outside the 80%-90% range. In general, carbonate content in Subunit IIB seems to exhibit smaller low-frequency variations than in Unit I or Subunit IIA.

Biogenic silica occurs in minor amounts throughout most of Subunit IIB, with a slight increase in abundance observed below 175.0 mbsf (Core 115-714A-20X). Other noncarbonate components include clay, volcanic glass, and quartz.

Evidence of natural disturbance and redeposition in Unit II occurs at the very bottom of Subunit IIB in the form of several small turbidites (one in Core 115-714A-22X and six in Core 115-714A-25X), and the occurrence in scattered intervals of large benthic foraminifers identified as shallower water forms (upper bathyal and carbonate shelf species; see benthic foraminifer discussion, "Biostratigraphy" section, this chapter). The very pale brown (10YR 7/3) turbidite intervals contain sand-size and larger limestone fragments and shallower-water benthic foraminifers, suggesting transport from shallow-shelf environments to intermediate depths.

BIOSTRATIGRAPHY

Introduction

Two holes at Site 714, which lie in a water depth of 2031.5 m, penetrated a 233-m-thick sedimentary sequence consisting of (1) 19.55 m of an upper Pleistocene nannofossil ooze; (2) a major unconformity spanning a time interval of approximately 8 m.y.; and (3) a continuous, expanded sequence (200 m thick) of lower upper Miocene through upper Oligocene nannofossil ooze and chalk.

Calcareous nannofossils are abundant throughout the section. They show excellent preservation in the Pleistocene and moderately good to good preservation in the Miocene and upper Oligocene. The diversity of the nannofossil assemblages is higher in the Oligocene-Miocene sediments of Site 714 than in any of the previous sites of Leg 115.

Planktonic foraminifers are abundant, being well preserved in the Pleistocene, well to moderately well preserved in the Miocene, and moderately well preserved in the Oligocene.

Benthic foraminifers are common and well preserved in all sediments, except in the lower Miocene interval where preservation deteriorates. Throughout the sequence, benthic foraminiferal assemblages are representative of middle bathyal depths, except in the upper Oligocene where assemblages are associated with redeposited shallower faunas.

Radiolarians, present in the entire stratigraphic interval, are moderately well to well preserved and vary in abundance from rare to common.

Diatoms are restricted to the upper Miocene through upper middle Miocene interval, and to a short interval in the upper Oligocene. Only traces of diatom valves are present in the Pleistocene. Assemblages are diversified and fairly well preserved in the upper Miocene (in contrast to the previous Leg 115 sites) and are poorly preserved in the middle Miocene.

A biostratigraphic summary for Site 714 is presented in Figure 5.

Calcareous Nannofossils

Hole 714A

Hole 714A yielded abundant calcareous nannofossil assemblages ranging in age from the late Oligocene to the late Pleistocene. A hiatus spanning approximately 8 m.y. is present in Section 115-714A-3H-5, in which middle Pleistocene sediments belonging to Zone CN14a (NN19) overlie upper Miocene sediments belonging to Zone CN8 (NN10).

An interesting feature of the calcareous nannofossil assemblages recorded here is the higher taxonomic diversity in comparison with that observed in other Leg 115 sites. Specifically, in the upper Oligocene and the lower Miocene, several species belonging to the Helicosphaeraceae (e.g., the index species *Helicosphaera recta* and *H. ampliaperta*) are present at Site 714 but are totally missing in previous sites. In the middle and upper Miocene, the Pontosphaeraceae (Perch-Nielsen, 1985) are also well represented by the genera *Scyphosphaera* and *Pontosphaera*. Both Helicosphaeraceae and many species of Pontosphaeraceae are more typical of "nearshore" environments and are often missing or rare in open-ocean sediments. Helicosphaeraceae seem to prefer upwelling areas or nutrient-rich water masses (Perch-Nielsen, 1985). This finding would suggest marginal marine conditions for this Maldivian sequence, in contrast to more open-ocean conditions for both the Mascarene and Chagos sites during late Oligocene and early Miocene times.

The high taxonomic diversity and good preservation allow us to consider the sequence at Site 714 as a reference section for the upper Oligocene through the lower-upper Miocene calcareous nannofossil biostratigraphy of the equatorial Indian Ocean.

Pleistocene

Emiliania huxleyi is present at the top of the Pleistocene sequence, and we placed its first occurrence (FO) at the base of Zone CN15 between Samples 115-714A-2H-4, 110 cm, and 115-714A-2H-5, 40 cm. The interval between Samples 115-714A-2H-5, 40 cm, and 115-714A-3H-4, 70 cm, is assigned to the upper Pleistocene Subzone CN14b. The entire Pleistocene sequence is relatively free of reworked forms, and we easily identified the last occurrence (LO) of *Pseudoemiliania lacunosa* in Sample 115-714A-3H-4, 150 cm. The interval between the latter sample and the sharp lithologic contact which marks the above-mentioned hiatus contains abundant large *Gephyrocapsa oceanica*, which show morphologic features typical of the upper Pleistocene morphotypes of the species. We assigned this interval, therefore, to the upper part of Subzone CN14a. By using the *P. lacunosa* event and the top of the sequence as control points for the sedimentation rate, an age of 0.5 Ma is obtained for the lowermost Pleistocene sediments just above the hiatus.

Miocene

The Miocene sequence of Site 714 is represented by a fairly uniform and homogeneous lithology with no evidence of reworking. Moreover, it appears to be continuous and complete from the Oligocene/Miocene boundary to the lower upper Miocene. We recognized all the Miocene zones of Martini (1971) and of Okada and Bukry (1980), which are given in Figure 5.

The youngest Miocene sediments recovered below the hiatus belong to the upper Miocene NN10 (CN8) Zone. The other upper Miocene biozones of both Martini (1971) and Okada and Bukry (1980) are easily recognized by the successive LO of *Discoaster hamatus*, the FO of *D. hamatus*, and the FO of *Catinaster coalitus* (Table 3 and Fig. 5). In this interval the assemblage contains common Pontosphaeraceae (represented by the genera *Scyphosphaera* and *Pontosphaera*) and Helicosphaeraceae. The boundary between the middle and upper Miocene occurs at approximately 55–60 mbsf within Zone NN8. The total thickness of the upper Miocene is between 35 and 40 m.

The boundary between middle Miocene Zones NN6 and NN7, and the corresponding boundary between Subzones CN5a and CN5b (FO of *Discoaster kugleri*), occurs in the upper part of Core 115-714A-9H. The boundary between Zones NN5 and NN6, and the corresponding boundary between Zones CN4 and CN5a, is easily recognized on the basis of the LO of *Sphenolithus heteromorphus*.

We identified the boundary between Zones NN4 and NN5, and the corresponding boundary between Zones CN3 and CN4, by means of the LO of *Helicosphaera ampliaperta*. The NN4–NN5 zonal boundary, which occurs at ~131–132 mbsf, identifies the boundary between the lower and the middle Miocene.

Sphenolithus belemnos seems to be missing above the *Triquetrorhabdulus carinatus* LO, and therefore the boundary between Zones NN3 and NN4, originally defined by the LO of *S. belemnos*, has been drawn by means of the FO of *S. heteromorphus*. These two events are known to be very close to each other (Perch-Nielsen, 1985). We identified the boundary between Zones NN2 and NN3 on the basis of the LO of *T. carinatus*, which is abundant in the sequence. In the early Miocene interval, the nannofossil assemblage is quite diversified. Several species of

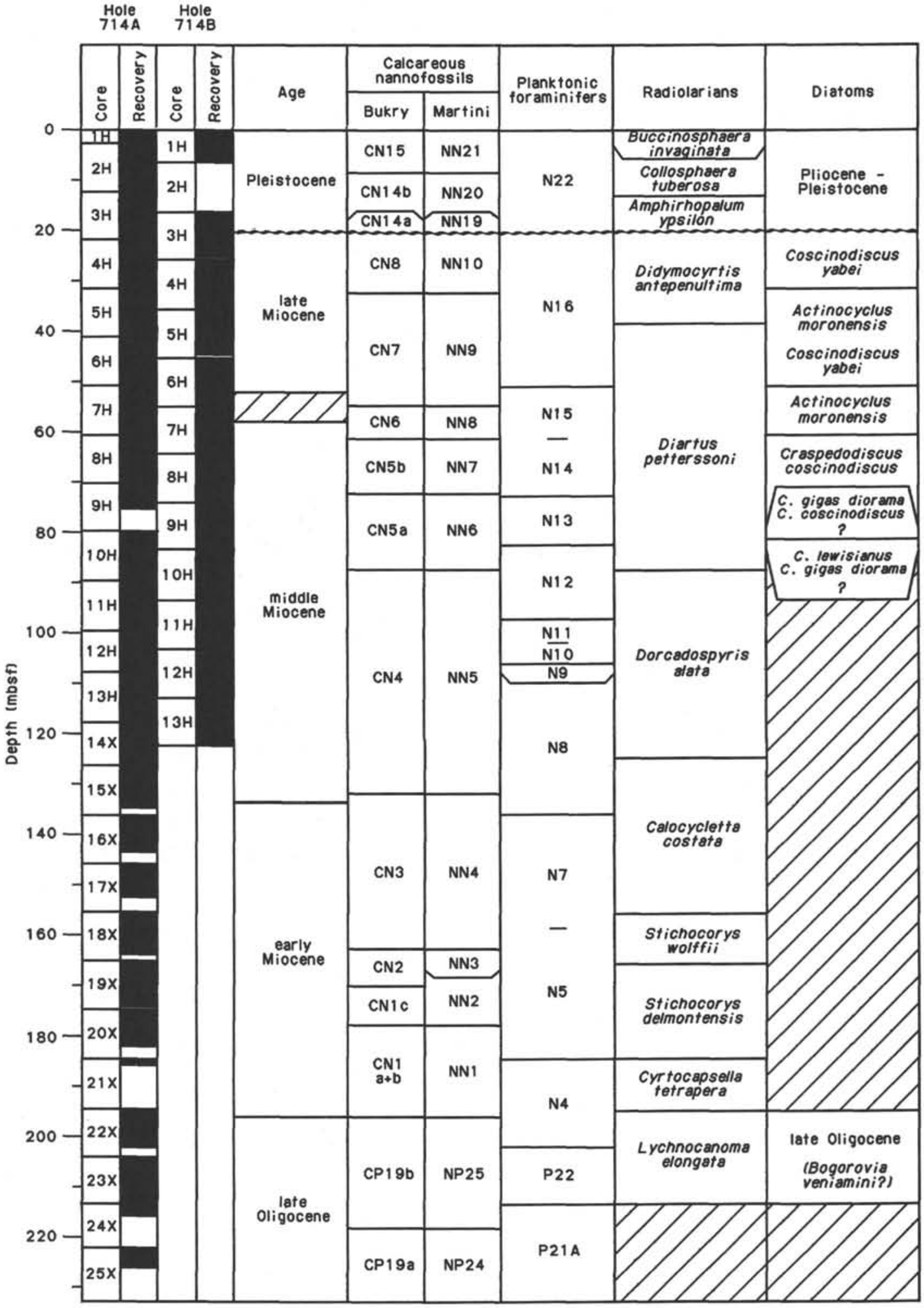

Figure 5. Biostratigraphic summary of Site 714. Black bars indicate recovery in Holes 714A and 714B.

sphenoliths (*Sphenolithus delphix*, *S. dissimilis*, *S. capricornutus*, and *S. conicus*) are restricted to this interval and to the uppermost Oligocene. Among the Helicosphaeraceae, *Helicosphaera euphratis*, *H. perch-nielseniae*, and small-sized *H. carteri* are well represented.

The LOs of *Sphenolithus ciperoensis* and of *Helicosphaera recta*, which define the base of the CN1 Zone and the NN1 Zone, respectively, and approximate the Oligocene/Miocene boundary, occur simultaneously in Sample 115-714A-22X-2, 130 cm.

Oligocene

As in the overlying lower Miocene sequence, the assemblages are characterized by the presence of Helicosphaeraceae, including low abundances of *H. recta*. The basal Oligocene sediments recovered in this hole contain abundant *S. ciperoensis* and, thus, are late Oligocene in age.

The upper Oligocene series (Zone CP19) is represented by about 35 m of sediments, from Section 115-714A-22X-4 to the bottom of the hole. We placed the LO of *Sphenolithus distentus* (base of Subzone CP19b) between Sample 115-714A-24X-6, 130 cm, and Section 115-714A-24X, CC.

Hole 714B

We drilled Hole 714B only 20 m away from Hole 714A and only examined the core-catcher samples. Because the sub-bottom depth of Core 115-714B-1H is 4 m lower than that of Core 115-714A-1H, zonal assignments were slightly different between the corresponding core catchers of these two holes. The zonal assignments for the 12 core-catcher samples recovered from Hole 714B are summarized in Table 2.

Table 2. Zonal assignments for core-catcher samples recovered from Hole 714B.

Section interval	Zone	Period
115-714B-		
1H, CC	Subzone CN14b	late Pleistocene
2H, CC	No recovery	
3H, CC	Zone CN8 (NN10)	late Miocene
4H, CC	Subzone CN7b (NN9)	late Miocene
5H, CC	Subzone CN7b (NN9)	late Miocene
6H, CC	Zone CN6 (NN8)	middle/late Miocene
7H, CC	Subzone CN5b (NN7)	middle Miocene
8H, CC	Subzone CN5a (NN6)	middle Miocene
9H, CC	Subzone CN5a (NN6)	middle Miocene
10H, CC	Zone CN4 (NN5)	middle Miocene
11H, CC	Zone CN4 (NN5)	middle Miocene
12H, CC	Zone CN4 (NN5)	middle Miocene
13H, CC	Zone CN4 (NN5)	middle Miocene

Planktonic Foraminifers

Neogene

The Neogene planktonic foraminiferal biostratigraphy of Hole 714A is based on data from core catchers and an additional two samples per core. Planktonic foraminifers are abundant throughout the Neogene sequence, being well preserved in the Pleistocene and well to moderately well preserved in the Miocene.

The upper part of Hole 714A down to Section 115-714A-3H-4, rich in *Globorotalia menardii*, is assigned to the Pleistocene zonal interval N23–N22 based on the presence of rare *Globorotalia truncatulinoides*.

An unconformity between sections 4 and 5 of Core 115-714A-3H spans the Pliocene and uppermost Miocene. The sequential order of planktonic foraminiferal events, allowing zonal assignment in the expanded middle to lower Miocene sequence, is as follows:

1. The simultaneous FO of *Neogloboquadrina acostaensis* and LO of *Paragloborotalia siakensis* in Section 115-714A- 6H, CC, marks the boundary between Zones N16 and N14. We could not identify Zone N15.
2. The FO of *Globigerina nepenthes* in Section 115-714A-10H-2 marks the base of N14.
3. The FO of *Sphaeroidinellopsis subdehiscens* in Section 115-714A-11H-2 marks the base of N13.
4. The FO of *Globorotalia fohsi fohsi* in Section 115-714A-11H-5 marks the base of N12.
5. The FO of *Globorotalia peripheroacuta* in Section 115-714A-12H-5 marks the base of N10.
6. The FO of *Orbulina* in Section 115-714A-12H, CC, marks the base of N9.
7. The FO of *Globigerinoides sicanus* in Sample 115-714A-15X, CC, marks the base of N8.

The interval from Sections 115-714A-15X, CC, through 115-714A-20X, CC, often dominated by abundant small-sized faunas, is assigned to the zonal interval N7–N5, whereas samples in Cores 115-714A-21X and -22X containing small-sized *Globorotalia kugleri* are assigned to the lowermost Miocene Zone N4.

Paleogene

We recovered Paleogene planktonic foraminifers in core catchers from Sections 115-714A-23X, CC, to 115-714A-25X, CC. One additional sample, 115-714A-23X-1, 50–55 cm, was surveyed in order to specify the Oligocene/Miocene boundary. Paleogene sediments were chalky, and foraminifers were only moderately well preserved. We recognized the following zones:

1. Zone P22 (Sample 115-714A-23X-1, 50–55 cm, and Section 115-714A-23X, CC) was identified by the presence of *Globigerina ciperoensis* and *Paragloborotalia pseudokugleri* and by the absence of *G. kugleri*. Despite only moderate preservation, the fauna contained a full range of species including such solution-susceptible forms as *Globigerina angulisuturalis*. *Paragloborotalia nana* and *P. siakensis* were common. Smaller species and *Globoquadrina tripartita* and *Globigerina binaiensis* dominated the coarse fractions.
2. Zone P21A (Sections 115-714A-24X, CC, and 115-714A-25X, CC) was determined by the co-occurrence of *Paragloborotalia opima* and common *Streptochilus cubensis*. Faunas contained large numbers of the *G. tripartita* group, *G. angulisuturalis*, and *Catapsydrax unicavus*.

Benthic Foraminifers

Benthic foraminifers were recovered from all cores in Holes 714A and 714B at Site 714. With the exception of the lower Miocene interval, benthic foraminifers were well preserved and numerous throughout the Pleistocene–upper Oligocene sequence. From the Pleistocene through the lower Miocene Zone CN1 (Section 115-714A-20X, CC), benthic foraminifers were in place and representative of middle bathyal depths. In upper Oligocene Zone P21 (Sections 115-714A-24X, CC, and 115-714A-25X, CC), middle bathyal benthic foraminifers were accompanied by upper bathyal and carbonate platform species such as *Amphistegina*. This implies that the site was still located at middle bathyal depths and that the shallower material was redeposited.

Pleistocene

The Pleistocene fauna (Sections 115-714A-1H, CC, and 115-714A-2H, CC) were well preserved and more abundant than at Site 707, which was drilled at approximately the same water depth. Nevertheless, the faunal composition was similar at both sites. Middle bathyal depths were indicated by the presence of *Osangularia bengalensis*, *Hoeglundina elegans*, and *Bulimina striata*, with *B. rostrata*, *Uvigerina proboscidea*, and *Anomalinoides globulosus* together with the truly carinate form of *Cassidulina laevigata carinata*. The low number of uvigerinids in both samples suggests deposition during interglacial episodes.

Upper Miocene

The upper Miocene (Sections 115-714A-3H, CC, through 115-714A-6H, CC) contains a series of faunas suggesting a more or less well-developed oxygen minimum at the bottom. These faunas are characteristic of the darker grey-green vs. grey sediment which occurred in cycles throughout this interval. The oxygen minimum was indicated by floods of small bolivinids, the majority of which are ornamented with reticulations, striations, or ridges; these occurred in the grey intervals. In the darker colored sediment, bolivinids may have been equally abundant, but the majority of forms are small and smooth. In Californian offshore basins, where bolivinid abundance correlates with lower oxygen levels in bottom waters, the lowest oxygen levels are characterized by smooth bolivinids. Slightly higher oxygen levels, on the other hand, are characterized by the ornamented, crenulate forms. This suggests that episodic color changes are primary and represent cycles of bottom-water oxygenation.

Upper Miocene faunas contain larger numbers and a greater diversity of uvigerinids than at any other Leg 115 site. Species include *Rectuvigerina spinea*, *Uvigerina auberiana*, *U. proboscidea*, and *U. spinulosa*. These were most abundant in Cores 115-714A-5H and -6H. The presence of uvigerinids suggests higher accumulation rates here than at the other Leg 115 sites, presumably as a result of increased overhead productivity.

Unusually good preservation in these sediments is indicated not only by the diverse benthic faunas, but by the high numbers of miliolids. *Pyrgo murrhina* and *Triloculina lucernula* occur together with *Quinqueloculina seminulum*, *Q. venusta*, and at least two other triloculinids and a spiroloculinid.

An intermediate water depth is suggested by the presence of the miliolids, and the co-occurrence of *Osangularia* trans. *bengalensis*, *Bulimina striata*, *Anomalinoides* cf. *aragonensis*, *A. alazanensis*, and *Rectuvigerina spinea*. Both *R. spinea* and *U. spinulosa* are restricted to areas above ~1500 m throughout the late Paleogene and the Neogene. In addition, *U. spinulosa* is a species characteristic of subtropical intermediate waters under gyre-margin current systems and the equatorial circulation. These ecologic features seem consistent with the location of Site 714 in the late Miocene.

Middle Miocene

A different bottom environment is indicated by the preservation and character of the faunas in middle Miocene Zones CN5–CN4 (Sections 115-714A-8H, CC, through 115-714A-10H, CC). Bolivinids, miliolids, uvigerinids, benthic diversity, and the siliceous component of the coarse fractions decrease dramatically. Typical intermediate faunas include *Nuttalides umbonifera*, a bottom water and/or corrosivity index. By Zone CN4 (Section 115-714A-10H, CC), only solution-resistant benthic foraminifers occur in the small faunas. Because the samples lie above the chalk/ooze transition and because preservation and abundance improve in the underlying cores, we cannot attribute the faunal change solely to diagenesis. The decrease in bolivinids and consistent occurrence of hispid uvigerinids, together with *N. umbonifera*, suggest the development of oxidizing, corrosive conditions at the bottom. Future studies of the ostracodes in this interval should test such interpretations because there are several ostracodal tracers for oxygen at the bottom.

During Zone CN4 (Section 115-714A-11H, CC), the benthic fauna becomes more diverse, sediment preservation improves, ornamented bolivinids flood the fine fraction, and a new component is added to the faunas. The austral species *Siphonina australis*, *Stilostomella basicarinata*, and a bolivinitid occur together only at this time. The siphoninids become more abundant in general at this time, as *Siphonina tenuicarinata* is also present. The siphoninids consistently co-occur with glauconite in areas of the North Atlantic, as well as in shallow-water environments, and are tentatively used to suggest micro-reducing (but macro-oxidizing) conditions at the bottom. The uvigerinid is *Rectuvigerina spinea*. The benthic fauna suggests higher productivity surface-water conditions and a possibly cooler, micro-reducing and macro-oxidizing bottom environment.

Lower Miocene

Preservation deteriorates in the interval from Zone CN4 through CN1 (Sections 115-714A-12H, CC, through 115-714A-22X, CC), so that benthic faunas are less diverse and probably unrepresentative of the original fauna in the area. As in other intermediate depth areas, benthic faunas are small, preservation is poor, unusual genera and species occur throughout, and bolivinids are only occasionally very abundant. This interval is important because it represents the transition from the Paleogene-type bottom environment to those typical of the Neogene. The majority of Paleogene benthic species become extinct, and typically Neogene species evolve throughout this interval.

Lower Miocene–Upper Oligocene

From the lowermost Miocene Zone CN1 through the upper Oligocene (Sections 115-714A-21X, CC, through 115-714A-25X, CC), shallow-water materials were added to the intermediate-depth benthic faunas in ever-increasing amounts. Only one or two shallow-water amphisteginids were found in Sections 115-714A-21X, CC, and 115-714A-22X, CC. By Section 115-714A-24X, CC, however, large upper bathyal specimens and carbonate-platform benthic foraminifers occur together with the intermediate benthic fauna. This fauna contains *Cibicidoides kullenbergi*, intermediate-size *Globocassidulina subglobosa*, *Stilostomella subspinosa*, and *Uvigerina pygmaea*, all intermediate- or deeper-water forms of this time. Site 714, therefore, was still situated at intermediate depths in the late Oligocene, but was receiving redeposited shallower-water material throughout the early CN1–CP18 zonal interval represented in the core catchers.

Radiolarians

Identifiable radiolarians are present in nearly the entire stratigraphic sequence recovered at Site 714. Two stratigraphic intervals are represented, with an unconformity between them: the upper Pleistocene (approximately 0–20.0 mbsf) and the upper Miocene to upper Oligocene (20.0–233.0 mbsf).

Pleistocene

Section 115-714A-1H, CC, is of late Pleistocene age, within the *Buccinosphaera invaginata* Zone. Section 115-714A-2H, CC, is also of late Pleistocene age, but within the *Collosphaera tuberosa* Zone. Diagnostic taxa include *C. tuberosa*, *Collosphaera orthoconus*, *Didymocyrtis tetrathalamus*, *Anthocyrtidium nigriniae*, *Pterocorys hertwigii*, *Spongaster tetras*, and *Amphirhopalum ypsilon*. Sample 115-714A-3H-4, 70 cm, corresponds with the *A. ypsilon* Zone. Radiolarians are common and well preserved at the top of the Pleistocene interval, but preservation deteriorates downward. A sharp unconformity is present in Section 115-714A-3H-5, at a level of about 20.0 mbsf.

Miocene

Section 115-714A-3H, CC, through Sample 115-714A-5H-4, 70 cm, are assigned to the *Didymocyrtis antepenultima* Zone of late Miocene age. Radiolarians are common and well preserved in the upper part of this interval, but preservation deteriorates downward. Diagnostic radiolarian taxa include *Diartus hughesi*, *Didymocyrtis antepenultima*, *Stichocorys delmontensis*, *Lithopera neotera*, *Siphostichartus corona*, and *Calocycletta caepa*.

We assigned Section 115-714A-5H, CC, through Sample 115-714A-10H-4, 70 cm (41.4–85.0 mbsf), to the *Diartus petterssoni* Zone of middle Miocene age. Radiolarian abundance varies from rare to common, and preservation varies from good to poor within this interval. Diagnostic taxa include *Lithopera thornburgi*, *L. neotera*, *Diartus petterssoni*, *Didymocyrtis laticonus*, *Calocycletta caepa*, *Cyrtocapsella japonica*, *C. cornuta*, *Siphostichartus corona*, and *Stichocorys delmontensis*.

Section 115-714A-10H, CC, through Sample 115-714A-14X-4, 70 cm (89.5–123.6 mbsf), are assigned to the *Dorcadospyris alata* Zone of middle Miocene age. Radiolarians are rare and moderately to poorly preserved in this interval. Diagnostic taxa include *Stichocorys wolffii*, *S. delmontensis*, *Carpocanopsis bramlettei*, *Calocycletta virginis*, *C. costata*, *Cyrtocapsella cornuta*, and *Dorcadospyris alata*.

The *Calocycletta costata* Zone of middle Miocene age occurs in Sections 115-714A-14X, CC, through 115-714A-17X, CC (126.8–155.7 mbsf). Radiolarians are common and moderately well preserved. Diagnostic taxa include *Calocycletta costata*, *C. virginis*, *Cyrtocapsella cornuta*, *C. japonica*, *Eucyrtidium diaphanes*, *Didymocyrtis tubaria*, *D. violina*, *Stichocorys wolffii*, *S. delmontensis*, and *Carpocanopsis bramlettei*.

Sample 115-714A-18X-4, 70 cm, through Section 115-714A-18X, CC (160.9–165.3 mbsf), are assigned to the *Stichocorys wolffii* Zone of early Miocene age. Radiolarians are rare and moderately preserved. Diagnostic taxa include *Stichocorys wolffii*, *S. delmontensis*, *Lychnocanoma elongata*, *Carpocanopsis cristatum*, *Eucyrtidium diaphanes*, *Calocycletta virginis*, and *Cyrtocapsella cornuta*.

We assigned Sample 115-714A-19X-4, 70 cm, through Section 115-714A-20X, CC (170.5–184.7 mbsf), to the *Stichocorys delmontensis* Zone of early Miocene age. Radiolarians are rare and poorly preserved; the faunal assemblage is dominated by sponge spicules. Poorly preserved radiolarian fragments include *Calocycletta virginis*, *Eucyrtidium cienkowskii*, *E. diaphanes*, *Stichocorys delmontensis*, *Cyrtocapsella elongata*, *C. cornuta*, and *Theocorys spongoconus*.

Section 115-714A-21X, CC (194.4 mbsf), is assigned to the *Cyrtocapsella tetrapera* Zone of early Miocene age. Radiolarians are rare and poorly preserved. Diagnostic taxa include *Lychnocanoma elongata*, *Artophormis gracilis*, and *Calocycletta virginis*.

Oligocene

Sample 115-714A-22X-4, 70 cm, through Section 115-714A-23X, CC (199.6–213.8 mbsf), are assigned to the *Lychnocanoma elongata* Zone of uppermost Oligocene age. Radiolarians are rare and poorly preserved. Diagnostic taxa include *Artophormis gracilis*, *Dorcadospyris ateuchus*, *Lychnocanoma elongata*, *L. trifolium*, *Eucyrtidium cienkowskii*, and *Theocyrtis annosa*.

All samples examined below Section 115-714A-23X, CC (213.8 mbsf), are barren of radiolarians.

Diatoms

A consistent occurrence of diatoms is restricted to the stratigraphic interval of upper to middle Miocene. Only traces of valve fragments are present in the Pleistocene sections. The upper Miocene assemblages are generally characterized by a fairly high abundance of diatoms showing a moderate to poor preservation. A late Miocene productivity increase may be deduced from the increase in the abundance of *Thalassionema* spp., a group of species which under present-day conditions occur in high abundances in upwelling areas. Both the middle and upper Miocene diatom assemblages have a fairly high content of neritic species. Diatoms are not present in the early Miocene section of Hole 714A, whereas a rare but fairly well-preserved flora is present in the upper Oligocene.

Site 714 differs significantly from the previous sites of Leg 115 in terms of the stratigraphic occurrence of diatoms. Diatoms have not been observed in a Miocene section older than late Miocene in any of the previous sites, nor has a true Paleogene flora been recovered in the previous sites.

Pleistocene and Pliocene

In the recovered Pleistocene core-catcher samples of Holes 714A and 714B, diatoms have a scattered occurrence due to dissolution. In Sections 115-714A-1H, CC, and 115-714A-2H, CC, valve fragments of Pliocene-Pleistocene diatoms are present. Diatoms are absent in the youngest core catchers of Hole 714B (Sections 115-714B-1H, CC, and 115-714B-2H, CC).

Miocene

The late Miocene *Coscinodiscus yabei* Zone is recognized in Holes 714A and 714B in Sections 115-714A-3H, CC, 115-714A-4H, CC, and 115-714B-4H, CC. The floras, which are fairly well preserved and diversified, include species such as *Coscinodiscus temperei delicata*, *C. yabei*, and *Actinocyclus ellipticus*.

Sections 115-714A-5H, CC, 115-714A-6H, CC, and 115-714B-5H, CC, are placed at the boundary between the *Actinocyclus moronensis* and *C. yabei* zones. The biogenic silica content is fairly high in these samples, but strong fragmentation has affected the assemblages. Sections 115-714A-7H, CC, and 115-714B-6H, CC, are assigned to the *A. moronensis* Zone.

The middle Miocene *Craspedodiscus coscinodiscus* Zone is recognized in Sections 115-714A-8H, CC, and 115-714A-9H, CC. Sections 115-714B-7H, CC, and 115-714B-8H, CC, are referred to the *Coscinodiscus gigas* var. *diorama–Craspedodiscus coscinodiscus* Zones. The abundance of diatom valves is low and preservation is poor. No diatoms of early Miocene age are present in Holes 714A and 714B.

Oligocene

In Sections 115-714A-22X, CC, and 115-714A-23X, CC, the siliceous microfossil assemblages are dominated by radiolarians and sponge spicules. Only a subordinate amount of moderately well-preserved diatoms are present. The diatom flora includes such age-diagnostic species as *Rocella vigilans*, *Coscinodiscus rhombicus*, and *Bogorovia veniamini*, which tentatively place the samples in the *B. veniamini* Zone.

All samples examined below Section 115-714A-23X, CC, are barren of diatoms.

PALEOMAGNETICS

Introduction

The results from sediments taken at Site 714 are disappointing; we will discuss them only briefly therefore. Data acquired from pass-through measurements showed no interpretable magnetics except perhaps from the topmost sediments (where the signal is marginal at best).

Results

The first few meters of Pleistocene sediment recovered proved promisingly stable; however, with increasing depth the intensity of magnetization decreases and the measured directions become erratic. Intensities remain low in all other cores measured (except, perhaps, near core tops), and the directions appear to be largely random.

Discussion

It appears that the NRM-carrying minerals are not preserved upon burial. Consequently, there seems to be little chance that we can establish an interpretable magnetic stratigraphy at this site. There is no evidence of consistent overprinting, and the directions measured probably reflect the noise of the instrument.

Occasional higher intensity sections (near core tops) most likely result from minor rust contamination.

Magnetic Susceptibility

Magnetic susceptibility was measured at varying intervals (6, 7, or 10 cm), depending on the lithologic homogeneity of the sequence, in all sections of cores from Hole 714A to a depth of 118 mbsf (Cores 115-714A-1H through -13H); and at intervals of 5 cm in two cores from Hole 714B (Cores 115-714B-1H and -3H) to a depth of 24 mbsf. A limited number of susceptibility measurements were made in Holes 714A and 714B because of the low signal-to-noise ratio exhibited by the sediments recovered. The Pleistocene sediments yielded low susceptibility values ($5–15 \times 10^{-6}$ cgs), and the underlying Miocene sediments were almost totally devoid of magnetizable material, with the single exception of a peak in susceptibility of about 40×10^{-6} cgs toward the top of each hole.

Within the sequence measured at Site 714, there are two main lithologic units (see "Lithostratigraphy" section, this chapter): one of Pleistocene age (0–19.54 mbsf) and one of Miocene age (19.54 mbsf to the base of the section measured for susceptibility).

The Pleistocene sequence (Unit I) consists of gray, dark gray, and greenish gray, clay-bearing (sometimes foraminifer-bearing) nannofossil oozes, which produce a malodorous gas (hydrogen sulfide) when the cores are split and which exhibit pyrite staining throughout. These features suggest that the Pleistocene sediments are strongly reduced, possibly as a result of high initial organic carbon concentrations and high rates of deposition. A large flux of organic carbon and a rapid rate of burial favors suboxic processes of organic matter diagenesis, which involve bacterial reduction (dissociation) of nitrates, followed by the precipitation of manganese oxides, iron oxides, oxyhydroxides, and eventually iron sulfides in the sediment (i.e., pyrite; see Froelich et al., 1979; Berner, 1980; Klinkhammer, 1980; Bender and Heggie, 1984).

The underlying Miocene sequence (a portion of Unit II) consists of foraminifer-bearing nannofossil oozes throughout (with occasional siliceous-bearing horizons), becoming lighter in color downhole: from light brownish gray with occasional pale green laminae at the top of the sequence (e.g., Cores 115-714A-3H, -4H, and -5H), to light greenish gray and pale green toward its base (e.g., Cores 115-714A-18X and -19X). Pyrite staining again was observed throughout the sequence, and the smell of hydrogen sulfide was detected in several of the Miocene cores upon splitting. Therefore, the Miocene sediments at Site 714 are likely to be reduced as strongly as the overlying Pleistocene sediments. The lighter colors and lower susceptibility values of the Miocene sequence are probably the result of their higher carbonate content (see "Geochemistry" section, this chapter) and lower lithogenic clay content. It is likely that most of the magnetic (NRM-carrying) iron oxides and oxyhydroxides originally present in the sediment have been destroyed by bacterial dissociation during suboxic diagenesis of organic matter in both the Pleistocene and Miocene sections. The measured susceptibility values are probably generated mainly by paramagnetic ferrous iron in clay minerals and pyrite.

Variations in magnetic susceptibility within the Pleistocene sequence (though possibly augmented by a significant authigenic component) are sufficiently consistent in a spatial sense to provide a reliable correlation between Holes 714A and 714B, as shown in Figure 6.

SEDIMENTATION RATES

Site 714 recovered a 233-m-thick Neogene and late Paleogene sequence, with a long hiatus spanning the interval from late Pleistocene to late Miocene.

Sedimentation rates for Hole 714A are presented in Figure 7 based on biostratigraphic datums from various fossil groups listed in Table 3. The curves are drawn without making corrections for compaction and without considering short-term fluctuations. The reduced sedimentation rates observed in most of the lower and middle upper Miocene sections of the previous sites of Leg 115 are not recorded at Site 714.

GEOCHEMISTRY

Interstitial Water Studies

Samples for interstitial water studies were taken from 12 cores at Site 714. The results of the analyses are presented in Table 4 and Figure 8. As a result of the potential for higher amounts of organic material at this site, phosphate determinations were made in addition to the usual analyses.

Calcium and Magnesium

The downhole gradient of Ca^{2+} is the lowest observed in any of the holes drilled during Leg 115. The concentration increases from 10.58 mmol/L at 1.45 mbsf to only 11.65 mmol/L at 224.75 mbsf. This corresponds to a gradient of 0.004 mmol/L/m. It must be remembered, however, that the titration technique used (see "Explanatory Notes" chapter, this volume) cannot distinguish between Ca^{2+} and Sr^{2+}, and therefore it is possible that the apparent increase in Ca^{2+} is really a result of an increase in Sr^{2+}. Normally, changes in the amount of Sr^{2+} are substantially less than variations in the concentration of Ca^{2+}. For example, the Sr^{2+} content of seawater, which is approximately 97 μmol/L, can rise to concentrations of between 700 and 1000 μmol/L (Baker, 1986; Swart and Guzikowski, 1988) because of the dissolution of organically produced low-magnesium calcite and aragonite, and the precipitation of low-magnesium calcite cements. This process can affect measured Ca^{2+} concentrations by up to 1 mmol/L. Such a contribution can be lost in the fluctuation of the typical downhole increase in calcium as observed at previous sites drilled during Leg 115.

An increase in pore-water Sr^{2+} concentration at Site 714 is even more likely since aragonite, which can contain between 7000 and 8000 ppm strontium, is a predominant component in the upper 30 m. As a result of the metastable nature of aragonite, it will tend to dissolve more easily than low-magnesium calcite and hence impart strontium to the pore fluids. The maximum rise of strontium in pore waters of deep-sea sediments appears to be limited by the solubility product of celestite ($SrSO_4$; Baker and Bloomer, 1988). In the absence of sulfate reduction, the strontium content of pore fluids cannot exceed approximately 700 μmol/L.

In contrast to most of the other sites examined during Leg 115, no significant changes were observed in the concentration of Mg^{2+} in Hole 714A (Fig. 9). This type of relationship typically is observed in situations where pore-water chemistry is dominated by carbonate dissolution and precipitation reactions (Gieskes, 1981).

Alkalinity, Sulfate, Ammonia, and Phosphate

The alkalinity of the pore fluids reaches a maximum of 4.44 mmol/L at 39.15 mbsf (Fig. 10). The maximum depletion in sulfate is achieved at 8.75 mbsf and coincides approximately with a rise in phosphate to between 6.99 and 6.22 μmol/L and in ammonia to 135 μmol/L. Below this depth, phosphate rapidly decreases to seawater values of approximately 2 μmol/L, while sulfate remains depressed and ammonia is enriched throughout the remainder of the core.

Chlorinity and Salinity

Chlorinity and, to a lesser extent, salinity show small variations: from 526.8 mmol/L at 1.45 mbsf, to a maximum of 564.7

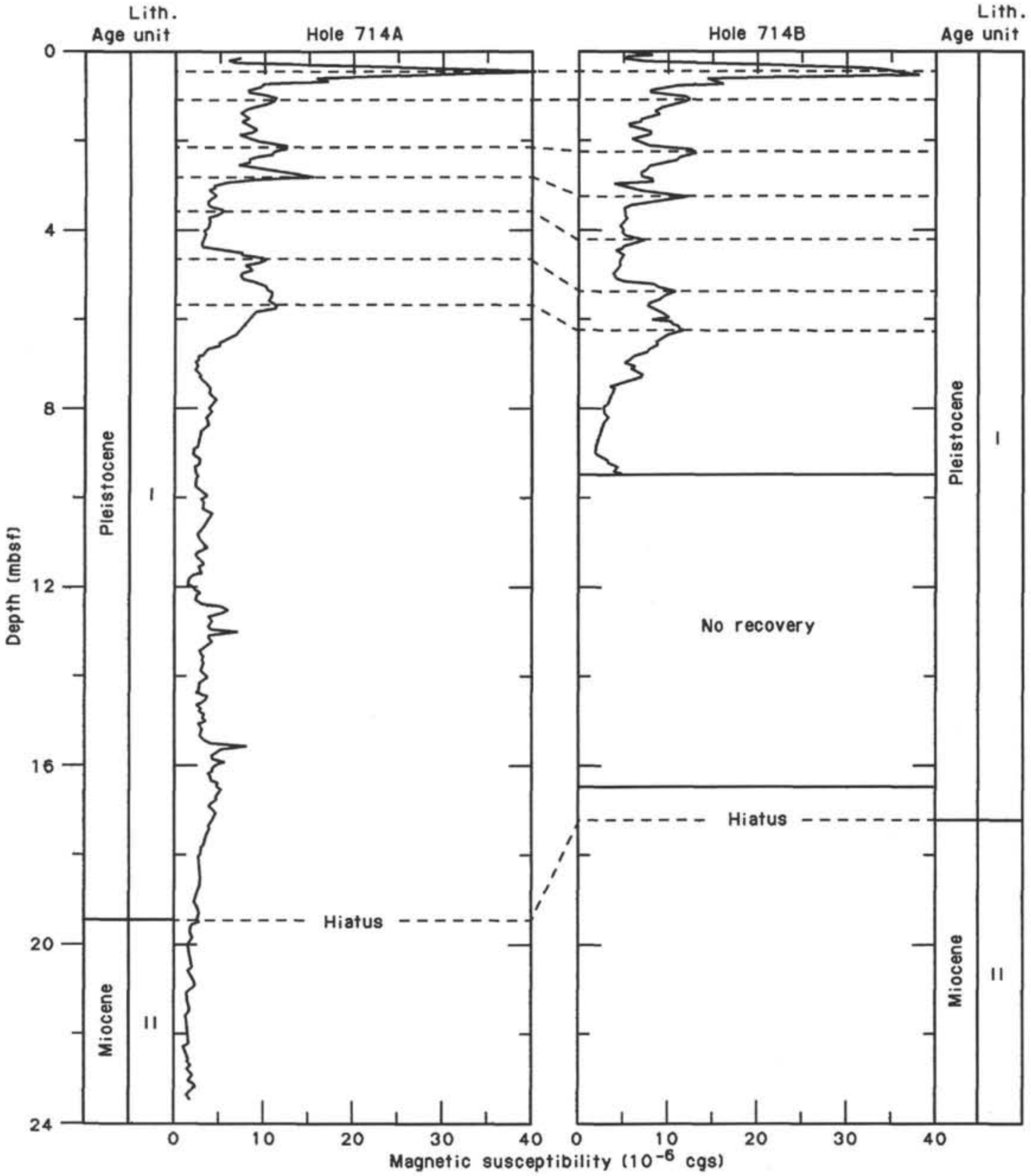

Figure 6. Correlation between the upper portion of Holes 714A and 714B, based on whole-core magnetic susceptibility profiles of each hole. Lithologic units correspond to those defined in "Lithostratigraphy" section, this chapter.

mmol/L at 8.75 mbsf, and finally back to 531.5 mmol/L. This type of change in chlorinity was also seen at Site 709 and may be an inherited signature related to paleosalinity variations of the oceans during Pleistocene times.

Silica

Concentrations of silica gradually rise from 575 μmol/L at 1.45 mbsf to 870 μmol/L at 200.10 mbsf. The gradual increase probably reflects dissolution of biogenic silica components in the hole.

X-ray Mineralogy, Carbonate, and Organic Analyses

X-ray Mineralogy and Carbonate Content

All sediment samples squeezed for interstitial waters were analyzed by X-ray diffraction in order to determine their carbonate mineralogy. These analyses revealed that aragonite and low-magnesium calcite were the dominant carbonate minerals throughout the upper 25 m of Hole 714A, an interval corresponding to sediments of Pleistocene age. Below the sharp hiatus visible in Core 115-714A-4H, aragonite disappears and low-magnesium calcite was the only mineral detected.

The carbonate content of Hole 714A varies between 60.05 and 94.74 wt%, with an overall average of 84.8 wt% (± 5.35; Table 5 and Fig. 11). The lowest concentrations of aragonite occur in the uppermost Pleistocene interval where carbonate contents average approximately 76 wt% (Fig. 12). The noncarbonate fraction of the samples is composed primarily of quartz, presumably detrital in nature. The amount of carbonate gradually rises in the lower Pleistocene, and the percentage of quartz decreases. The upper Miocene is characterized by an average carbonate content of 82.77 wt%, which gradually increases to

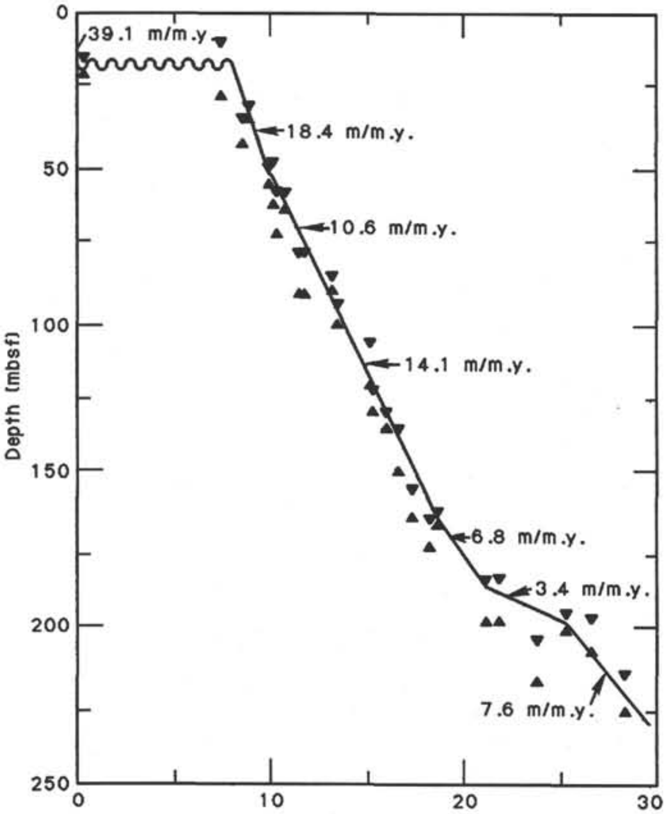

Figure 7. Sedimentation rates in Hole 714A based on the biostratigraphic events listed in Table 3.

an average of 89.4 wt% in the middle Miocene. The concentration of carbonate remains at approximately this level throughout the remainder of the core.

Organic Carbon Analysis

The concentration of organic material in Hole 714A was the highest observed during Leg 115. In the Pleistocene interval, concentrations were all in excess of 0.18%, and in some instances were as high as 0.78% (Fig. 11). However, there did not appear to be a downhole decrease consistent with the continued oxidation of organic material, as was suggested by the sharp decrease in sulfate and increase in phosphate. Below the hiatus marking the boundary between the Pleistocene and Miocene, concentrations of organic material rapidly decrease to background concentrations (Table 6 and Fig. 11).

In addition, concentrations of methane obtained by headspace analysis (see "Explanatory Notes" chapter, this volume) were detectable above background levels of approximately 2 ppm (Fig. 13 and Table 7). As methane concentrations decrease with depth, the concentrations of methane are related to methanogenesis taking place on an extremely small scale within the sediments themselves. Locally, it is possible that more drastic reductions in the concentration of sulfate have occurred than is observed from squeezing bulk sediment samples.

PHYSICAL PROPERTIES

Introduction

The following physical properties were measured at Site 714: index properties including carbonate content, compressional-wave velocities on discrete samples, shear-wave velocities, shear strengths, and thermal conductivities. We completed the transfer of the *P*-wave logger and GRAPE to a vertical tracking system during the drilling of Hole 714A. However, a number of problems arose with implemention of the new system, prohibiting any measurements at this hole.

Table 3. Biostratigraphic datum levels, Hole 714A.

	Species event	Depth (mbsf)	Age (Ma)
LO	*P. lacunosa* (N)	17.3–18.8	0.46
LO	*C. yabei* (D)	12.4–26.0	7.5
	D. petterssoni–D. hughesi (R)	36.9–41.4	8.6
LO	*D. hamatus* (N)	33.0–33.3	8.9
FO	*D. hamatus* (N)	52.6–54.1	10.0
FO	*N. acostaensis* (F)	51.0–60.6	10.2
LO	*P. siakensis* (F)	60.6–70.2	10.4
FO	*C. coalitus* (N)	60.7–62.2	10.8
FO	*C. coalitus* (N)	60.7–62.2	10.8
FO	*D. petterssoni* (R)	79.8–89.5	11.5
FO	*S. subdehiscens* (F)	79.8–89.5	11.8
LO	*S. heteromorphus* (N)	87.1–88.0	13.2
FO	*G. foshi foshi* (F)	96.5–99.1	13.5
FO	*Orbulina* (F)	108.7–118.4	15.2
	D. dentata–D. alata (R)	123.6–126.8	15.3
LO	*H. ampliaperta* (N)	131.1–132.4	16.0
FO	*G. sicanus* (F)	136.4–146.1	16.6
FO	*S. heteromorphus* (N)	163.0–163.3	18.6
FO	*C. costata* (R)	155.7–160.9	17.3
FO	*S. wolffii* (R)	165.3–170.5	18.2
FO	*S. delmontensis* (R)	184.7–194.4	21.1
LO	*G. kugleri* (F)	184.7–194.4	21.8
FO	*G. kugleri* (F)	204.1–213.8	23.7
LO	*S. ciperoensis* (N)	195.7–197.2	25.2
	B. veniamini (D)	204.1–213.8	26.5
LO	*S. distentus* (N)	215.3–223.5	28.2

Note: FO = first occurrence, LO = last occurrence, N = nannofossil, F = foraminifer, D = diatom, and R = radiolarian.

Index Properties

The calculated results for wet-bulk density, porosity, water content, and grain density for Site 714 are shown in Figures 14 and 15 and are listed in Table 8. The measured carbonate contents of the same samples are plotted in Figure 16. The wet-bulk density gradually increases with increasing depth, whereas the other index properties generally decrease with depth. However, porosity and water content are constant between 75 and 175 mbsf. There is little scatter in the porosity and water content data, and only sightly more in the bulk- and grain-density results. There are three anomalously low porosity values: at 186, 216, and 217 mbsf. They were measured on samples obtained from core catchers.

Compressional-Wave Velocity and Acoustic Impedance

The compressional-wave velocities (V_p) obtained from discrete samples from Site 714 are shown in Figure 17 and in Table 9. These data show a fair agreement between Holes 714A and 714B; a trend of increasing V_p with increasing depth is also observed. There is a large amount of scatter in the data below 150 mbsf. The discrete acoustic impedances for Site 714 are shown in Figure 18 and in Table 9. Generally, there is a gradual increase of impedance with depth, but no strong impedance contrasts are resolvable.

The GRAPE and *P*-wave logger were mounted on a vertical tracking system for Site 714. The effect of the transfer increased the uncertainty in V_p (determined from the *P*-wave logger) to approximately 2% for the distilled water standard. More importantly, there was an increase in background noise with the vertical tracking system, which introduced spurious readings. The

Table 4. Interstitial water analyses, Hole 714A.

Sample interval (cm)	Depth (mbsf)	Ca (mmol/L)	Mg (mmol/L)	Cl (mmol/L)	Al (mmol/L)	pH	Salinity (‰)	Si (μmol/L)	SO_4 (mmol/L)	NH_4 (μmol/L)	PO_4 (μmol/L)
Seawater	0	10.58	55.21	562.9	2.47	8.5	35.4	0	29.48	0	1.85
115-714A-											
1H-1, 145–150	1.45	10.58	51.21	526.8	3.30	7.6	35.2	575	27.46	46.5	6.99
2H-4, 145–150	8.75	10.72	53.95	564.7	3.88	7.5	35.2	621	26.51	112.0	6.22
3H-4, 145–150	18.75	10.68	52.23	531.5	4.32	7.6	34.8	663	26.88	135.0	4.16
4H-5, 145–150	28.08	10.83	52.16	567.5	4.08	7.5	35.5	746	27.03	106.0	2.62
5H-5, 145–150	39.15	10.81	52.10	562.0	4.44	7.6	35.2	568	27.17	125.0	3.78
6H-4, 145–150	47.35	10.94	51.89	551.8	4.23	7.6	35.4	704	26.51	114.0	2.36
9H-2, 145–150	73.15	10.92	50.71	558.3	3.99	7.7	35.0	769	26.30	111.0	2.24
12H-4, 120–125	104.80	11.01	49.98	545.3	4.19	7.6	35.2	783	26.29	129.0	2.49
15X-3, 120–125	131.00	11.27	50.04	538.9	4.00	7.5	35.2	797	26.64	112.0	2.11
18X-4, 120–125	161.40	11.07	50.64	544.4	3.78	7.5	34.8	808	26.42	94.0	2.24
22X-4, 120–125	200.10	11.43	50.77	547.2	3.63	7.6	35.2	870	26.67	69.0	1.98
25X-1, 145–150	224.75	11.65	52.54	556.4	3.36	7.8	35.8	771	26.46	42.0	1.98

new tracking system did not affect the GRAPE wet-bulk density results, although the vertical tracking caused slumping and upward migration of gas bubbles for soupy and partially filled core liners.

The *P*-wave logger measurements for V_p, GRAPE wet-bulk density results, and acoustic impedances for Hole 714B are shown in Figure 19. The wet-bulk densities, determined by the GRAPE, increase gradually with depth and are in good agreement with the discrete measurements. The V_p measurements are highly variable and contain a number of spurious readings. These uncorrected measurements should be viewed with caution, as should the continuous impedance profile which is calculated from these data.

Shear Strength and Shear-Wave Velocity

Measurements for shear-wave velocity (V_s) and shear strength taken at Site 714 are shown in Tables 10 and 11 and Figures 20 and 21. Both V_s and shear strength increase with depth, although there is a large amount of scatter in both sets of data. Shear strength measurements were not taken in the stiffer, more brittle chalks below 127 mbsf.

Thermal Conductivity

Thermal conductivity measurements for Holes 714A and 714B are shown in Figure 22 and Table 12. Almost all of the measurements were made in Hole 714A. The measurements in Hole 714B were confined to Core 115-714B-1H in order to fill in a small gap in the data at the top of Hole 714A. The thermal conductivity data show a certain amount of small-scale variability in the upper 50 m of this site, but below that depth the magnitude of the variability is reduced in comparison with the other sites of this leg.

There are a few isolated values at depths greater than 100 mbsf that are much lower than the surrounding values; these may be disturbed areas of the core which have a much higher water content. The higher water content would also account for the lower thermal conductivity. The general pattern shown by the thermal conductivity at this site is a steady increase with depth.

Summary

The physical properties measurements obtained at Site 714 all varied gradually with increasing depth. There was no major change in physical properties at the hiatus at ~20 mbsf nor at the deeper transition from soft nannofossil oozes to chalks. Porosity decreased to a depth of 75 mbsf, where it leveled off at 60%. A similar leveling off occurred for the other index properties. The carbonate content, shear strength, V_s, V_p, impedance, and thermal conductivity all increased with depth with varying amounts of scatter. The quality of the continuous V_p data was reduced because of the new vertical tracking system; hence, one should view the continuous V_p and impedance profiles with caution.

SEISMIC STRATIGRAPHY

Site 714 is located on the eastern shoulder of the Maldives Ridge, in 2031.5-m water depths (Fig. 23). This elevated plateau extends northward from the Chagos Bank to the Laccadive Islands and is part of the proposed volcanic trace of the Réunion hotspot left on the Indian plate. In this region the ridge is capped by a 100-km-wide carbonate bank of perhaps 1–1.5 km thickness. We intended to position this site on the top of a satellite spur that connects with the main carbonate platform, where pelagic carbonate oozes might be protected from disruption by turbidites. From previous seismic surveys, it appeared as though several hundred meters of soft sediment rested on harder strata (Fig. 24).

The *JOIDES Resolution* surveys of the site, however, revealed that the ridge was scoured of soft sediment everywhere and only a hard reflector could be seen at or near the sediment-water interface (Fig. 25). We continued to survey down the eastern slope of this ridge in the vicinity of a piston core location (V29-26) known to have recovered 12 m of Pleistocene carbonate ooze. The 3.5- and 12-kHz recordings show a 1-km-wide basin bounded by sediment hills (Fig. 26). This sediment appears to have accumulated at the base of the ridge by a combination of downslope transport and normal pelagic sedimentation. From the results of the piston coring, we felt there was a reasonable chance that a Quaternary section might be preserved in the small basin.

The single-channel seismic (SCS), water-gun reflection profile run by the *JOIDES Resolution* over Site 714 (Fig. 25) reveals a series of acoustic reflectors. Any evidence of impedance contrast across the Pleistocene-Miocene unconformity (see "Biostratigraphy" section, this chapter) is masked by reflection from the sediment-water contact. A strong reflector that appears to be continuous with strata near the surface of the nearby ridge occurs at 0.24 s below the seafloor. From drilling we know this is a late Oligocene shallow-water limestone, intersected at about 230 mbsf. *In situ P*-wave velocities of about 1500 m/s, then, seem appropriate for the overlying Neogene oozes. A second strong reflector appears at 0.36 sbsf and is most likely a basaltic basement.

REFERENCES

Baker, P. A., and Bloomer, S. H., 1988. The solubility of celestite in deep-sea sediments, *Geochim. Cosmochim. Acta*, 52:335–339.

Baker, P. A., 1986. Pore-water chemistry of carbonate-rich sediments, Lord Howe Rise, southwest Pacific Ocean. *In* Kennett, J. P., von der

Borch, C. C., et al., *Init. Repts. DSDP*, 90: Washington (U.S. Govt. Printing Office), 1249-1256.

Bender, M. L., and Heggie, D. T., 1984. Fate of organic carbon reaching the deep sea floor: a status report. *Geochim. Cosmochim. Acta*, 48:977-986.

Berner, R. A., 1980. *Early Diagenesis: A Theoretical Approach*: Princeton, NJ (Princeton Univ. Press).

Boardman, M. R., Neumann, A. C., Baker, P. A., Dulin, L. A., Kenter, R. J., Hunter, G. E., and Keifer, K. B., 1986. Banktop response to Quaternary fluctuations in sea level recorded in periplatform sediments. *Geology*, 14:28-31.

Boardman, M. R., and Neumann, A. C., 1986. Reply on "Banktop response to Quaternary fluctuations in sea level recorded in periplatform sediments." *Geology*, 14:1040-1041.

Droxler, A. W., Schlager, W., and Whallon, C. C., 1983. Quaternary aragonite cycles and oxygen-isotope record in Bahamian carbonate ooze. *Geology*, 11:235-239.

Droxler, A. W., 1986. Comment on "Banktop response to Quaternary fluctuations in sea level recorded in periplatform sediments." *Geology*, 14:1039-1040.

Froelich, P. N., Klinkhammer, G. P., Bender, M. L., Luedtke, N. A., Heath, G. R., Cullen, D., Dauphin, P., Hartman, B., Hammond, D., and Maynard, V., 1979. Early oxidation of organic matter in pelagic sediments of the eastern Equatorial Atlantic: suboxic diagenesis. *Geochim. Cosmochim. Acta*, 43:1075-1090.

Gieskes, J. M., 1981. Deep-sea drilling interstitial water studies: implications for chemical alteration of the ocean crust, Layers I and II. *Soc. Econ. Paleontol. Mineral. Spec. Publ.*, 32:149-167.

Kier, J. S., and Pilkey, O. H., 1971. The influence of sea level changes on sediment carbonate mineralogy, Tongue of the Oceans, Bahamas. *Mar. Geol.* 11:189-200.

Klinkhammer, G. P., 1980. Early diagenesis in sediments from the eastern Equatorial Pacific: II. Pore water metal results. *Earth Planet. Sci. Lett.*, 49:81-101.

Martini, E., 1971. Standard Tertiary and Quaternary calcareous nannoplankton zonation. *In* Farinacci, A. (Ed.), *Proc. II Planktonic Conf. Roma, 1971*: Rome (Ed. Tecnoscienza), 739-785.

Okada, H., and Bukry, D., 1980. Supplementary modification and introduction of code numbers to the low-latitude coccolith biostratigraphic zonation (Bukry, 1973; 1975). *Mar. Micropaleontol.*, 5:321-325.

Perch-Nielsen, K., 1985. Cenozoic calcareous nannofossils. *In* Bolli, H. M., Saunders, J. B., and Perch-Nielsen, K. (Eds.), *Plankton Stratigraphy:* Cambridge (Cambridge Univ. Press), 427-554.

Swart, P. K., and Guzikowski, M., 1988. Interstitial water chemistry and diagenesis of periplatform sediments from the Bahamas, Leg 101. *In* Austin, J., Schlager, W., et al., *Proc. ODP, Sci. Results*, 101: College Station, TX (Ocean Drilling Program), 363-380.

Ms 115A-112

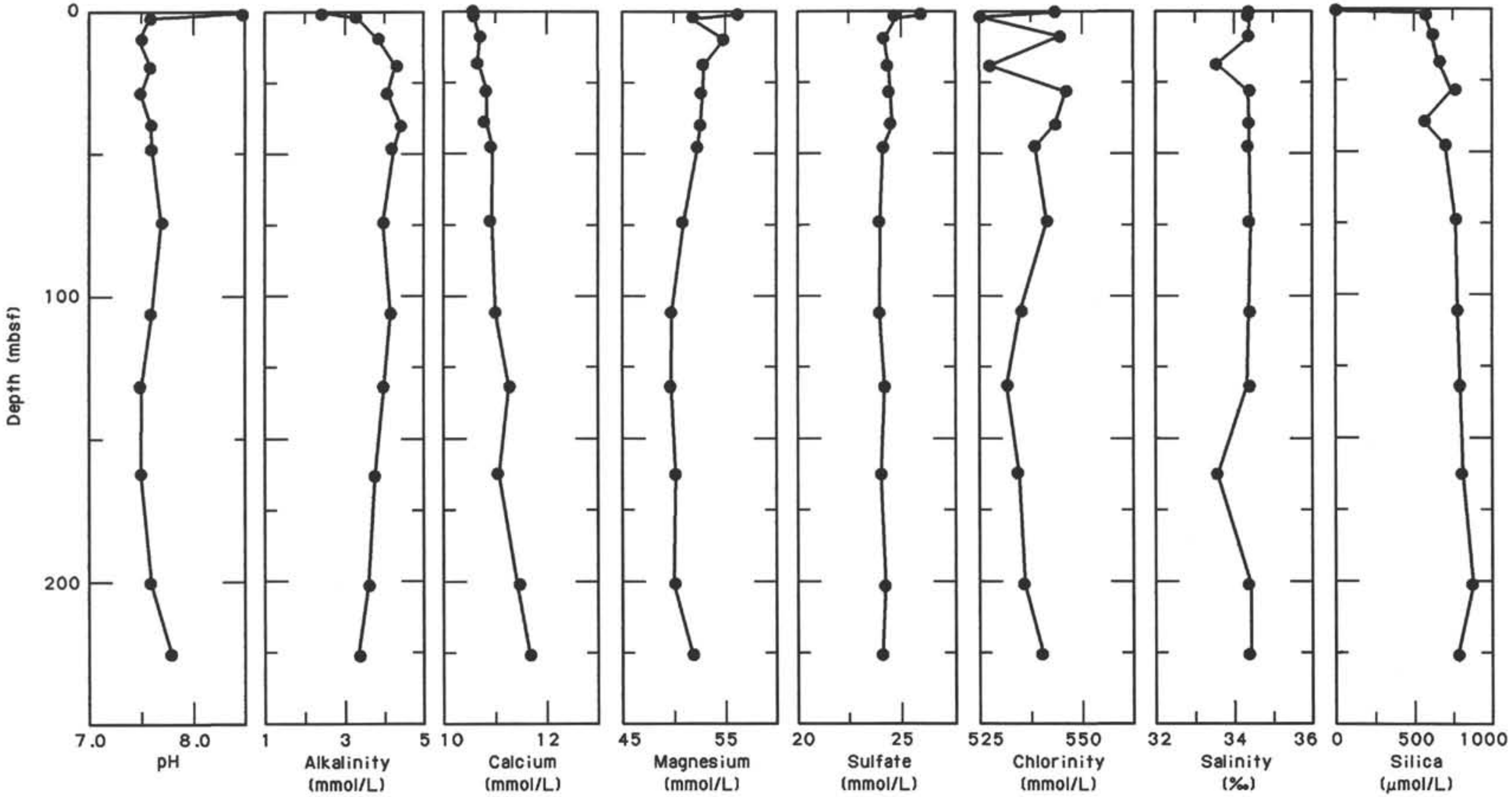

Figure 8. Summary of interstitial water analyses, Hole 714A, as a function of sub-bottom depth. Surface seawater is plotted at 0 mbsf.

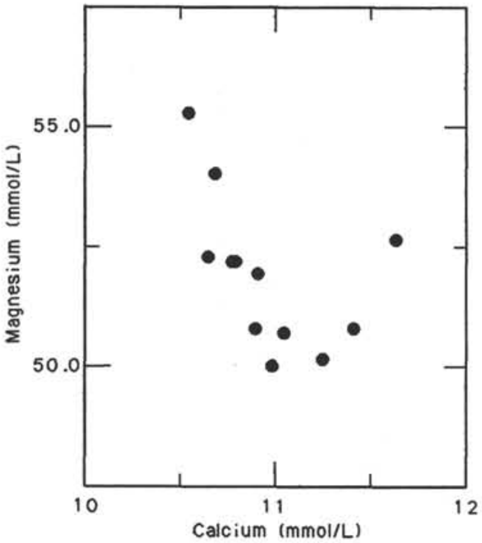

Figure 9. Relationship between calcium and magnesium concentrations, Hole 714A.

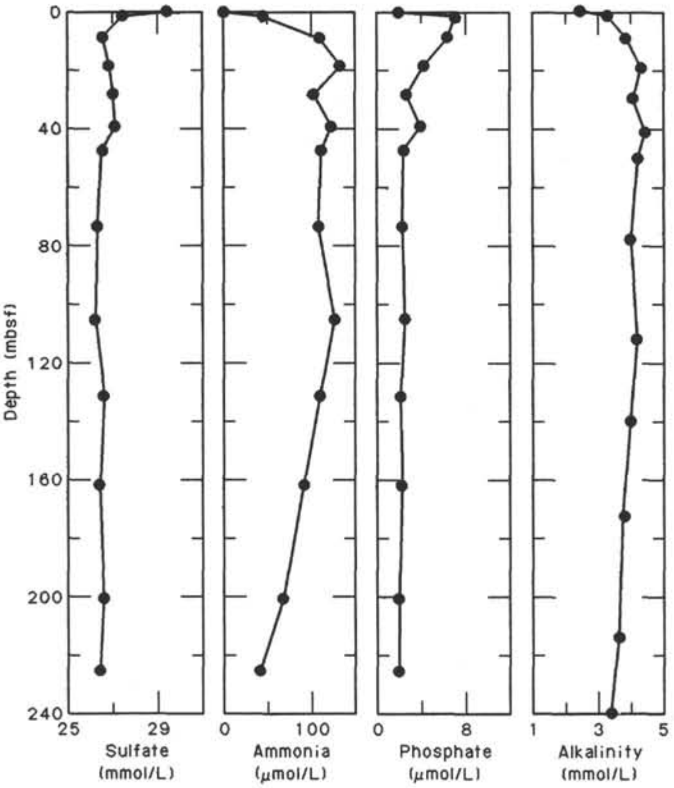

Figure 10. Downhole changes in alkalinity, sulfate, phosphate, and ammonia in Hole 714A. Note the dramatic increase in the concentration of phosphate at 1.45 mbsf and the corresponding decrease in sulfate.

Table 5. Carbonate content of samples from Hole 714A.

Sample interval (cm)	Depth (mbsf)	Carbonate (wt%)
115-714A-		
1H-1, 30–31	0.30	81.86
1H-1, 100–101	1.00	67.47
1H-2, 30–31	1.80	72.56
1H-2, 69–71	2.19	67.98
1H-2, 100–101	2.50	60.05
2H-1, 30–31	3.10	79.41
2H-1, 60–62	3.40	80.70
2H-1, 100–101	3.80	80.09
2H-2, 30–31	4.60	70.81
2H-2, 100–101	5.30	71.58
2H-3, 30–31	6.10	71.49
2H-3, 100–101	6.80	80.78
2H-4, 30–31	7.60	73.17
2H-4, 100–101	8.30	76.04
2H-5, 30–31	9.10	75.81
2H-5, 100–101	9.80	74.82
2H-6, 30–31	10.60	75.22
2H-6, 100–101	11.30	84.10
2H-7, 30–31	12.10	84.06
3H-1, 30–31	12.70	72.32
3H-1, 60–62	13.00	81.05
3H-1, 100–101	13.40	80.55
3H-2, 30–31	14.20	78.40
3H-2, 100–101	14.90	80.67
3H-3, 30–31	15.70	66.56
3H-3, 60–62	16.00	73.65
3H-3, 100–101	16.40	71.86
3H-4, 30–31	17.20	74.78
3H-4, 60–62	17.50	80.50
3H-4, 100–101	17.90	80.07
3H-5, 30–31	18.70	81.31
3H-5, 60–62	19.00	83.64
3H-5, 100–101	19.40	81.39
3H-6, 30–31	20.20	81.84
3H-6, 60–62	20.50	88.56
3H-6, 100–101	20.90	74.21
3H-7, 30–31	21.70	88.99
4H-2, 30–31	22.48	77.19
4H-2, 60–62	22.78	89.70
4H-2, 100–101	23.18	83.34
4H-3, 30–31	23.93	85.69
4H-3, 100–101	24.63	83.07
4H-4, 30–31	25.43	86.62
4H-4, 86–88	25.99	87.60
4H-4, 100–101	26.13	87.12
4H-5, 30–31	26.93	86.14
4H-5, 100–101	27.63	69.77
4H-6, 30–31	28.43	86.73
4H-6, 88–90	29.01	81.60
4H-6, 100–101	29.13	81.86
4H-7, 30–31	29.93	79.47
4H-7, 100–101	30.63	82.98
4H-8, 30–31	31.43	83.52
5H-1, 30–31	32.00	83.57
5H-1, 100–101	32.70	80.71
5H-2, 30–31	33.50	77.45
5H-2, 60–62	33.80	78.03
5H-2, 100–101	34.20	83.38
5H-3, 30–31	35.00	86.00
5H-3, 100–101	35.70	82.54
5H-4, 30–31	36.50	81.74
5H-4, 60–62	36.80	79.54
5H-4, 100–101	37.20	80.30
5H-5 30–31	38.00	84.61
5H-6, 100–101	38.70	80.47
5H-6, 30–31	39.50	81.38
5H-6, 60–62	39.80	82.67
5H-6, 100–101	40.20	75.79
5H-7, 30–31	41.00	83.57
6H-1, 30–31	41.70	80.77
6H-1, 100–101	42.40	82.27
6H-2, 30–31	43.20	77.45
6H-2, 60–62	43.50	82.88
6H-2, 100–101	43.90	73.40

Table 5 (continued).

Sample interval (cm)	Depth (mbsf)	Carbonate (wt%)
115-714A-		
6H-3, 30–31	44.70	84.80
6H-3, 100–101	45.40	72.14
6H-4, 30–31	46.20	84.84
6H-4, 60–62	46.50	86.18
6H-4, 100–101	46.90	69.82
6H-5, 30–31	47.70	83.80
6H-5, 100–101	48.40	86.71
6H-6, 30–31	49.20	80.99
6H-6, 60–62	49.50	82.35
6H-6, 100–101	49.90	83.51
6H-7, 30–31	50.70	80.09
7H-1, 30–31	51.30	85.20
7H-1, 100–101	52.00	84.20
7H-2, 30–31	52.80	79.70
7H-2, 40–41	52.90	74.15
7H-2, 60–62	53.10	86.18
7H-2, 100–101	53.50	79.73
7H-3, 30–31	54.30	79.95
7H-3, 40–41	54.40	75.93
7H-3, 100–101	55.00	86.33
7H-4, 30–31	55.80	79.03
7H-4, 40–41	55.90	83.10
7H-4, 60–62	56.10	81.43
7H-4, 100–101	56.50	75.26
7H-5, 30–31	57.30	85.53
7H-5, 100–101	58.00	80.76
7H-6, 30–31	58.80	76.19
7H-6, 56–58	59.06	85.32
7H-6, 100–101	59.50	82.22
7H-7, 30–31	60.30	84.55
8H-1, 30–31	60.90	84.21
8H-1, 100–101	61.60	79.19
8H-2, 30–31	62.40	84.67
8H-2, 60–62	62.70	86.18
8H-2, 100–101	63.10	86.43
8H-3, 30–31	63.90	84.41
8H-3, 100–101	64.60	86.04
8H-4, 30–31	65.40	87.55
8H-4, 60–62	65.70	87.74
8H-4, 100–101	66.10	86.46
8H-5, 30–31	66.90	90.60
8H-5, 100–101	67.60	88.14
8H-6, 30–31	68.40	83.29
8H-6, 60–62	68.70	88.61
8H-6, 100–101	69.10	82.10
8H-7, 30–31	69.90	87.71
9H-1, 30–31	70.50	88.65
9H-1, 100–101	71.20	87.96
9H-2, 30–31	72.00	84.35
9H-2, 60–62	72.30	81.26
9H-2, 100–101	72.70	84.88
9H-3, 30–31	73.50	86.01
9H-3, 75–77	73.95	86.58
9H-3, 100–101	74.20	82.99
9H-4, 30–31	75.00	86.42
10H-1, 30–31	80.10	86.21
10H-1, 100–101	80.80	86.17
10H-2, 30–31	81.60	87.50
10H-2, 60–62	81.90	86.31
10H-2, 100–101	82.30	79.36
10H-3, 30–31	83.10	85.21
10H-3, 60–62	83.40	94.74
10H-3, 100–101	83.80	86.89
10H-4, 30–31	84.60	87.08
10H-4, 100–101	85.30	88.12
10H-5, 30–31	86.10	89.11
10H-5, 60–62	86.40	86.68
10H-5, 100–101	86.80	89.97
10H-6, 30–31	87.60	90.96
10H-6, 100–101	88.30	86.52
10H-7, 30–31	89.10	91.30
10H-7, 60–62	89.40	89.99
11H-1, 30–31	89.80	89.85
11H-1, 100–101	90.50	90.98
11H-2, 30–31	91.30	90.95
11H-2, 100–101	92.00	89.03
11H-3, 30–31	92.80	90.89
11H-3, 70–72	93.20	92.35
11H-3, 100–101	93.50	90.08
11H-4, 30–31	94.30	88.41
11H-4, 100–101	95.00	88.40
11H-5, 30–31	95.80	87.61
11H-5, 100–101	96.50	86.17
11H-6, 30–31	97.30	88.66
11H-6, 52–54	97.52	88.21
11H-6, 100–101	98.00	92.08
12H-1, 30–31	99.40	88.44
12H-1, 100–101	100.10	90.60
12H-2, 30–31	100.90	85.56
12H-2, 60–62	101.20	92.14
12H-2, 100–101	101.60	89.47
12H-3, 30–31	102.40	90.79
12H-3, 100–101	103.10	88.96
12H-4, 30–31	103.90	89.42
12H-4, 61–63	104.21	94.73
12H-4, 100–101	104.60	88.10
12H-5, 30–31	105.40	88.50
12H-5, 63–65	105.73	89.54
12H-5, 100–101	106.10	86.82
12H-6, 30–31	106.90	89.84
12H-6, 100–101	107.60	88.41
12H-7, 30–31	108.40	85.77
13H-1, 30–31	109.00	90.25
13H-1, 100–101	109.70	87.02
13H-2, 30–31	110.50	90.37
13H-2, 58–60	110.78	88.10
13H-2, 100–101	111.20	92.57
13H-3, 30–31	112.00	90.20
13H-3, 100–101	112.70	90.84
13H-4, 30–31	113.50	90.34
13H-4, 65–67	113.85	87.03
13H-4, 100–101	114.20	88.21
13H-5, 30–31	115.00	91.35
13H-5, 100–101	115.70	85.34
13H-6, 30–31	116.50	87.46
13H-6, 100–101	117.20	87.34
13H-7, 30–31	118.00	86.25
14X-1, 30–31	118.70	87.73
14X-1, 100–101	119.40	87.36
14X-2, 30–31	120.20	88.32
14X-2, 63–65	120.53	88.81
14X-2, 100–101	120.90	86.95
14X-3, 30–31	121.70	88.59
14X-3, 100–101	122.40	85.99
14X-4, 30–31	123.20	85.44
14X-4, 63–65	123.53	87.40
14X-4, 100–101	123.90	82.54
14X-5, 30–31	124.70	88.80
14X-5, 100–101	125.40	84.83
14X-6, 30–31	126.20	88.38
14X-6, 54–56	126.44	85.91
14X-6, 65–67	126.55	89.49
14X-6, 100–101	126.90	88.42
15X-1, 30–31	127.10	79.94
15X-1, 92–93	127.72	86.82
15X-2, 30–31	128.60	85.30
15X-2, 92–93	129.22	87.26
15X-2, 100–102	129.30	87.56
15X-3, 30–31	130.10	83.56
15X-3, 92–93	130.72	86.58
15X-4, 26–28	131.56	86.78
15X-4, 30–31	131.60	85.69
15X-4, 92–93	132.22	87.18
15X-5, 30–31	133.10	87.50
15X-5, 92–93	133.72	85.20
15X-6, 22–24	134.19	89.14
15X-6, 30–31	134.27	84.59
16X-1, 30–31	136.70	85.44
16X-1, 100–101	137.40	83.25
16X-2, 30–31	138.20	86.09
16X-2, 100–101	138.90	83.35
16X-3, 30–31	139.70	78.83
16X-3, 50–52	139.90	86.42
16X-3, 100–101	140.40	83.26
16X-4, 30–31	141.20	80.73
16X-4, 100–101	141.90	84.59
16X-5, 30–31	142.70	84.44
16X-5, 100–101	143.40	83.53
16X-6, 25–27	144.60	83.75
17X-1, 30–31	146.40	84.82
17X-1, 100–101	147.10	85.60
17X-2, 30–31	147.90	86.17
17X-2, 92–94	148.52	85.22
17X-2, 100–101	148.60	85.33
17X-3, 30–31	149.40	85.45
17X-3, 100–101	150.10	86.50
17X-4, 30–31	150.90	87.95
17X-4, 100–101	151.60	82.09
17X-4, 148–150	152.08	85.96
17X-5, 30–31	152.40	87.07
18X-1, 30–31	156.00	87.76
18X-1, 100–101	156.70	84.35
18X-2, 30–31	157.50	85.69
18X-2, 100–101	158.20	78.50
18X-3, 8–10	158.78	88.40
18X-3, 30–31	159.00	87.42
18X-3, 100–101	159.70	81.00
18X-4, 30–31	160.50	82.82
18X-4, 100–101	161.20	88.14
18X-5, 10–12	161.80	82.93
18X-5, 30–31	162.00	81.82
18X-5, 100–101	162.70	88.80
18X-6, 30–31	163.50	88.30
18X-7, 30–31	163.82	86.02
19X-1, 30–31	165.60	86.51
19X-1, 100–101	166.30	84.80
19X-2, 30–31	167.10	86.54
19X-2, 52–54	167.32	88.01
19X-2, 100–101	167.80	85.00
19X-3, 30–31	168.60	83.17
19X-3, 100–101	169.30	87.44
19X-4, 30–31	170.10	85.61
19X-4, 100–101	170.80	88.63
19X-5, 30–31	171.60	90.78
19X-5, 56–58	171.86	88.77
19X-5, 100–101	172.30	89.49
19X-6, 30–31	173.10	90.71
19X-6, 100–101	173.80	90.94
20X-1, 30–31	175.30	86.68
20X-1, 100–101	176.00	87.25
20X-2, 30–31	176.80	89.53
20X-2, 60–62	177.10	92.58
20X-2, 100–101	177.50	86.91
20X-3, 30–31	178.30	86.71
20X-3, 100–101	179.00	88.46
20X-4, 30–31	179.80	76.81
20X-4, 100–101	180.50	87.35
20X-5, 30–31	181.30	85.81
20X-5, 64–66	181.64	88.14
20X-5, 100–101	182.00	87.86
21X-1, 33–34	185.03	86.05
21X, CC, 2–4	185.49	60.72
22X-1, 30–31	194.70	87.36
22X-1, 100–101	195.40	87.35
22X-2, 30–31	196.20	89.19
22X-2, 60–62	196.50	88.21
22X-2, 100–101	196.90	88.46
22X-3, 30–31	197.70	88.17
22X-3, 100–101	198.40	89.09
22X-4, 14–15	199.04	91.60
22X-4, 60–62	199.50	91.73
22X-4, 100–101	199.90	90.05
22X-5, 30–31	200.70	90.46

Table 5 (continued).

Sample interval (cm)	Depth (mbsf)	Carbonate (wt%)
115-714A-		
22X-6, 54-56	202.40	91.03
23X-1, 30-31	204.40	87.77
23X-1, 100-101	205.10	87.77
23X-2, 30-31	205.90	87.20
23X-2, 63-65	206.23	91.16
23X-2, 100-101	206.60	87.60
23X-3, 30-31	207.40	86.36
23X-3, 62-65	207.72	90.46
23X-3, 100-101	208.10	89.09
23X-4, 30-31	208.90	89.44
23X-4, 100-101	209.60	88.76
23X-5, 30-31	210.40	89.40
23X-5, 100-101	211.10	88.81
23X-6, 30-31	211.90	85.65
23X-6, 63-65	212.23	88.42
23X-6, 100-101	212.60	89.61
24X-1, 30-31	214.10	86.94
24X-1, 100-101	214.80	88.57
25X-1, 30-31	223.60	89.99
25X-1, 100-101	224.30	89.34
25X-, 30-31	226.60	89.97

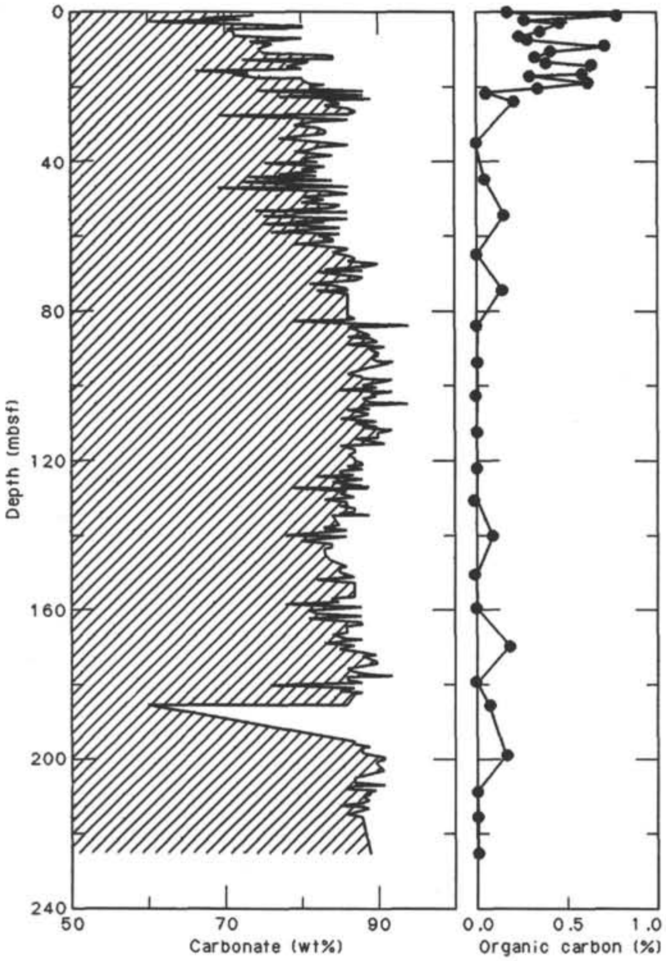

Figure 11. Carbonate and organic carbon content of sediments from Hole 714A.

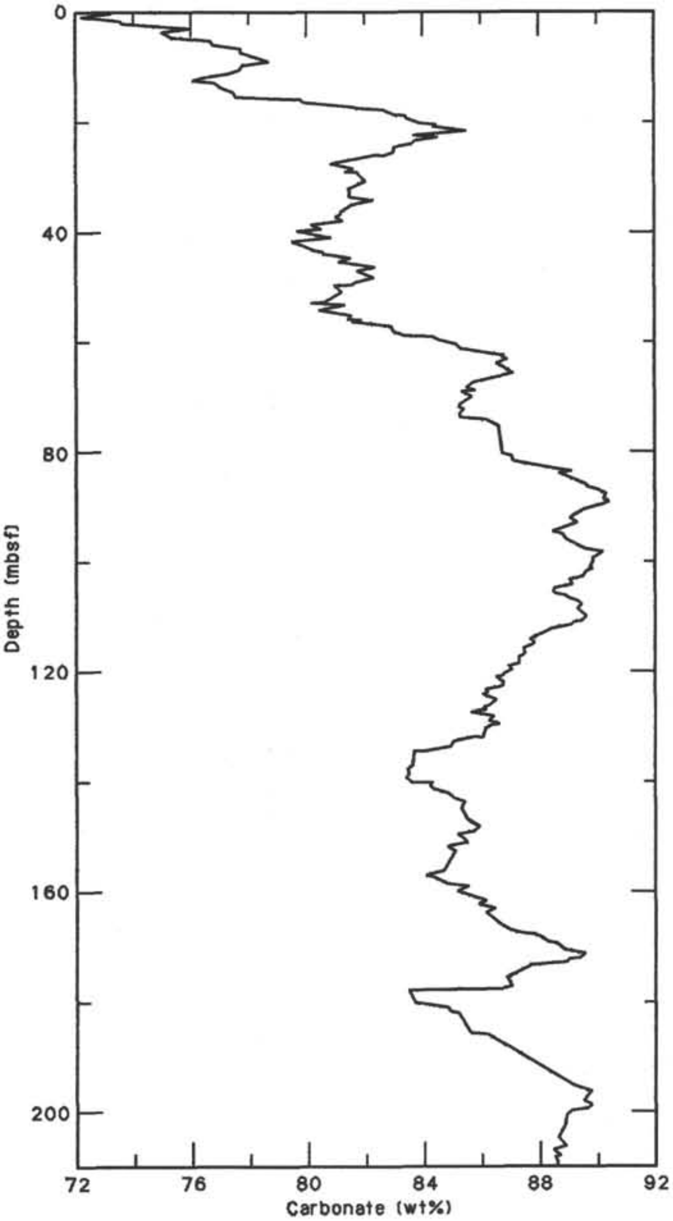

Figure 12. Smoothed variations in carbonate content, Hole 714A.

Table 6. Organic carbon analyses, Hole 714A.

Sample interval (cm)	Depth (mbsf)	Organic carbon (%)
115-714A-		
1H-1, 30–31	0.30	0.18
1H-1, 100–101	1.00	0.78
1H-2, 100–101	2.50	0.27
2H-1, 30–31	3.10	0.46
2H-2, 100–101	5.30	0.35
2H-3, 100–101	6.80	0.24
2H-4, 30–31	7.60	0.28
2H-5, 30–31	9.10	0.71
2H-6, 30–31	10.60	0.41
2H-7, 30–31	12.10	0.33
3H-1, 100–101	13.40	0.39
3H-2, 30–31	14.20	0.64
3H-3, 100–101	16.40	0.59
3H-4, 30–31	17.20	0.30
3H-5, 30–31	18.70	0.62
3H-6, 30–31	20.20	0.34
3H-7, 30–31	21.70	0.06
4H-3, 30–31	23.93	0.21
5H-3, 30–31	35.00	0
6H-3, 30–31	44.70	0.05
7H-3, 30–31	54.30	0.16
8H-3, 100–101	64.60	0
9H-3, 100–101	74.20	0.15
10H-3, 100–101	83.80	0
11H-3, 100–101	93.50	0
12H-3, 30–31	102.40	0
13H-3, 30–31	112.00	0
14X-3, 30–31	121.70	0
15X-3, 30–31	130.10	0
16X-3, 30–31	139.70	0.10
17X-3, 100–101	150.10	0
18X-3, 30–31	159.00	0
19X-3, 100–101	169.30	0.19
20X-3, 100–101	179.00	0
21X-1, 33–34	185.03	0.08
22X-3, 101–101	198.41	0.17
23X-3, 100–101	208.10	0
24X-1, 100–101	214.80	0
25X-1, 100–101	224.30	0

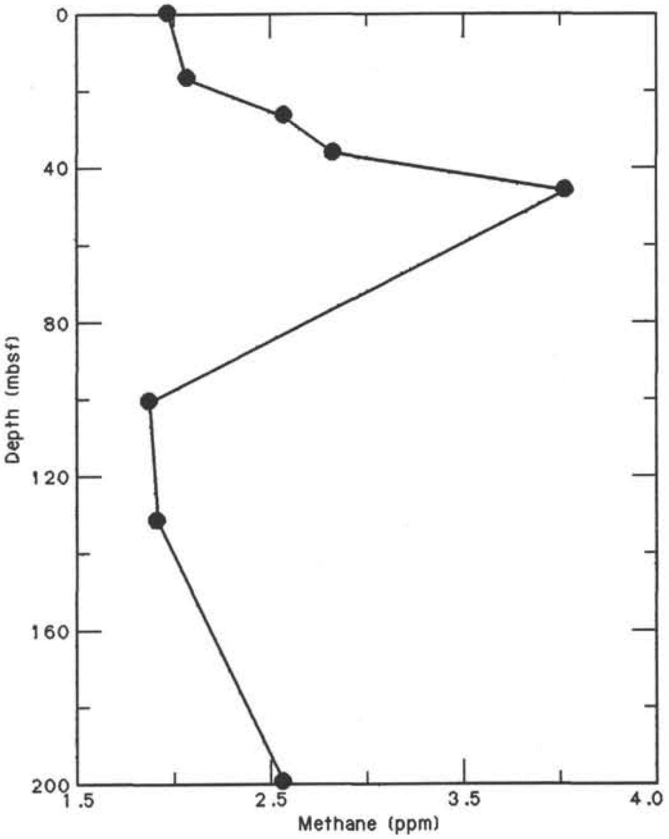

Figure 13. Methane measurements, Hole 714A.

Table 7. Concentrations of methane (CH_4), Hole 714A.

Sample interval (cm)	Depth (mbsf)	Methane (ppm)
115-714A-		
1H-1, 145–150	1.45	2.0
3H-4, 145–150	18.35	2.1
4H-5, 145–150	28.08	2.6
5H-4, 145–150	37.65	2.86
6H-4, 145–150	47.35	4.06
12H-2, 120–125	101.80	1.91
15X-4, 120–125	132.50	1.95
22X-4, 120–125	200.10	2.6

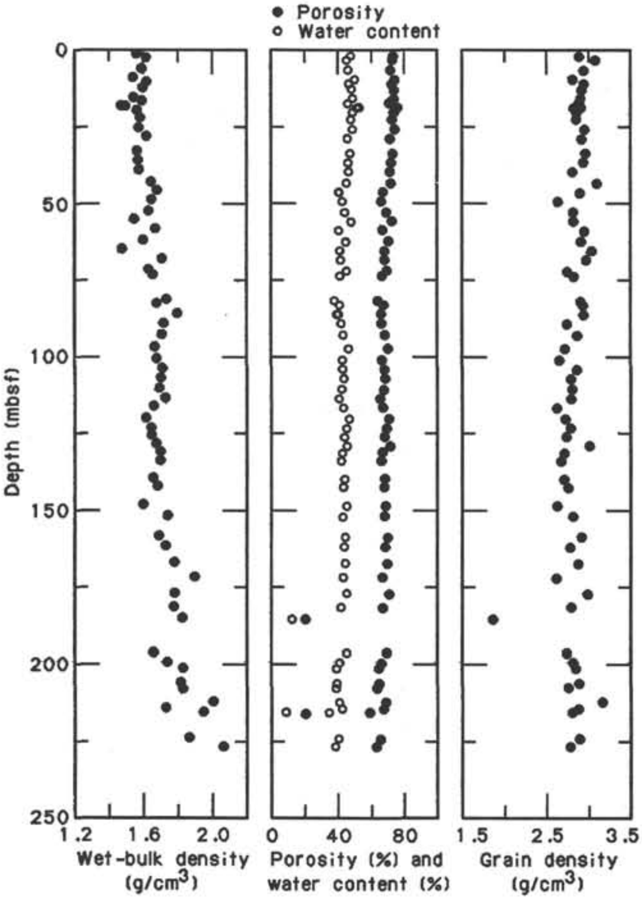

Figure 14. Index properties (wet-bulk density, water content, porosity, and grain density) at Hole 714A.

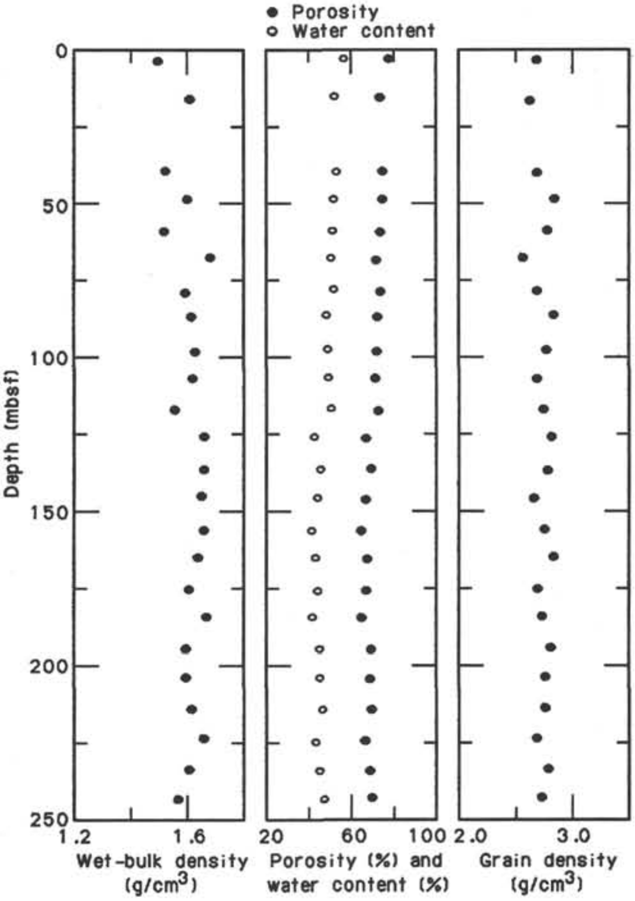

Figure 15. Index properties (wet-bulk density, water content, porosity, and grain density) at Hole 714B.

Table 8. Index-properties data, Site 714.

Section interval (cm)	Depth (mbsf)	Water content (%)	Porosity (%)	Wet-bulk density (g/cm^3)	Dry-bulk density (g/cm^3)	Grain density (g/cm^3)	Carbonate content (wt%)
115-714A-							
1H-2, 71	2.21	47.98	72.47	1.56	0.81	2.89	67.98
2H-1, 60	3.40	45.53	71.86	1.62	0.88	2.90	80.70
2H-3, 100	6.80	45.99	71.27	1.59	0.86	2.95	83.42
2H-5, 100	9.80	49.94	73.58	1.54	0.77	2.82	72.44
2H-6, 100	11.30	46.55	71.76	1.62	0.86	2.95	83.24
3H-1, 60	13.00	47.98	72.77	1.60	0.83	2.93	81.05
3H-3, 60	16.00	48.79	73.35	1.54	0.79	2.92	73.65
3H-4, 60	17.50	45.82	70.76	1.59	0.86	2.89	80.50
3H-5, 60	19.00	52.46	75.66	1.47	0.70	2.84	83.64
3H-6, 60	20.50	48.71	72.95	1.56	0.80	2.87	88.56
4H-2, 60	22.78	47.76	72.15	1.58	0.83	2.86	89.70
4H-4, 86	25.99	48.74	73.57	1.57	0.81	2.96	87.60
4H-6, 88	29.01	45.76	71.00	1.62	0.88	2.93	81.60
5H-2, 60	33.80	47.33	72.54	1.56	0.82	2.97	78.03
5H-4, 60	36.80	46.32	71.59	1.57	0.84	2.95	79.54
5H-6, 60	39.80	46.61	70.88	1.57	0.84	2.82	82.67
6H-2, 60	43.50	45.33	71.84	1.64	0.89	2.85	82.88
6H-4, 60	46.50	40.73	66.32	1.68	1.00	2.90	86.18
6H-6, 60	49.50	42.68	66.02	1.65	0.95	2.64	82.35
7H-2, 60	53.10	44.24	68.93	1.63	0.91	2.83	85.93
7H-4, 60	56.10	48.02	72.12	1.55	0.81	2.83	81.43
7H-6, 56	59.06	40.69	66.75	1.67	0.99	2.96	85.32
8H-2, 60	62.70	44.79	70.07	1.60	0.88	2.92	86.18
8H-4, 60	65.70	41.31	67.89	1.48	0.87	2.86	87.74
8H-6, 60	68.70	41.85	67.96	1.71	0.99	2.98	88.61
9H-2, 60	72.30	45.19	69.26	1.63	0.89	2.76	81.26
9H-3, 75	73.95	41.11	66.15	1.66	0.98	2.83	86.58
10H-2, 60	81.90	38.08	63.91	1.73	1.07	2.92	86.31
10H-3, 60	83.40	41.03	66.87	1.68	0.99	2.94	84.74
10H-5, 60	86.40	39.82	65.83	1.80	1.08	2.95	86.68
10H-7, 60	89.40	42.07	66.36	1.72	1.00	2.75	89.99
11H-3, 70	93.20	43.32	68.47	1.71	0.97	2.87	92.35
11H-6, 52	97.52	46.41	70.03	1.67	0.89	2.73	88.21
12H-2, 60	101.20	42.96	66.56	1.68	0.96	2.67	92.14
12H-4, 61	104.21	42.67	67.86	1.71	0.98	2.87	94.73
12H-6, 63	107.23	43.73	68.24	1.70	0.96	2.80	89.54
13H-2, 58	110.78	42.48	67.23	1.69	0.97	2.81	88.10
13H-4, 65	113.85	40.69	65.45	1.73	1.03	2.80	87.03
13H-6, 65	116.85	43.37	66.60	1.66	0.94	2.63	89.49
14X-2, 63	120.53	47.01	70.55	1.62	0.86	2.73	88.81
14X-4, 63	123.53	45.23	69.47	1.65	0.91	2.79	87.40
14X-6, 54	126.44	44.11	68.25	1.65	0.92	2.75	85.91
15X-2, 100	129.30	45.60	71.36	1.67	0.91	2.73	87.56
15X-4, 26	131.56	42.82	66.78	1.70	0.97	2.72	86.78
15X-6, 22	134.19	42.17	65.96	1.70	0.98	2.69	89.14
16X-3, 58	139.98	44.30	68.16	1.66	0.92	2.72	86.42
16X-5, 25	142.65	43.56	67.78	1.68	0.95	2.76	83.75
17X-2, 92	148.52	45.61	68.69	1.60	0.87	2.64	85.22
17X-4, 148	152.08	43.35	68.09	1.74	0.99	2.82	85.96
18X-3, 8	158.78	44.61	69.90	1.69	0.94	2.92	88.40
18X-5, 10	161.80	43.91	68.36	1.73	0.97	2.79	82.93
19X-2, 52	167.32	44.64	69.64	1.78	0.98	2.88	88.01
19X-5, 56	171.86	43.38	66.56	1.90	1.08	2.63	88.77
20X-2, 60	177.10	45.38	71.03	1.78	0.97	2.99	92.58
20X-5, 64	181.64	42.18	66.84	1.78	1.03	2.80	88.14
21X, CC, 2	185.49	12.32	20.56	1.83	1.61	1.87	60.72
22X-2, 60	196.50	45.28	69.24	1.66	0.91	2.75	88.21
22X-4, 60	199.50	41.20	66.13	1.74	1.03	2.82	91.73
22X-5, 54	201.44	39.48	64.75	1.83	1.11	2.85	91.03
23X-2, 63	206.23	39.24	64.82	1.82	1.11	2.89	91.16
23X-3, 63	207.73	38.75	63.26	1.83	1.12	2.76	90.46
23X-6, 63	212.23	40.90	68.33	2.01	1.19	2.80	88.82
24X-1, 60	214.40	42.40	67.69	1.73	0.99	2.88	86.94
24X, CC, 21	215.51	34.50	59.33	1.95	1.27	2.81	88.57
24X, CC, 24	215.54	8.53	20.45	2.79	2.55	2.80	89.99
25X-1, 60	223.90	40.04	65.56	1.87	1.12	2.89	89.34
25X, CC, 20	226.50	37.92	62.69	2.07	1.28	2.78	89.97
115-714B-							
1H-2, 60	2.10	55.52	76.83	1.49	0.66	2.68	71.06
1H-6, 60	8.10	50.85	72.85	1.60	0.79	2.62	79.97
3H-3, 60	20.00	51.70	74.04	1.52	0.74	2.69	79.04
3H-6, 60	24.50	50.33	74.03	1.59	0.79	2.84	83.85
4H-3, 60	29.60	49.91	73.22	1.51	0.76	2.77	80.70
4H-6, 60	34.10	49.22	71.12	1.67	0.85	2.56	82.07

Table 8 (continued).

Section interval (cm)	Depth (mbsf)	Water content (%)	Porosity (%)	Wet-bulk density (g/cm^3)	Dry-bulk density (g/cm^3)	Grain density (g/cm^3)	Carbonate content (wt%)
115-714B-							
5H-3, 60	39.30	50.27	72.88	1.59	0.79	2.68	80.67
5H-6, 32	43.52	47.20	71.46	1.61	0.85	2.83	83.04
6H-3, 60	49.00	47.38	71.05	1.62	0.85	2.76	77.69
6H-6, 60	53.50	47.44	70.46	1.61	0.85	2.67	82.48
7H-3, 60	58.60	48.13	71.50	1.55	0.80	2.73	79.07
7H-6, 60	63.10	40.78	65.60	1.65	0.98	2.80	85.41
8H-3, 60	68.20	43.31	67.70	1.65	0.93	2.78	85.11
8H-6, 60	72.70	41.94	65.44	1.64	0.95	2.65	84.93
9H-3, 71	78.01	39.40	63.79	1.65	1.00	2.74	84.50
9H-6, 64	82.44	41.26	66.20	1.63	0.96	2.82	84.41
10H-3, 85	87.75	42.12	65.77	1.60	0.93	2.67	84.45
10H-6, 67	92.07	40.01	64.07	1.66	0.99	2.71	89.01
11H-3, 68	97.28	43.23	67.76	1.59	0.90	2.79	82.21
11H-6, 76	101.86	43.29	67.40	1.59	0.90	2.74	85.64
12H-3, 71	106.91	43.94	68.00	1.61	0.90	2.74	87.36
12H-6, 92	111.62	41.55	65.16	1.65	0.96	2.66	88.52
13H-3, 76	116.66	43.02	67.35	1.60	0.91	2.76	82.34
13H-6, 97	121.37	45.03	68.65	1.56	0.86	2.70	83.96

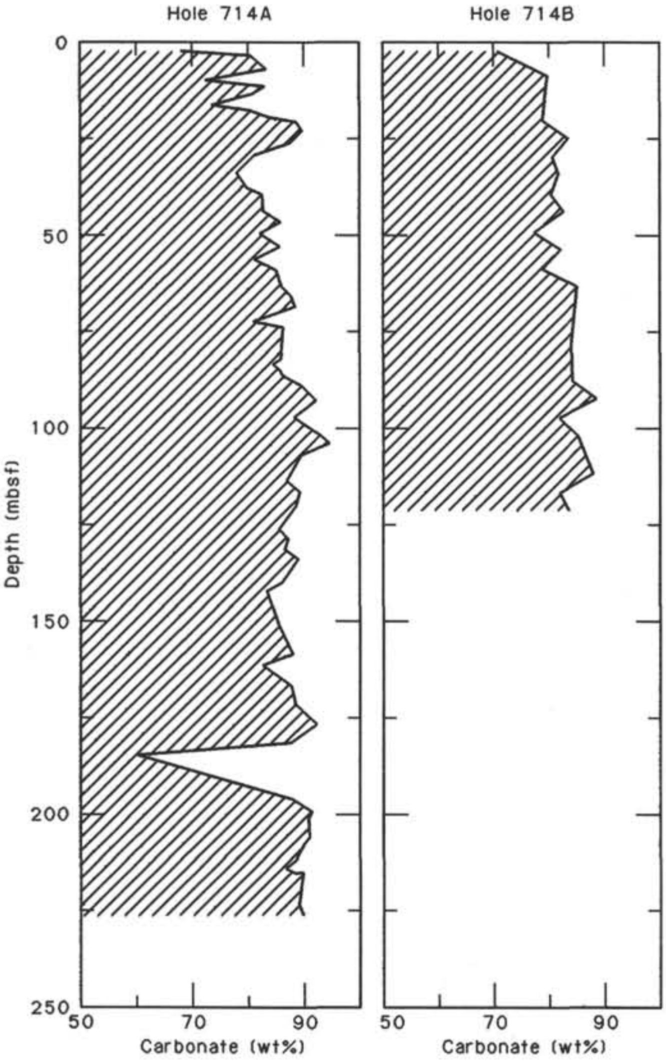

Figure 16. Carbonate content of samples for which the index properties were measured at Site 714.

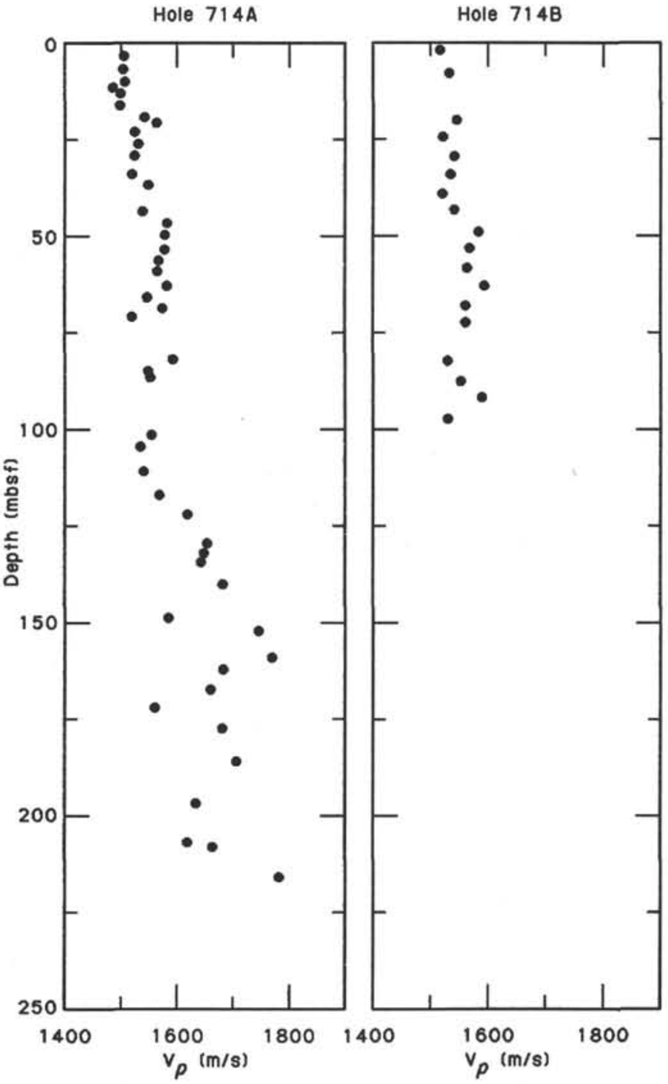

Figure 17. Compressional-wave velocities measured from discrete samples at Site 714.

Table 9. Compressional-wave velocity and acoustic impedance data, Site 714.

Section interval (cm)	Depth (mbsf)	V_p (m/s)	Impedance ($g/cm^2 \cdot s \cdot 10^4$)
115-714A-			
2H-1, 60	3.40	1507	24.41
2H-3, 100	6.80	1505	23.93
2H-5, 100	9.80	1508	23.22
2H-6, 100	11.30	1485	24.06
3H-1, 60	13.00	1500	24.00
3H-3, 60	16.00	1499	23.08
3H-5, 60	19.00	1541	22.62
3H-6, 60	20.50	1562	24.36
4H-2, 60	22.78	1524	24.08
4H-4, 86	25.99	1532	24.06
4H-6, 88	29.01	1525	24.40
5H-2, 60	33.80	1521	23.72
5H-4, 60	36.80	1549	24.32
6H-2, 60	43.50	1539	25.24
6H-4, 60	46.50	1582	26.58
6H-6, 60	49.50	1579	26.05
7H-2, 60	53.10	1578	25.72
7H-4, 60	56.10	1568	24.30
7H-6, 56	59.06	1565	26.13
8H-2, 60	62.70	1582	25.31
8H-4, 60	65.70	1548	22.91
8H-6, 60	68.70	1574	26.92
9H-1, 60	70.80	1521	24.79
10H-2, 60	81.90	1593	27.56
10H-4, 60	84.90	1549	26.03
10H-5, 60	86.40	1552	27.94
12H-2, 60	101.20	1554	26.11
12H-4, 61	104.21	1535	26.25
13H-2, 58	110.78	1541	26.04
13H-6, 65	116.85	1569	26.04
14X-3, 54	121.94	1618	26.68
15X-2, 100	129.30	1654	27.62
15X-4, 26	131.56	1649	28.03
15X-6, 22	134.19	1642	27.91
16X-3, 58	139.98	1681	27.95
17X-2, 92	148.52	1584	25.34
17X-4, 148	152.08	1744	30.34
18X-3, 8	158.78	1767	29.86
18X-5, 12	161.82	1682	29.10
19X-2, 50	167.30	1660	29.55
19X-5, 56	171.86	1559	27.75
20X-2, 60	177.10	1680	29.90
21X, CC, 2	185.49	1705	31.20
22X-2, 60	196.50	1633	27.11
23X-2, 63	206.23	1619	29.47
23X-3, 63	207.73	1663	30.43
24X, CC, 21	215.51	1779	34.69
24X, CC, 23	215.53	4787	133.50
115-714B-			
1H-2, 60	2.10	1516	22.59
1H-6, 60	8.10	1532	24.51
3H-3, 60	20.00	1544	23.47
3H-6, 60	24.50	1520	24.17
4H-3, 60	29.60	1539	23.24
4H-6, 60	34.10	1533	25.60
5H-3, 60	39.30	1520	24.17
5H-6, 32	43.52	1540	24.79
6H-3, 60	49.00	1584	25.66
6H-6, 60	53.50	1567	25.23
7H-3, 60	58.60	1563	24.22
7H-6, 60	63.10	1594	26.30
8H-3, 60	68.20	1560	25.74
8H-6, 60	72.70	1560	25.58
9H-6, 64	82.44	1529	24.92
10H-3, 85	87.75	1551	24.82
10H-6, 67	92.07	1589	26.38
11H-3, 68	97.28	1529	24.31

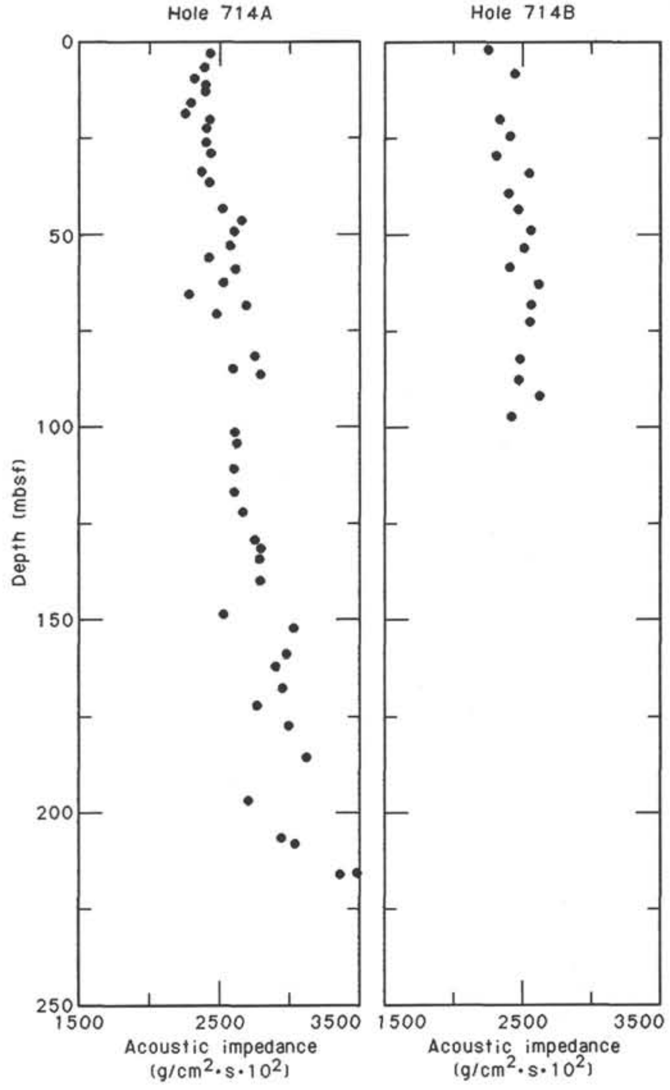

Figure 18. Acoustic impedance calculated from wet-bulk density and compressional-wave velocity of discrete samples at Site 714.

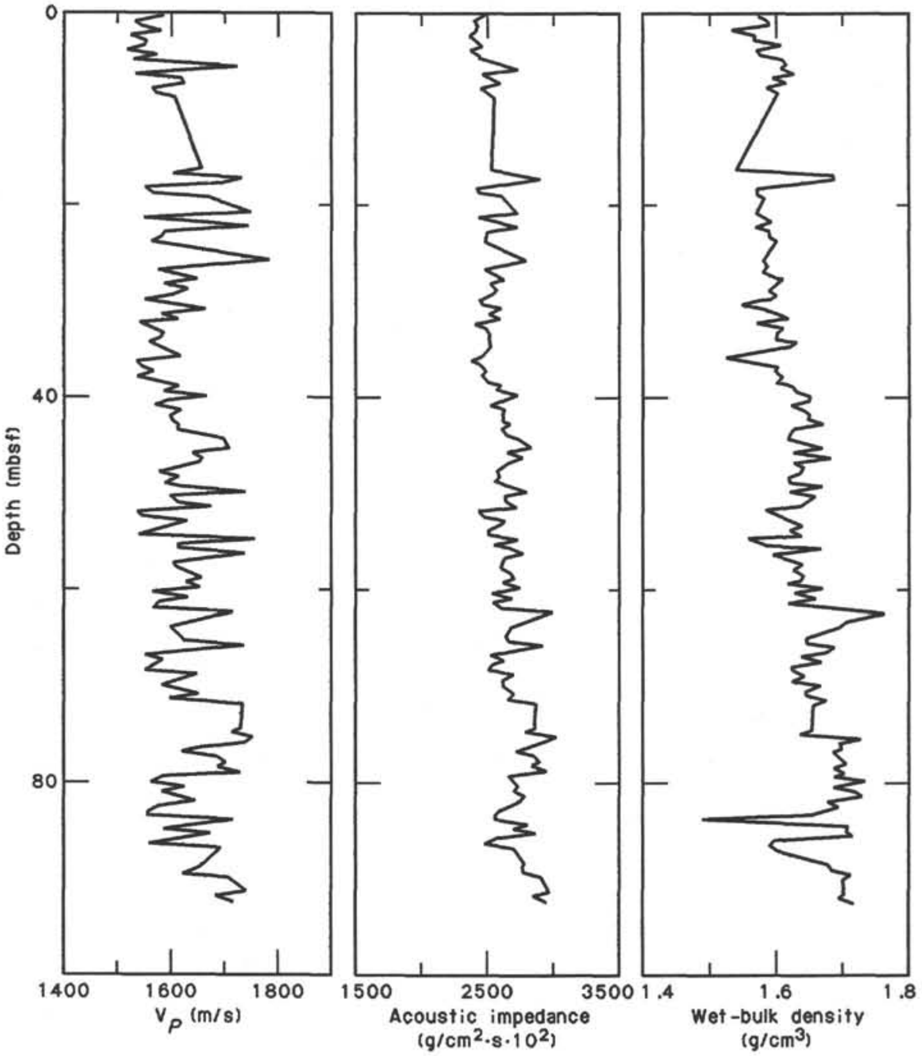

Figure 19. Continuous *P*-wave logger, computed acoustic impedance, and GRAPE wet-bulk density records for Hole 714B.

Table 10. Shear-wave velocity data, Hole 714A.

Section interval (cm)	Depth (mbsf)	V_s (m/s)
115-714A-		
1H-2, 69	2.19	69
2H-2, 90	5.20	36
2H-4, 89	8.19	43
2H-6, 49	10.79	41
3H-2, 61	14.51	48
3H-4, 60	17.50	60
4H-5, 47	27.10	84
4H-7, 58	30.21	102
5H-6, 52	39.72	90
6H-2, 53	43.43	74
6H-4, 48	46.38	84
6H-6, 52	49.42	93
7H-2, 43	52.93	131
7H-4, 46	55.96	78
7H-6, 48	58.98	91
8H-2, 50	62.60	75
8H-4, 50	65.60	201
8H-6, 54	68.64	139
9H-1, 50	70.70	115
9H-3, 53	73.73	203
10H-2, 49	81.79	94
10H-4, 52	84.82	154
10H-3, 51	83.31	173

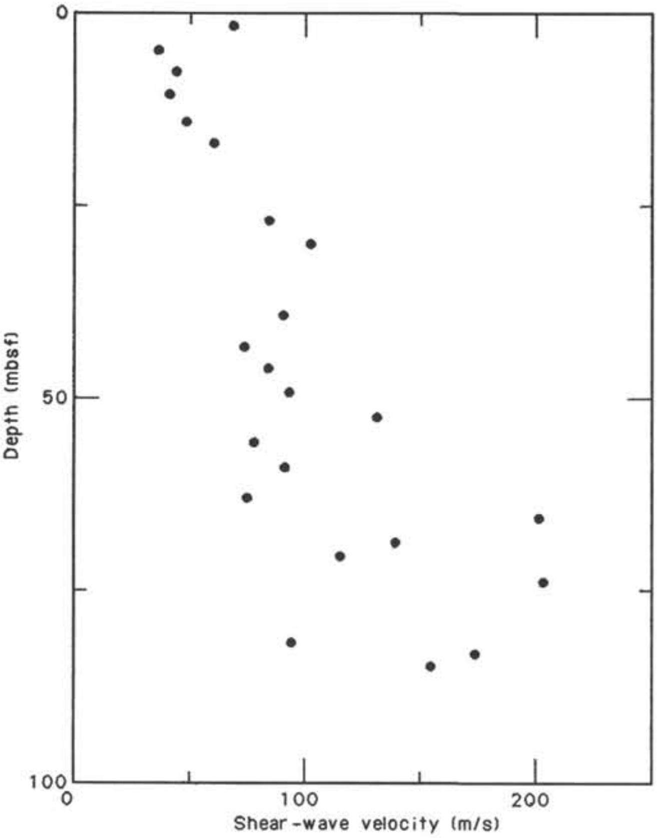

Figure 20. Shear-wave velocity at Hole 714A.

Table 11. Motorized shear strength data, Site 714.

Section interval (cm)	Depth (mbsf)	Peak (kPa)
115-714A-		
2H-2, 102	5.32	4.7
2H-4, 96	8.26	2.3
2H-6, 61	10.91	5.2
3H-2, 80	14.70	4.1
3H-4, 20	17.10	6.4
3H-6, 93	20.83	12.2
4H-3, 64	24.27	10.5
4H-5, 62	27.25	17.5
4H-7, 63	30.26	16.9
5H-2, 56	33.76	16.3
5H-4, 67	36.87	19.8
5H-6, 57	39.77	20.9
6H-2, 56	43.46	11.1
6H-4, 58	46.48	2.9
6H-6, 54	49.44	27.9
7H-2, 56	53.06	14.0
7H-2, 66	53.16	23.3
7H-4, 60	56.10	20.9
8H-2, 57	62.67	12.3
8H-4, 60	65.70	35.5
8H-6, 59	68.69	38.4
9H-1, 66	70.86	20.4
9H-2, 66	72.36	11.1
9H-3, 66	73.86	19.2
10H-6, 63	87.93	26.8
10H-4, 59	84.89	18.6
10H-2, 59	81.89	21.5
11H-6, 45	97.45	40.7
11H-3, 54	93.04	29.7
11H-3, 60	93.10	30.3
12H-2, 54	101.14	39.6
12H-4, 57	104.17	33.7
12H-6, 59	107.19	69.8
13H-2, 47	110.67	42.5
13H-4, 55	113.75	33.7
13H-4, 61	113.81	42.5
13H-6, 54	116.74	64.0
14X-2, 57	120.47	44.8
115-714B-		
1H-2, 84	2.34	3.5
1H-6, 84	8.34	3.5
3H-1, 128	17.68	23.3
3H-1, 140	17.80	14.0
3H-4, 86	21.76	13.4
4H-2, 68	28.18	18.6
4H-6, 68	34.18	17.8
5H-3, 68	39.38	11.6
5H-5, 68	42.38	11.9
6H-3, 72	49.12	11.1
6H-6, 72	53.62	28.2
7H-3, 73	58.73	9.3
7H-6, 72	63.22	25.0
8H-3, 72	68.32	22.7
8H-6, 72	72.82	32.6
9H-3, 67	77.97	37.2
9H-6, 71	82.51	27.3
10H-3, 82	87.72	160.0
10H-6, 63	92.03	26.8
11H-3, 73	97.33	36.7
11H-6, 72	101.82	51.8
12H-3, 66	106.86	39.6
12H-6, 68	111.38	42.5
12H-6, 72	111.42	21.5
13H-4, 71	118.11	46.0
13H-6, 94	121.34	35.2

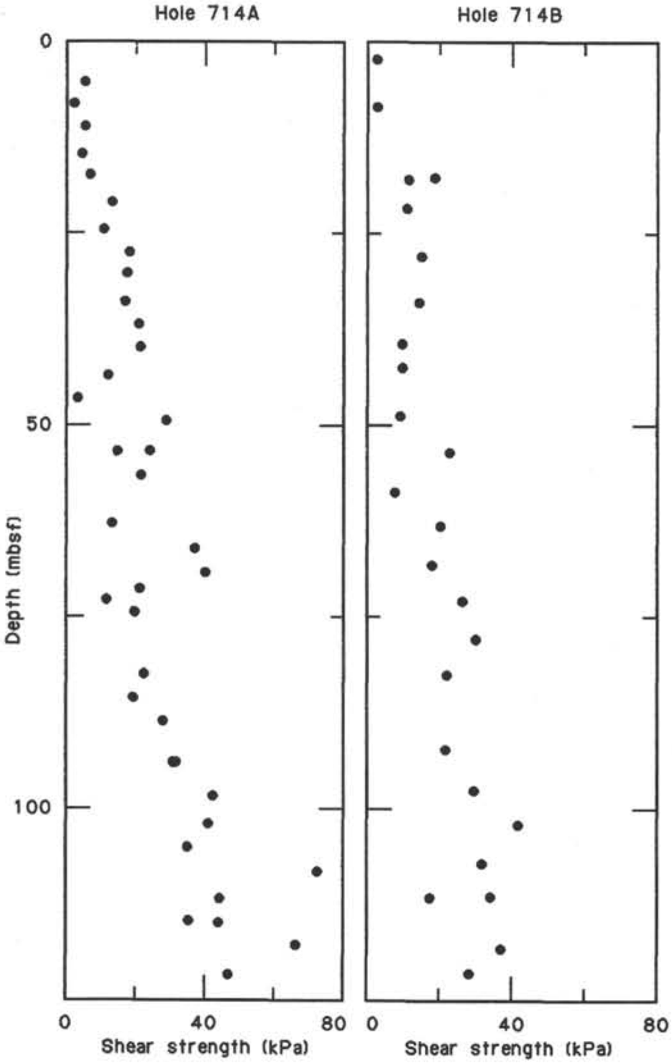

Figure 21. Shear strength at Site 714.

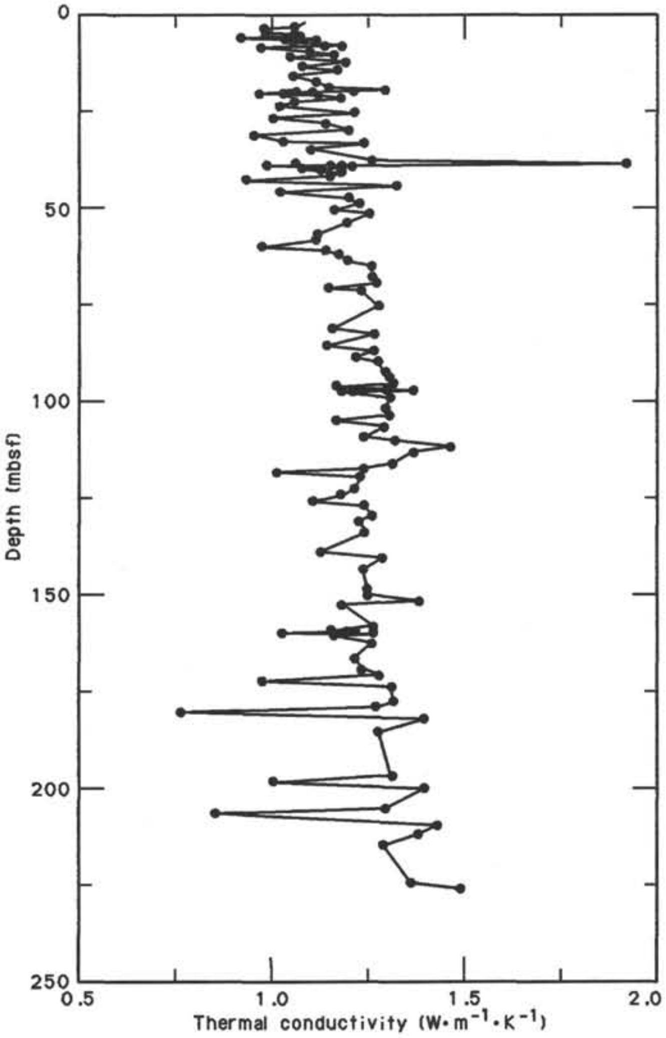

Figure 22. Thermal conductivity at Hole 714A.

Table 12. Thermal conductivity data, Site 714.

Section interval (cm)	Depth (mbsf)	Thermal conductivity $(W \cdot m^{-1} \cdot K^{-1})$
115-714A-		
2H-1, 100	3.80	1.057
2H-2, 80	5.10	1.030
2H-3, 100	6.80	1.173
2H-4, 80	8.10	1.093
2H-5, 80	9.60	1.045
2H-6, 80	11.10	1.182
2H-7, 35	12.15	1.076
3H-1, 80	13.20	1.163
3H-2, 80	14.70	1.051
3H-3, 80	16.20	1.111
3H-4, 80	17.70	1.144
3H-5, 10	18.50	1.284
3H-5, 20	18.60	1.209
3H-5, 30	18.70	1.059
3H-5, 40	18.80	1.098
3H-5, 60	19.00	1.039
3H-5, 70	19.10	1.023
3H-5, 80	19.20	1.037
3H-5, 90	19.30	1.111
3H-5, 100	19.40	0.964
3H-5, 110	19.50	1.054
3H-5, 120	19.60	1.050
3H-5, 130	19.70	1.071
3H-5, 140	19.80	1.117
3H-6, 80	20.70	1.173
3H-7, 18	21.58	1.050
4H-2, 80	22.98	1.017
4H-3, 80	24.43	1.202
4H-4, 80	25.93	1.000
4H-5, 80	27.43	1.136
4H-6, 80	28.93	1.192
4H-7, 80	30.43	0.956
4H-8, 80	31.93	1.027
5H-1, 80	32.50	1.232
5H-2, 80	34.00	1.096
5H-4, 80	37.00	1.253
5H-5, 10	37.80	1.910
5H-5, 20	37.90	1.057
5H-5, 30	38.00	1.130
5H-5, 40	38.10	1.149
5H-5, 50	38.20	0.988
5H-5, 60	38.30	1.182
5H-5, 70	38.40	1.166
5H-5, 80	38.50	1.196
5H-5, 90	38.60	1.159
5H-5, 100	38.70	1.124
5H-5, 120	38.90	1.077
5H-5, 130	39.00	1.127
5H-5, 140	39.10	1.120
5H-6, 80	40.00	1.174
5H-7, 25	40.95	1.146
6H-1, 80	42.20	0.933
6H-2, 80	43.70	1.315
6H-3, 80	45.20	1.020
6H-4, 80	46.70	1.193
6H-5, 80	48.20	1.217
6H-6, 80	49.70	1.158
6H-7, 40	50.80	1.247
7H-2, 80	53.30	1.189
7H-4, 80	56.30	1.113
7H-5, 80	57.80	1.108
7H-6, 80	59.30	0.974
7H-7, 40	60.40	1.134
8H-1, 80	61.40	1.168
8H-2, 80	62.90	1.192
8H-3, 80	64.40	1.253
8H-5, 80	67.40	1.254
8H-6, 80	68.90	1.260
8H-7, 40	70.00	1.145
9H-1, 80	71.00	1.224
9H-4, 18	74.88	1.268
10H-1, 80	80.60	1.155
10H-2, 80	82.10	1.257
10H-4, 80	85.10	1.138
10H-5, 80	86.60	1.256
10H-6, 80	88.10	1.212
10H-7, 40	89.20	1.267
11H-2, 80	91.80	1.288
11H-3, 80	93.30	1.298
11H-4, 80	94.80	1.306
11H-5, 10	95.60	1.166
11H-5, 20	95.70	1.237
11H-5, 30	95.80	1.279
11H-5, 40	95.90	1.314
11H-5, 60	96.10	1.277
11H-5, 70	96.20	1.246
11H-5, 80	96.30	1.200
11H-5, 90	96.40	1.292
11H-5, 100	96.50	1.360
11H-5, 120	96.70	1.231
11H-5, 130	96.80	1.202
11H-5, 140	96.90	1.180
11H-7, 15	98.65	1.301
12H-2, 80	101.40	1.292
12H-3, 80	102.90	1.297
12H-4, 80	104.40	1.162
12H-5, 80	105.90	1.287
12H-7, 40	108.50	1.237
13H-1, 80	109.50	1.314
13H-2, 80	111.00	1.457
13H-3, 80	112.50	1.360
13H-5, 80	115.50	1.308
13H-6, 80	117.00	1.232
13H-7, 40	118.10	1.013
14X-1, 80	119.20	1.225
14X-3, 80	122.20	1.208
14X-4, 80	123.70	1.177
14X-5, 95	125.35	1.104
14X-6, 80	126.70	1.233
15X-2, 80	129.10	1.254
15X-3, 80	130.60	1.223
15X-5, 80	133.60	1.239
16X-2, 80	138.70	1.126
16X-3, 80	140.20	1.282
16X-5, 80	143.20	1.231
17X-2, 80	148.40	1.244
17X-3, 80	149.90	1.247
17X-4, 80	151.40	1.376
17X-5, 30	152.40	1.179
18X-2, 80	158.00	1.257
18X-3, 10	158.80	1.154
18X-3, 40	159.10	1.192
18X-3, 60	159.30	1.214
18X-3, 70	159.40	1.255
18X-3, 80	159.50	1.264
18X-3, 90	159.60	1.025
18X-3, 100	159.70	1.243
18X-3, 120	159.90	1.185
18X-3, 130	160.00	1.162
18X-5, 50	162.20	1.257
19X-1, 80	166.10	1.208
19X-3, 80	169.10	1.232
19X-4, 80	170.60	1.276
19X-5, 80	172.10	0.978
19X-6, 80	173.60	1.306
20X-2, 80	177.30	1.315
20X-3, 80	178.80	1.266
20X-4, 80	180.30	0.770
20X-5, 80	181.80	1.393
21X-1, 56	185.26	1.275
22X-2, 80	196.70	1.309
22X-3, 80	198.20	1.009
22X-4, 80	199.70	1.391
23X-1, 80	204.90	1.290
23X-2, 80	206.40	0.861
23X-4, 80	209.40	1.426
23X-6, 14	211.74	1.375
24X-1, 80	214.60	1.288
25X-1, 80	224.10	1.361
25X-2, 80	225.60	1.482
115-715B-		
1H-1, 80	0.80	1.082
1H-2, 40	1.90	1.052
1H-2, 80	2.30	0.979
1H-3, 40	3.40	0.985
1H-3, 120	4.20	1.070
1H-4, 40	4.90	0.917
1H-4, 80	5.30	1.108
1H-4, 120	5.70	1.052
1H-5, 80	6.80	1.132
1H-5, 120	7.20	0.974
1H-7, 20	9.20	1.152

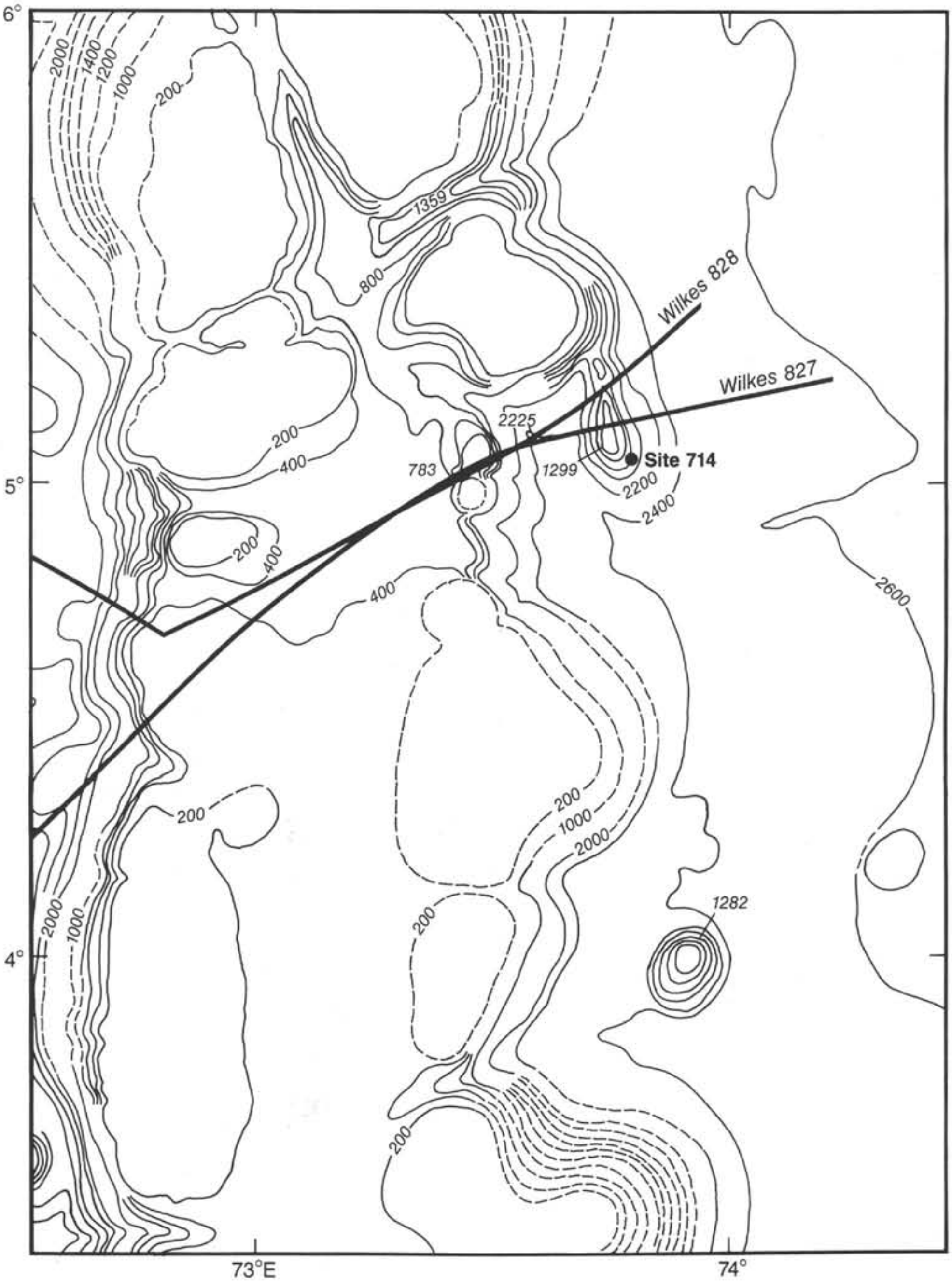

Figure 23. Bathymetry in the region of Site 714, eastern margin of the Maldives Ridge (after unpublished data from NAVOCEANO, U.S. Navy surveys).

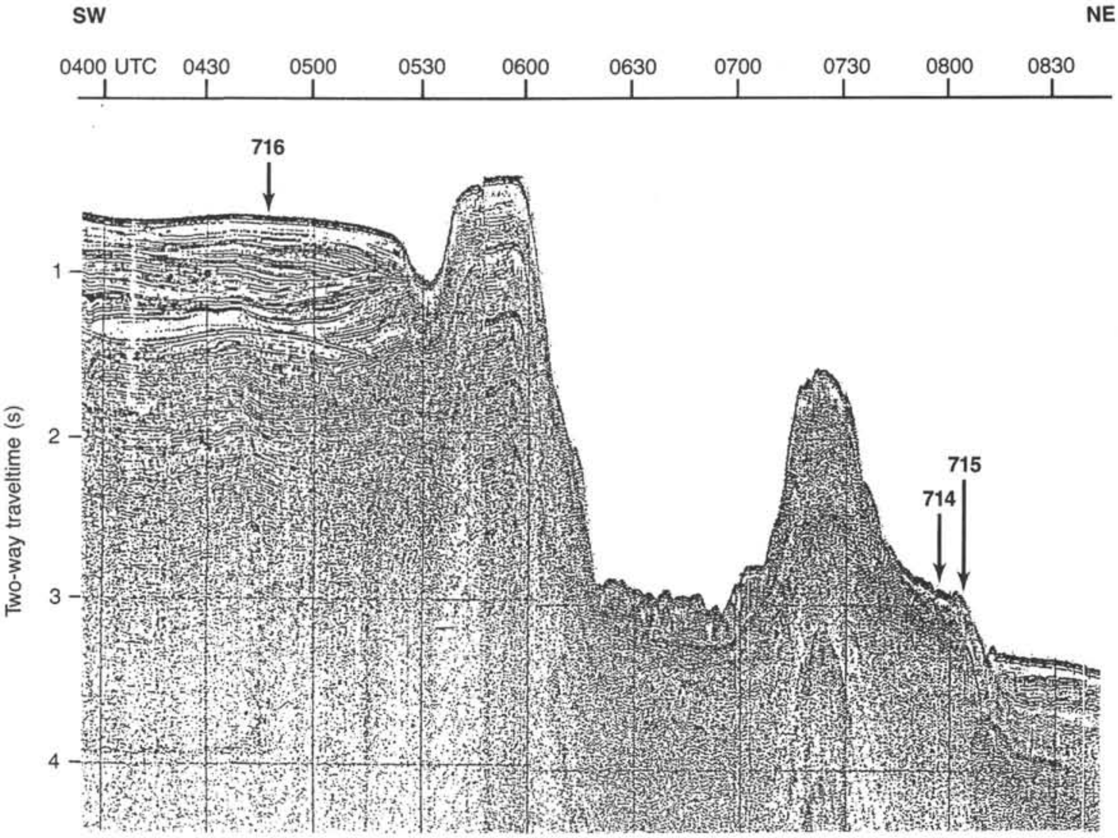

Figure 24. Wilkes 827 (17 September 1976) single-channel seismic (SCS) reflection line near Site 714. A narrow ridge effectively protects the site from turbidites flowing down from carbonate banks to the west.

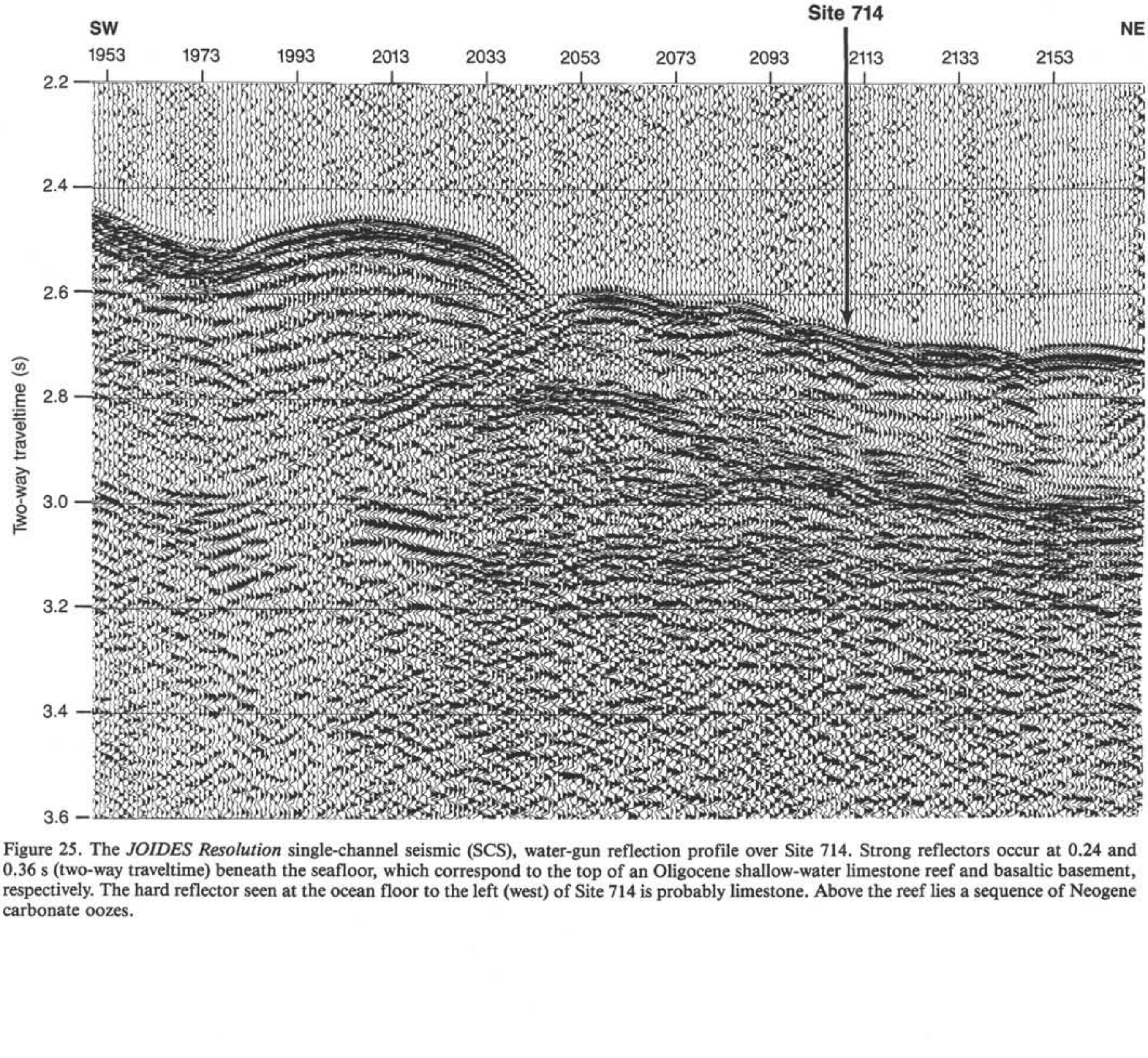

Figure 25. The *JOIDES Resolution* single-channel seismic (SCS), water-gun reflection profile over Site 714. Strong reflectors occur at 0.24 and 0.36 s (two-way traveltime) beneath the seafloor, which correspond to the top of an Oligocene shallow-water limestone reef and basaltic basement, respectively. The hard reflector seen at the ocean floor to the left (west) of Site 714 is probably limestone. Above the reef lies a sequence of Neogene carbonate oozes.

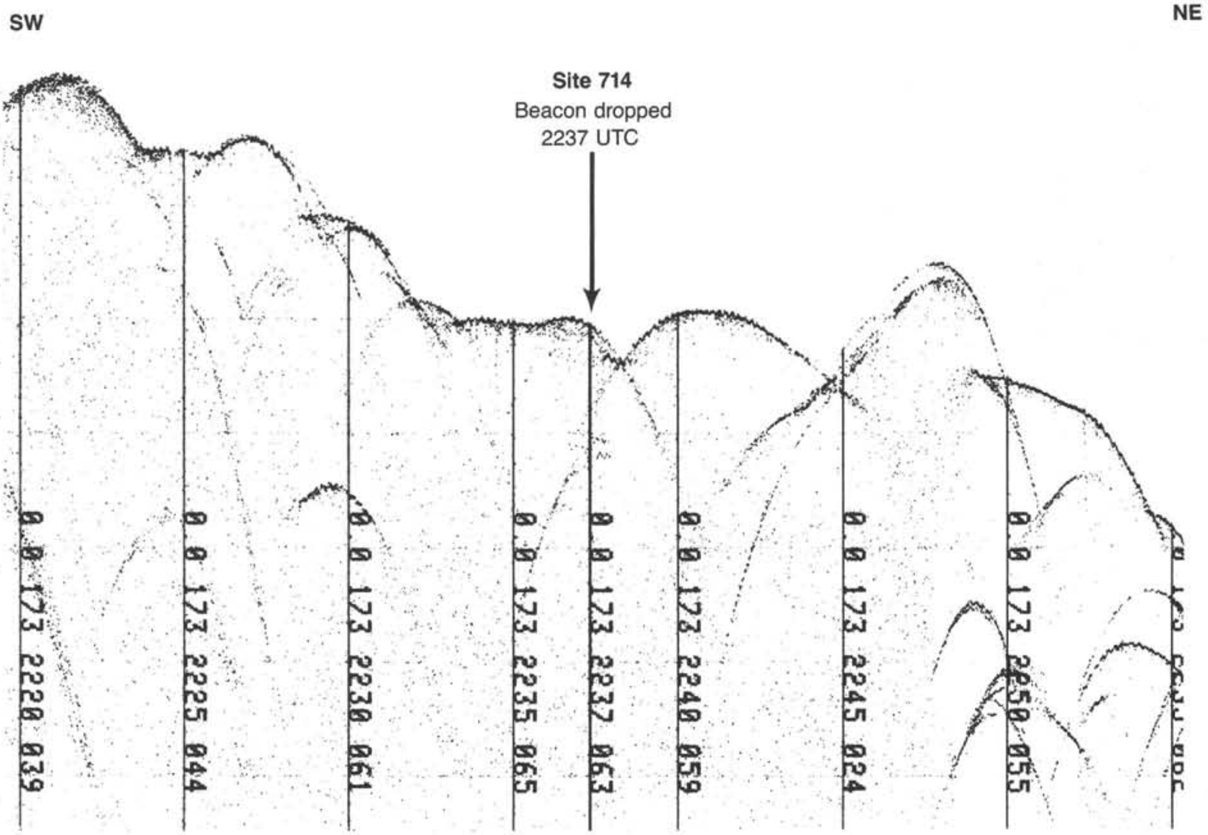

Figure 26. The *JOIDES Resolution* 12-kHz profile over Site 714. This site is located in a small basin bounded by sediment hills (slump structures?). See Figure 20 in "Underway Geophysics" chapter, this volume, for location of Site 714 track line.

SITE 714 HOLE A CORE 1H CORED INTERVAL 2031.5-2034.3 mbsl; 0-2.8 mbsf

TIME-ROCK UNIT	BIOSTRAT. ZONE/ FOSSIL CHARACTER					PALEOMAGNETICS	PHYS. PROPERTIES	CHEMISTRY
	FORAMINIFERS	NANNOFOSSILS	RADIOLARIANS	DIATOMS				
UPPER PLEISTOCENE	N 22	CN 15 (NN 21)	*B. invaginata*	TRACE				
	AG	AG	CG					

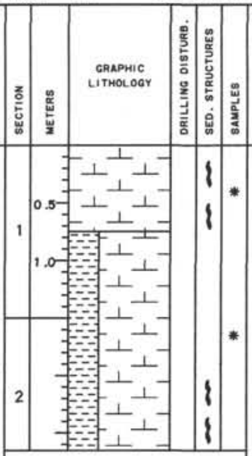

LITHOLOGIC DESCRIPTION

FORAMINIFER-BEARING CLAY-BEARING NANNOFOSSIL OOZE and FORAMINIFER-BEARING CLAYEY NANNOFOSSIL OOZE

Major lithologies: Foraminifer-bearing clay-bearing nannofossil ooze and foraminifer-bearing clayey nannofossil ooze, slightly burrow-mottled, alternating colors of dark gray (5GY 4/1) and gray (5G 5/1); color changes are gradational due to bioturbation; lighter layers appear finer grained than darker layers; oxidized, yellowish brown (10YR 5/4) interval in Section 1, 0-7 cm.

SMEAR SLIDE SUMMARY (%):

	1, 40 D	2, 17 D
TEXTURE:		
Sand	20	25
Silt	20	20
Clay	60	55
COMPOSITION:		
Quartz	3	2
Mica	—	Tr
Clay	15	20
Volcanic glass	2	1
Accessory minerals:		
Aragonite needles	5	1
Foraminifers	15	25
Nannofossils	49	48
Diatoms	1	—
Radiolarians	5	1
Sponge spicules	5	1
Fish remains	Tr	1

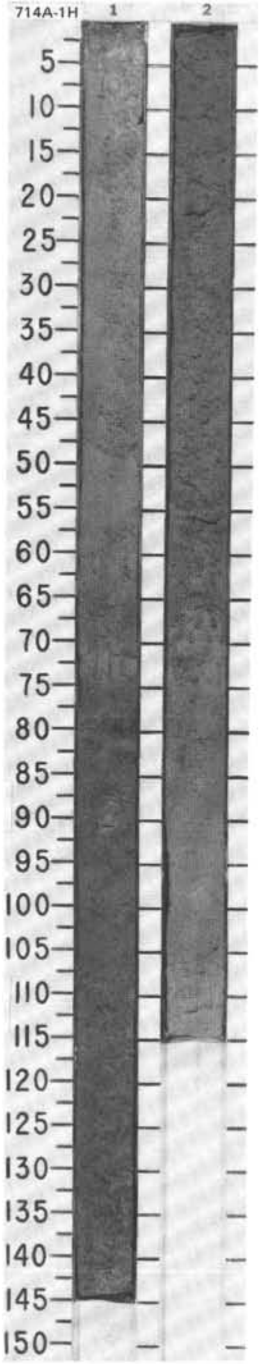

SITE 714 HOLE A CORE 2H CORED INTERVAL 2034.3-2043.9 mbsl; 2.8-12.4 mbsf

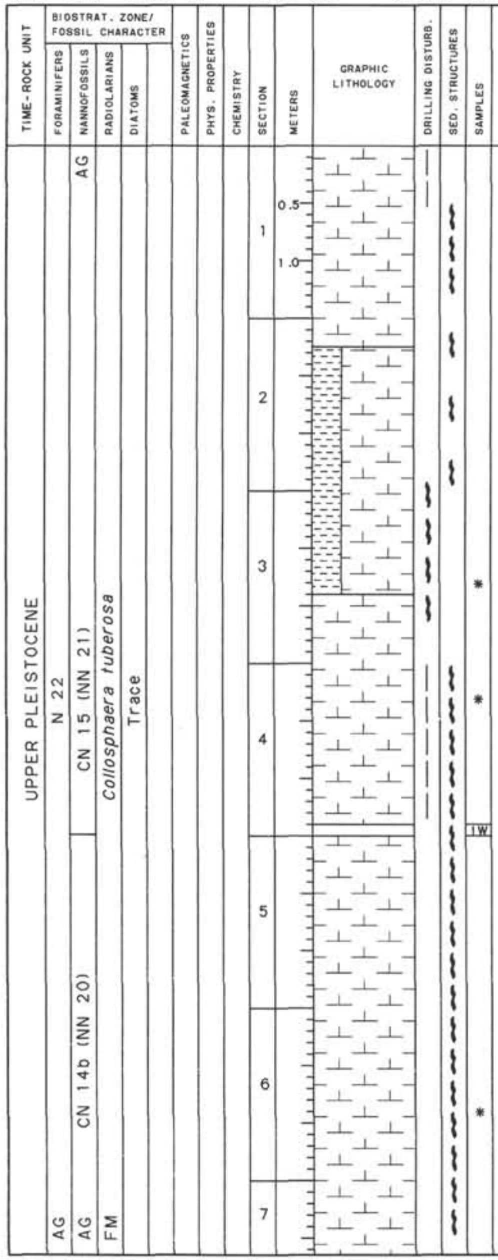

LITHOLOGIC DESCRIPTION

FORAMINIFER-BEARING CLAY-BEARING NANNOFOSSIL OOZE and FORAMINIFER-BEARING CLAYEY NANNOFOSSIL OOZE

Major lithologies: Foraminifer-bearing clay-bearing nannofossil ooze and foraminifer-bearing clayey nannofossil ooze, burrow-mottled, greenish gray (5GY 5/1), gray (5Y 5/1), and olive (10Y 5/2), alternating with greenish gray (5GY 6/1) and light gray (5Y 6/1); intermittent pyrite staining throughout core.

Minor lithology: Clay-bearing nannofossil ooze, mildly burrow-mottled, greenish gray (5GY 5/1, 6/1).

SMEAR SLIDE SUMMARY (%):

	3, 75 D	4, 36 M	6, 100 D
TEXTURE:			
Sand	20	10	10
Silt	15	15	20
Clay	65	75	70
COMPOSITION:			
Quartz	3	Tr	2
Feldspar	Tr	—	Tr
Mica	Tr	—	Tr
Clay	20	25	10
Volcanic glass	1	Tr	—
Dolomite	—	Tr	—
Accessory minerals:			
Aragonite needles	1	—	Tr
Pyrite	Tr	1	—
Foraminifers	20	12	8
Nannofossils	51	57	69
Diatoms	—	Tr	—
Radiolarians	1	2	7
Sponge spicules	2	2	4
Silicoflagellates	—	—	Tr
Fish remains	1	1	Tr
Mollusk debris	Tr	—	—

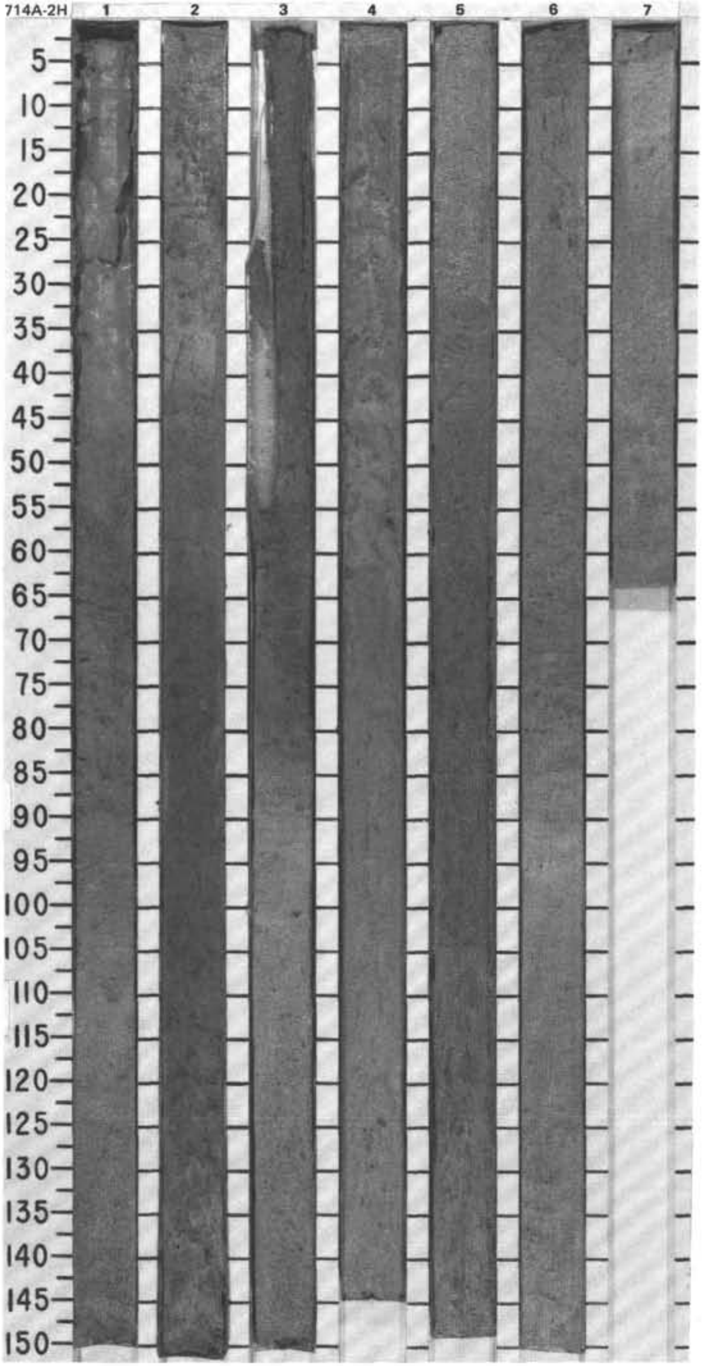

SITE 714 HOLE A CORE 3H CORED INTERVAL 2043.9-2053.5 mbsl; 12.4-22.0 mbsf

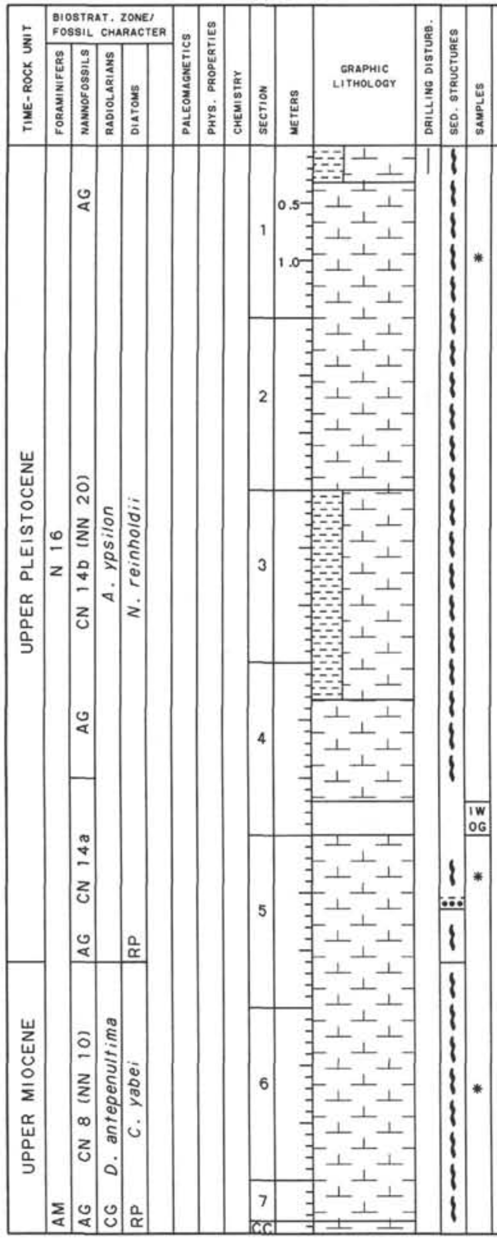

LITHOLOGIC DESCRIPTION

FORAMINIFER-BEARING CLAY-BEARING NANNOFOSSIL OOZE and FORAMINIFER-BEARING CLAYEY NANNOFOSSIL OOZE

Major lithologies: Foraminifer-bearing clay-bearing nannofossil ooze and foraminifer-bearing clayey nannofossil ooze, greenish gray (5GY 5/1, 6/1) changing to light brownish gray (2.5 Y 6/2), light gray (5G 7/1), and very light gray (5G 8/1); intermittent pyrite staining throughout core; two thin horizons of light greenish gray (5G 7/1) in Section 6.

Minor lithology: Clay-bearing foraminifer-nannofossil ooze, turbidite, greenish gray (5GY 6/1), in Section 5, 65–67 cm.

Very sharp color change from greenish gray (5GY 5/1) to light brownish gray (2.5 6/2), at Section 5, 114 cm, unconformity separating Pleistocene sediments above from Miocene sediments below.

SMEAR SLIDE SUMMARY (%):

	1, 80 D	5, 30 D	6, 80 D
TEXTURE:			
Sand	15	15	12
Silt	10	10	8
Clay	70	70	80
COMPOSITION:			
Quartz	3	Tr	1
Mica	Tr	—	—
Clay	20	5	5
Volcanic glass	Tr	Tr	Tr
Dolomite	Tr	Tr	Tr
Accessory minerals:			
Aragonite needles	Tr	Tr	Tr
Pyrite	1	—	—
Foraminifers	12	12	12
Nannofossils	60	78	74
Diatoms	—	—	1
Radiolarians	2	2	3
Sponge spicules	3	3	4
Fish remains	Tr	Tr	—

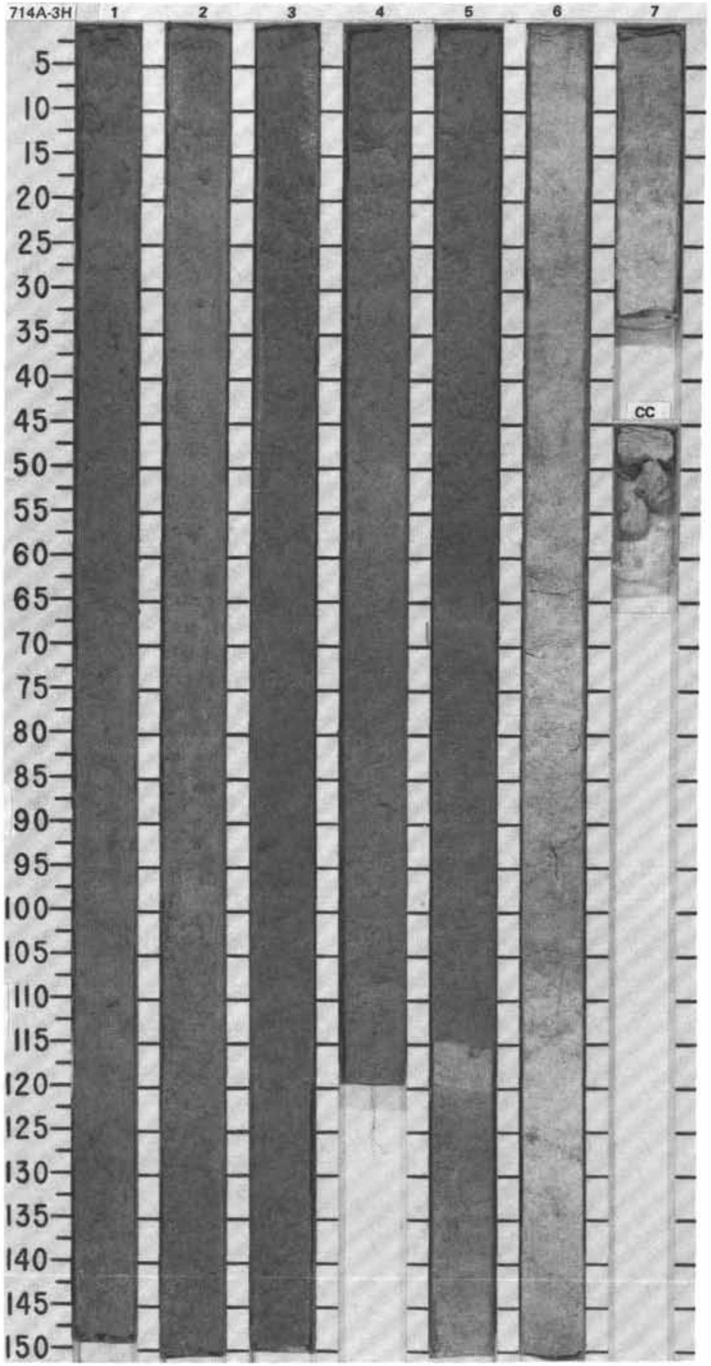

SITE 714 HOLE A CORE 4H CORED INTERVAL 2053.5-2063.2 mbsl; 22.0-31.7 mbsf

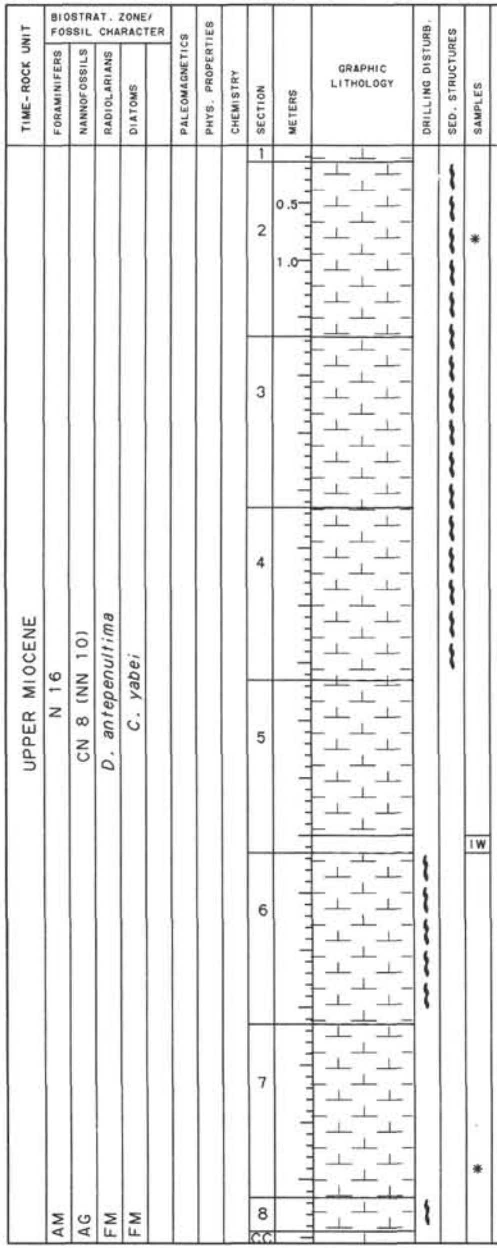

LITHOLOGIC DESCRIPTION

FORAMINIFER-BEARING CLAY-BEARING NANNOFOSSIL OOZE

Major lithology: Foraminifer-bearing clay-bearing nannofossil ooze, mildly burrow-mottled, with alternating intervals of light greenish gray (5GY 7/1) and light gray (5Y 7/1); mild pyrite staining throughout the core.

Minor lithology: Sponge spicule-bearing foraminifer-bearing clay-bearing nannofossil ooze, light brownish gray (2.5Y 6/2), in distinct layer at Section 7, 115-135 cm.

SMEAR SLIDE SUMMARY (%):

	2, 80 D	7. 124 M
TEXTURE:		
Sand	20	20
Silt	10	20
Clay	70	60
COMPOSITION:		
Quartz	—	Tr
Clay	5	5
Volcanic glass	—	Tr
Dolomite	Tr	—
Foraminifers	15	13
Nannofossils	67	60
Diatoms	Tr	—
Radiolarians	7	5
Sponge spicules	6	10
Fish remains	Tr	7
Aragonite	Tr	—

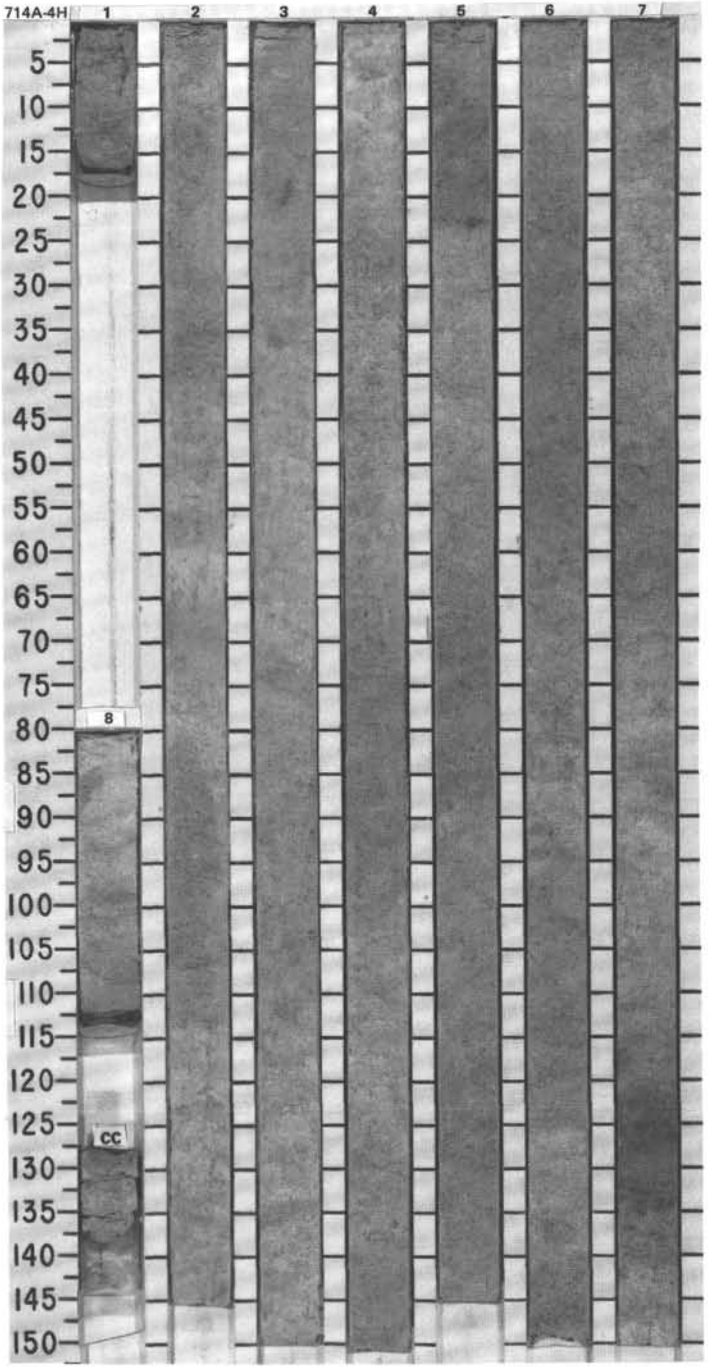

SITE 714 HOLE A CORE 5H CORED INTERVAL 2063.2-2072.9 mbsl; 31.7-41.4 mbsf

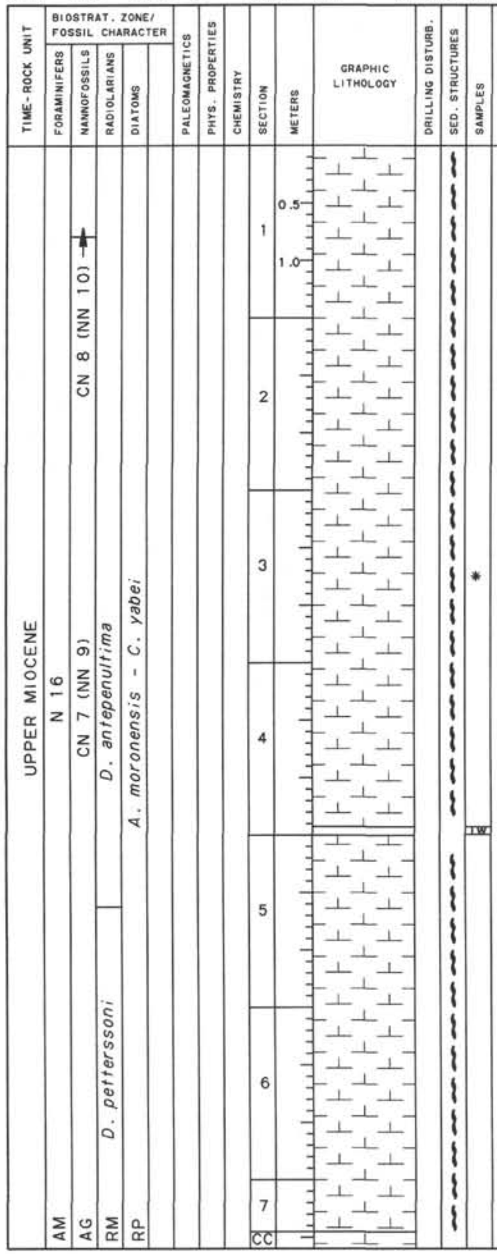

LITHOLOGIC DESCRIPTION

FORAMINIFER-BEARING CLAY-BEARING NANNOFOSSIL OOZE

Major lithology: Foraminifer-bearing clay-bearing nannofossil ooze, burrow-mottled, including a number of long (up to 15 cm) vertical burrows, light greenish gray (5GY 7/1) colors alternate with light gray (5Y 7/1) in distinct layers; mildly pyrite-stained, hydrogen sulfide odor detectable over freshly cut sections.

SMEAR SLIDE SUMMARY (%):

	3, 80 D
TEXTURE:	
Sand	15
Silt	15
Clay	70
COMPOSITION:	
Quartz	Tr
Mica	Tr
Clay	5
Volcanic glass	Tr
Accessory minerals:	
Pyrite	Tr
Foraminifers	10
Nannofossils	73
Diatoms	Tr
Radiolarians	5
Sponge spicules	6
Fish remains	1

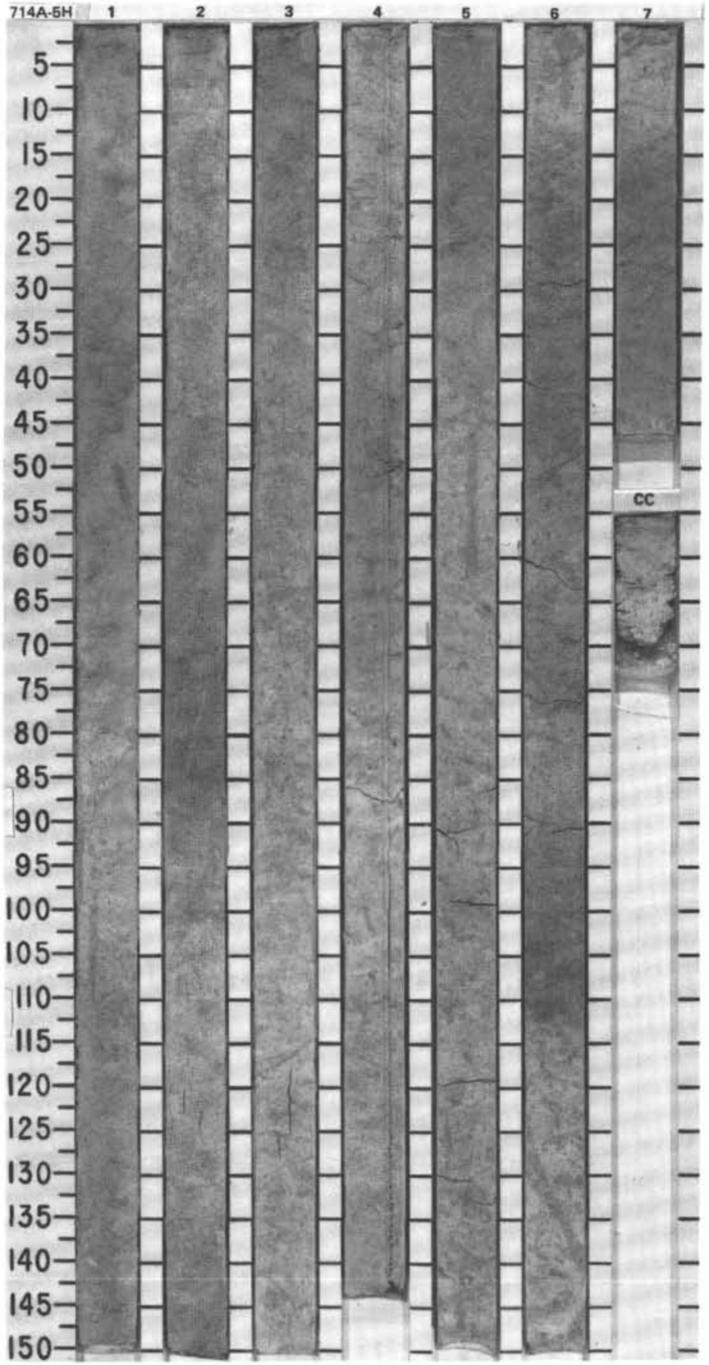

SITE 714 HOLE A CORE 6H CORED INTERVAL 2072.9-2082.5 mbsl; 41.4-51.0 mbsf

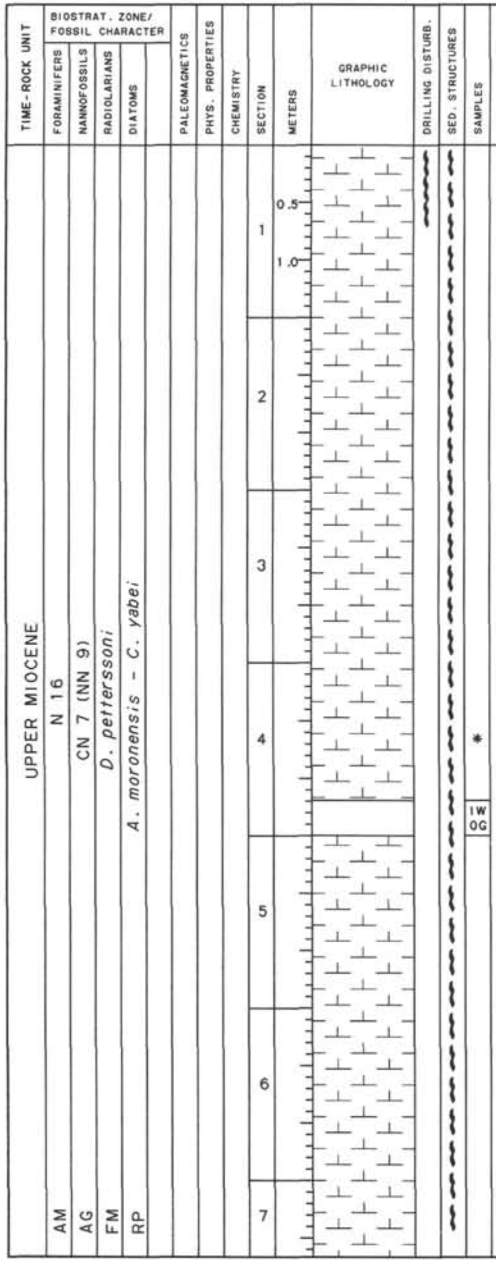

LITHOLOGIC DESCRIPTION

FORAMINIFER-BEARING CLAY-BEARING NANNOFOSSIL OOZE

Major lithology: Foraminifer-bearing clay-bearing nannofossil ooze, light greenish gray (5GY 7/1) colors alternate with light gray (5Y 7/1), mildly pyrite-stained, hydrogen sulfide odor detectable over freshly cut sections, drilling disturbance at top of Section 1.

Minor lithology: Foraminifer-bearing clayey nannofossil ooze, burrow-mottled; light gray (5Y 7/1), three small intervals (near Section 2, 100 cm; Section 3, 100 cm; and Section 4, 100 cm) grade to major lithology above and below.

SMEAR SLIDE SUMMARY (%):

	4, 60 D
TEXTURE:	
Sand	20
Silt	20
Clay	60
COMPOSITION:	
Quartz	Tr
Clay	8
Volcanic glass	Tr
Cement	Tr
Foraminifers	15
Nannofossils	62
Diatoms	1
Radiolarians	5
Sponge spicules	8
Silicoflagellates	Tr
Fish remains	1

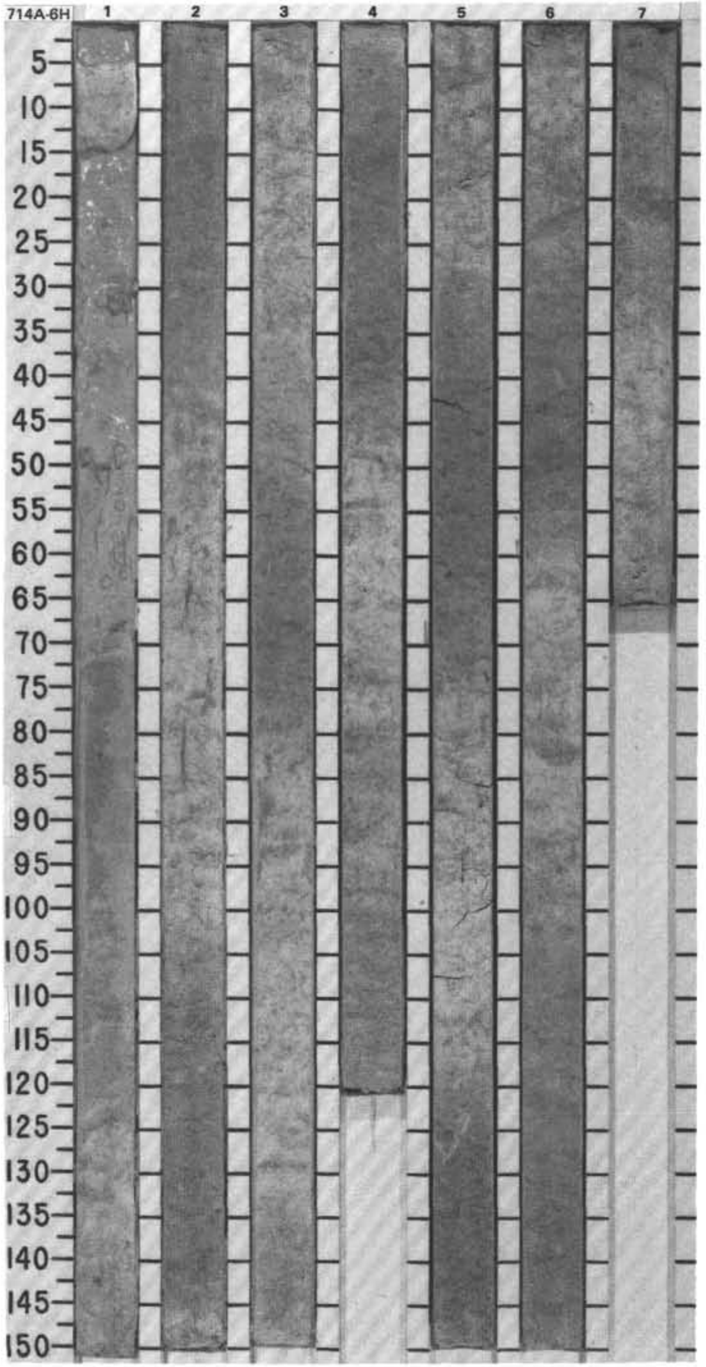

SITE 714 HOLE A CORE 7H CORED INTERVAL 2082.5-2092.1 mbsl; 51.0-60.6 mbsf

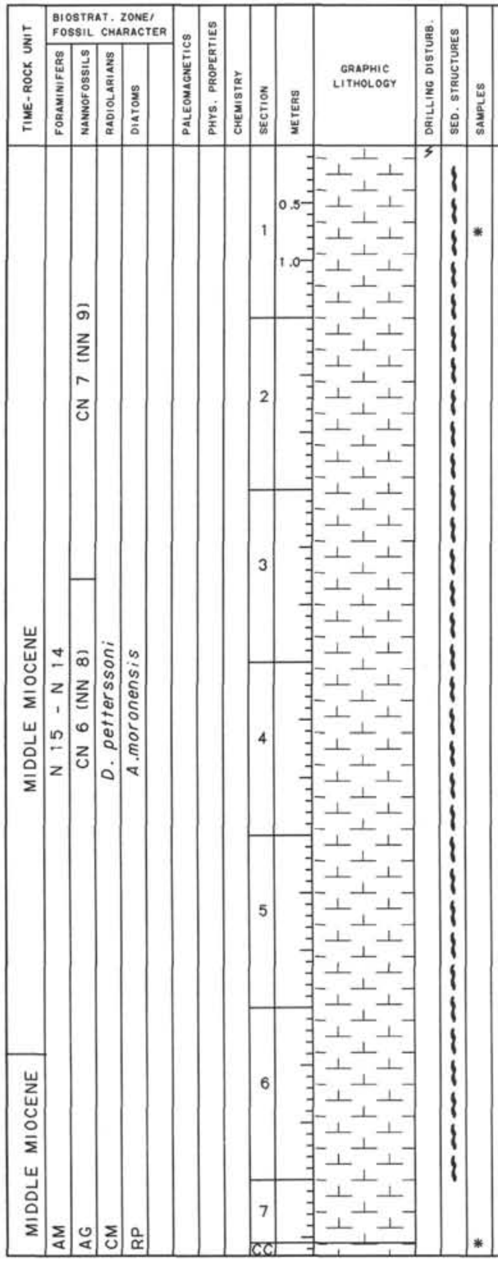

LITHOLOGIC DESCRIPTION

FORAMINIFER-BEARING CLAY-BEARING NANNOFOSSIL OOZE

Major lithology: Foraminifer-bearing clay-bearing nannofossil ooze, burrow-mottled; light greenish gray (5GY 7/1) colors alternate with light gray (5Y 7/1); pyrite stains throughout, hydrogen sulfide odor detectable over freshly cut sections.

Minor lithology: Sponge spicule-bearing foraminifer-bearing nannofossil ooze, light greenish gray (5GY 7/1), in Section 7, 50 cm, to CC.

SMEAR SLIDE SUMMARY (%):

	1, 80 D	CC D
TEXTURE:		
Sand	30	20
Silt	15	15
Clay	55	65
COMPOSITION:		
Quartz	Tr	1
Clay	5	8
Volcanic glass	—	Tr
Accessory minerals:		
Pyrite	Tr	Tr
Foraminifers	20	15
Nannofossils	50	61
Diatoms	2	1
Radiolarians	8	8
Sponge spicules	14	6
Silicoflagellates	Tr	Tr
Fish remains	1	Tr

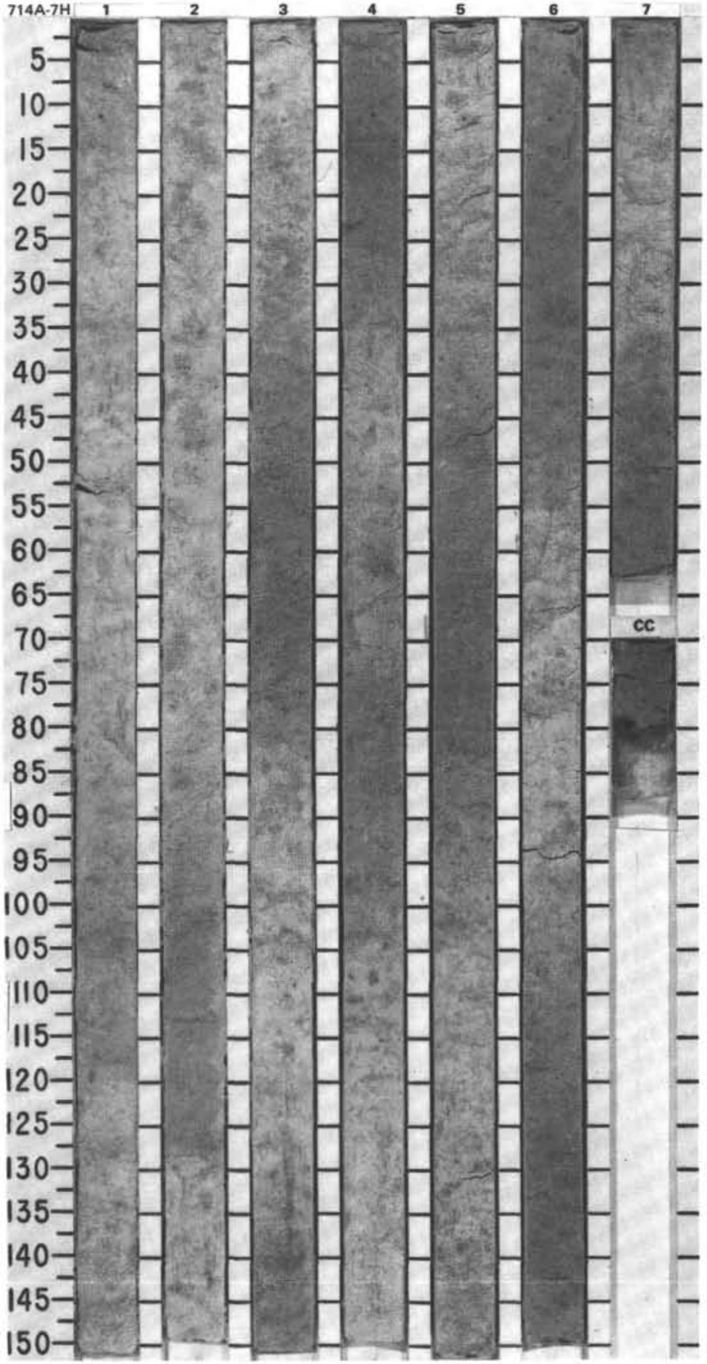

SITE 714 HOLE A CORE 8H CORED INTERVAL 2092.1-2101.7 mbsl; 60.6-70.2 mbsf

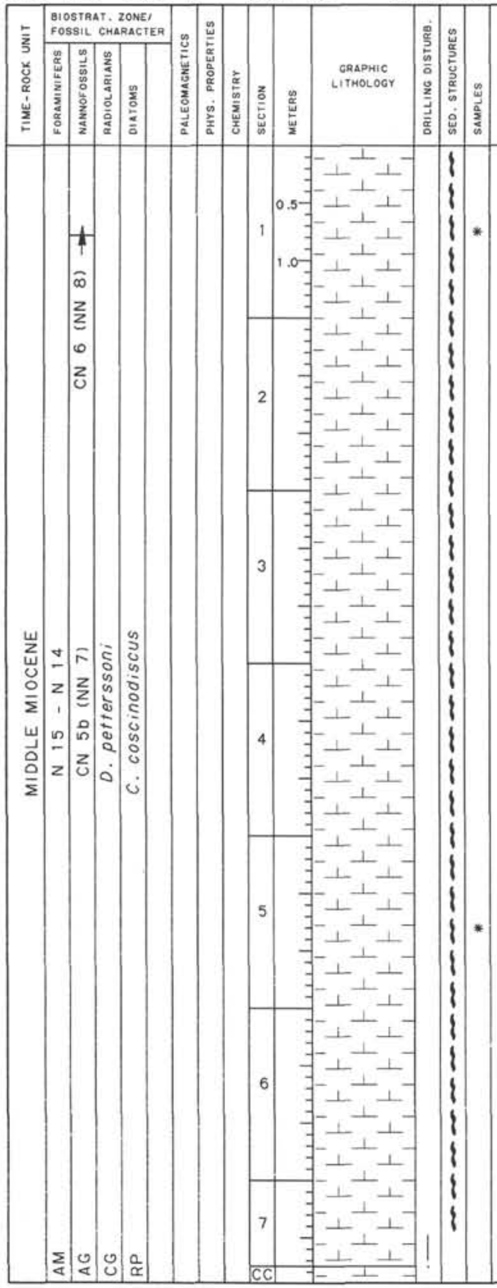

LITHOLOGIC DESCRIPTION

FORAMINIFER-BEARING NANNOFOSSIL OOZE

Major lithology: Foraminifer-bearing nannofossil ooze, burrow-mottled; light greenish gray (5GY 7/1) alternates with light gray (5Y 7/1) and very light greenish gray (5G 8/1); mildly pyrite-stained throughout with local dark gray (N4) pyrite.

SMEAR SLIDE SUMMARY (%):

	1, 80 D	5, 80 D
TEXTURE:		
Sand	30	25
Silt	15	15
Clay	55	60
COMPOSITION:		
Quartz	1	Tr
Clay	8	5
Volcanic glass	Tr	Tr
Accessory minerals:		
Pyrite	Tr	—
Foraminifers	25	20
Nannofossils	50	57
Diatoms	Tr	2
Radiolarians	7	8
Sponge spicules	9	8
Silicoflagellates	Tr	Tr
Fish remains	Tr	Tr
Mollusk debris	Tr	—

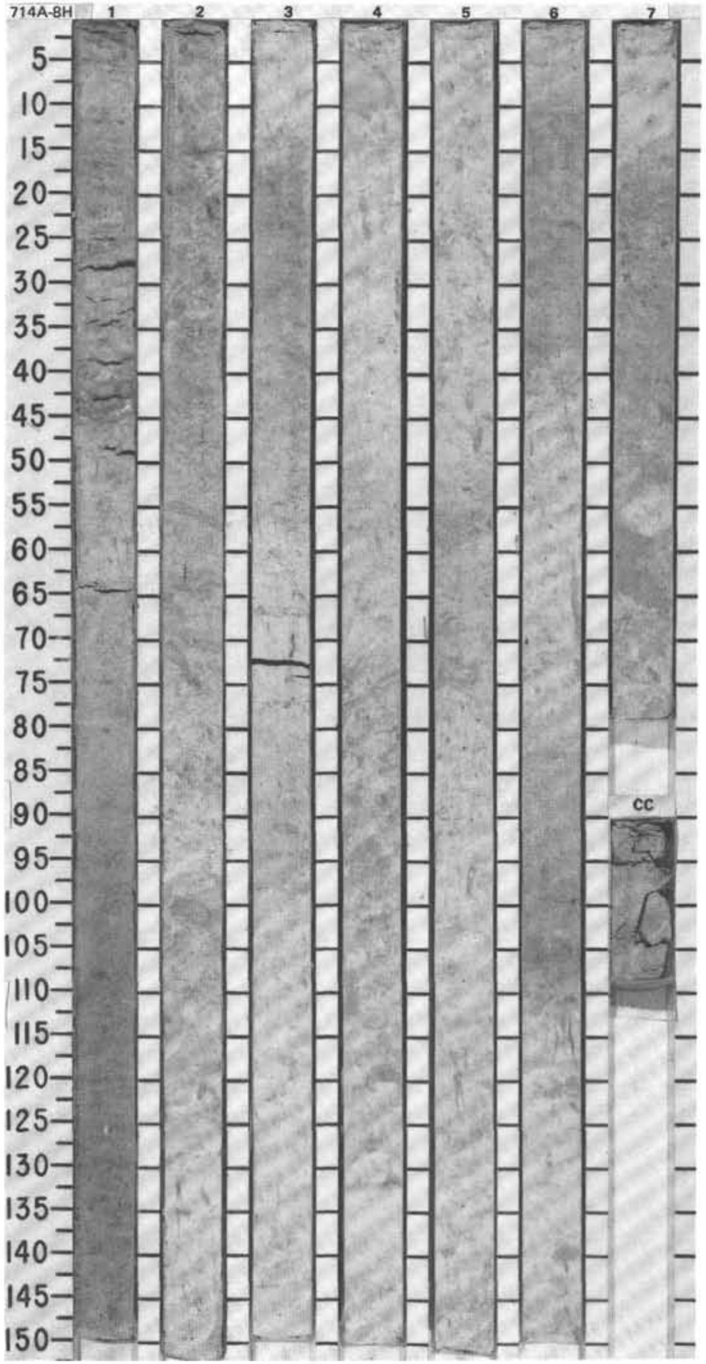

SITE 714 HOLE A CORE 9H CORED INTERVAL 2101.7-2111.3 mbsl; 70.2-79.8 mbsf

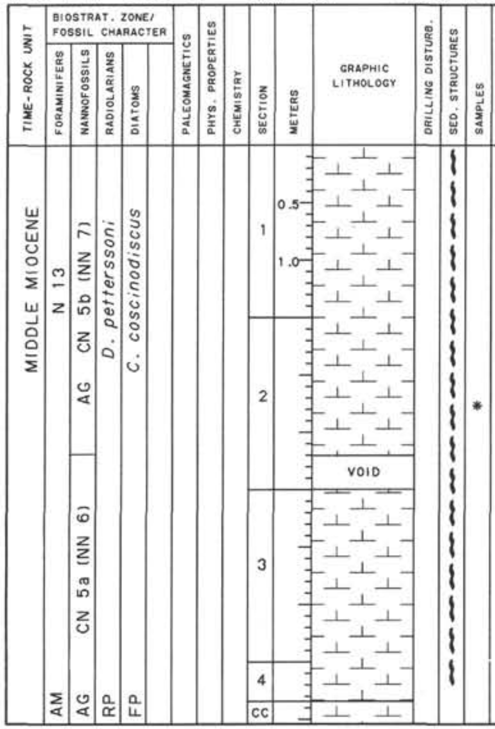

LITHOLOGIC DESCRIPTION

SPONGE SPICULE-BEARING FORAMINIFER-BEARING NANNOFOSSIL OOZE

Major lithology: Sponge spicule-bearing foraminifer-bearing nannofossil ooze, burrow-mottled; light greenish gray (5YR 7/1) alternates with light gray (5Y 7/1) and very light greenish gray (5G 8/1); moderately pyrite-stained.

SMEAR SLIDE SUMMARY (%):

	2, 80 D
TEXTURE:	
Sand	20
Silt	15
Clay	65
COMPOSITION:	
Quartz	Tr
Mica	Tr
Clay	5
Volcanic glass	1
Foraminifers	15
Nannofossils	63
Diatoms	1
Radiolarians	5
Sponge spicules	10
Silicoflagellates	Tr

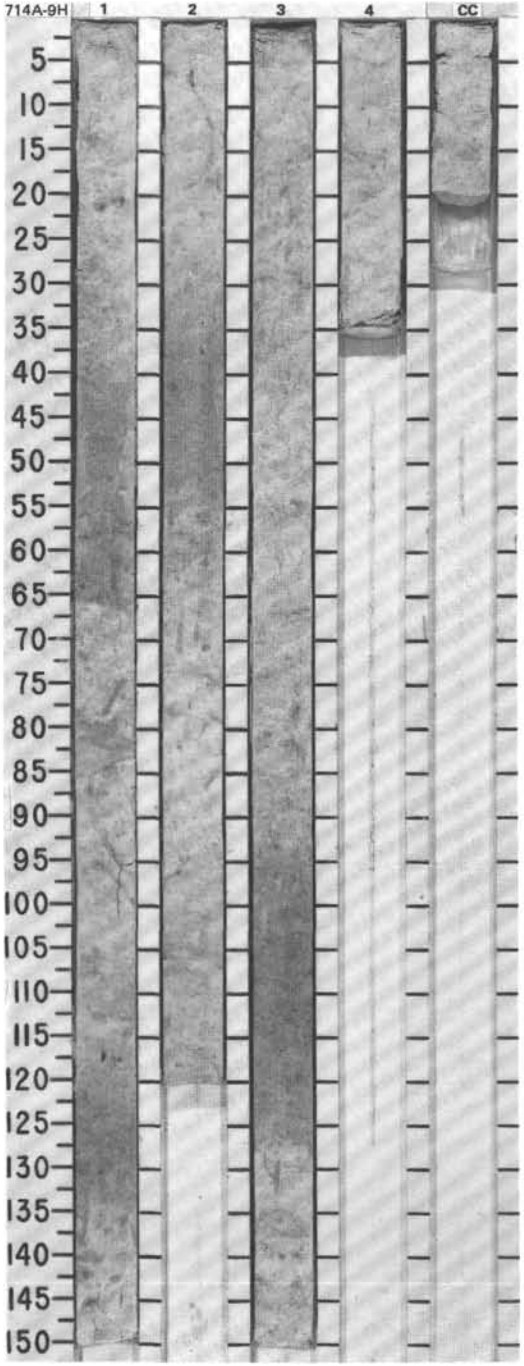

SITE 714 HOLE A CORE 10H CORED INTERVAL 2111.3-2121.0 mbsl; 79.8-89.5 mbsf

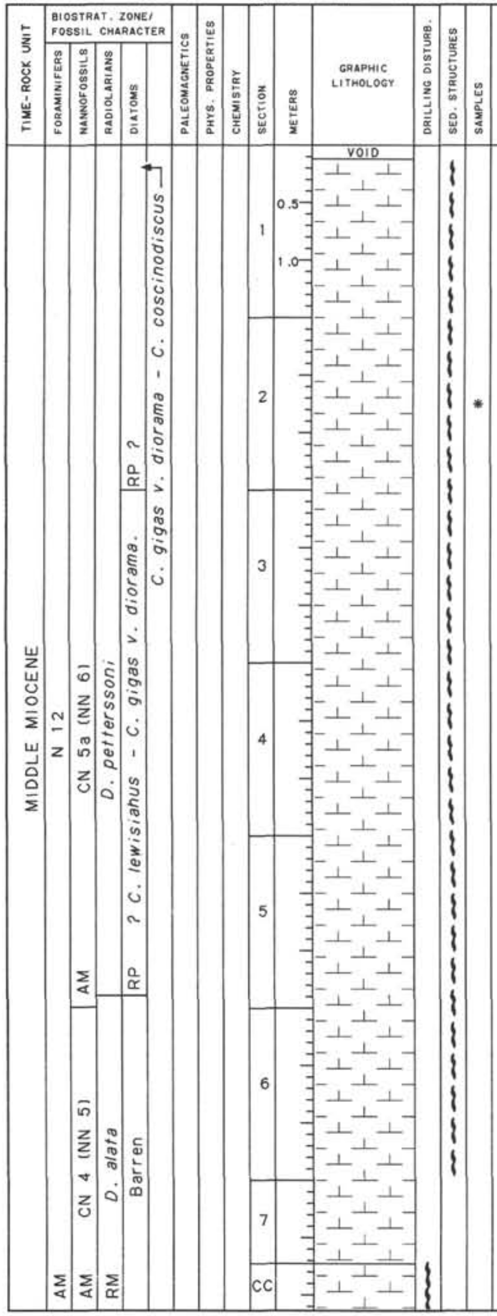

LITHOLOGIC DESCRIPTION

FORAMINIFER-BEARING NANNOFOSSIL OOZE

Major lithology: Foraminifer-bearing nannofossil ooze, burrow-mottled, very light greenish gray (5G 8/1) alternates with light gray (5Y 7/1), intermittent subhorizontal gray (N6) pyrite-stained bands throughout core.

Minor lithology: Foraminifer-bearing nannofossil chalk, light gray (5Y 7/1), occurs in a few 3-4 cm nodules in Sections 5 and 6.

SMEAR SLIDE SUMMARY (%):

	2, 80 D
TEXTURE:	
Sand	25
Silt	15
Clay	60
COMPOSITION:	
Quartz	Tr
Clay	5
Volcanic glass	Tr
Foraminifers	24
Nannofossils	59
Diatoms	Tr
Radiolarians	5
Sponge spicules	7

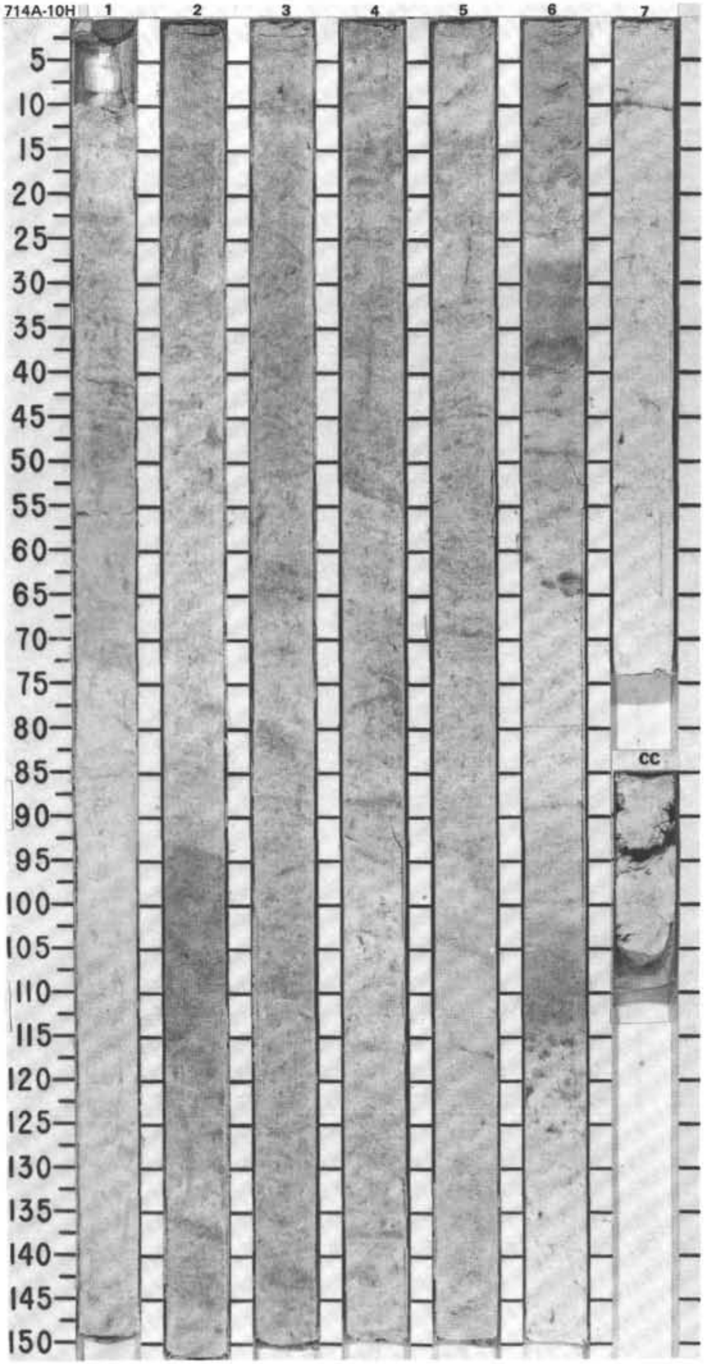

SITE 714 HOLE A CORE 11H CORED INTERVAL 2121.0-2130.6 mbsl; 89.5-99.1 mbsf

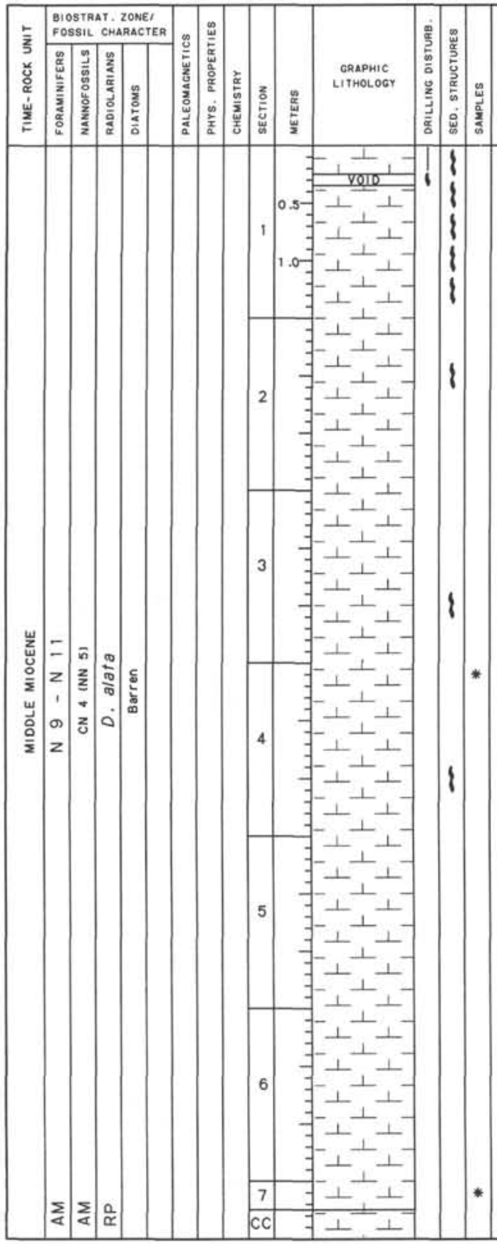

LITHOLOGIC DESCRIPTION

FORAMINIFER-BEARING NANNOFOSSIL OOZE and FORAMINIFER-BEARING CLAY-BEARING NANNOFOSSIL OOZE

Major lithologies: Foraminifer-bearing nannofossil ooze, and foraminifer-bearing clay-bearing nannofossil ooze, very light greenish gray (5G 8/1) alternates with greenish gray (5G 7/1); burrow-mottling and pyritic burrows in Section 1, thin subhorizontal horizons of gray (N6) bands in Sections 1 and 2.

SMEAR SLIDE SUMMARY (%):

	4, 16 D	7, 16 D
TEXTURE:		
Sand	15	10
Silt	15	15
Clay	70	75
COMPOSITION:		
Clay	5	5
Volcanic glass	—	Tr
Dolomite	Tr	Tr
Foraminifers	20	13
Nannofossils	74	80
Radiolarians	—	Tr
Sponge spicules	1	2
Bioclasts (bivalve?)	Tr	—

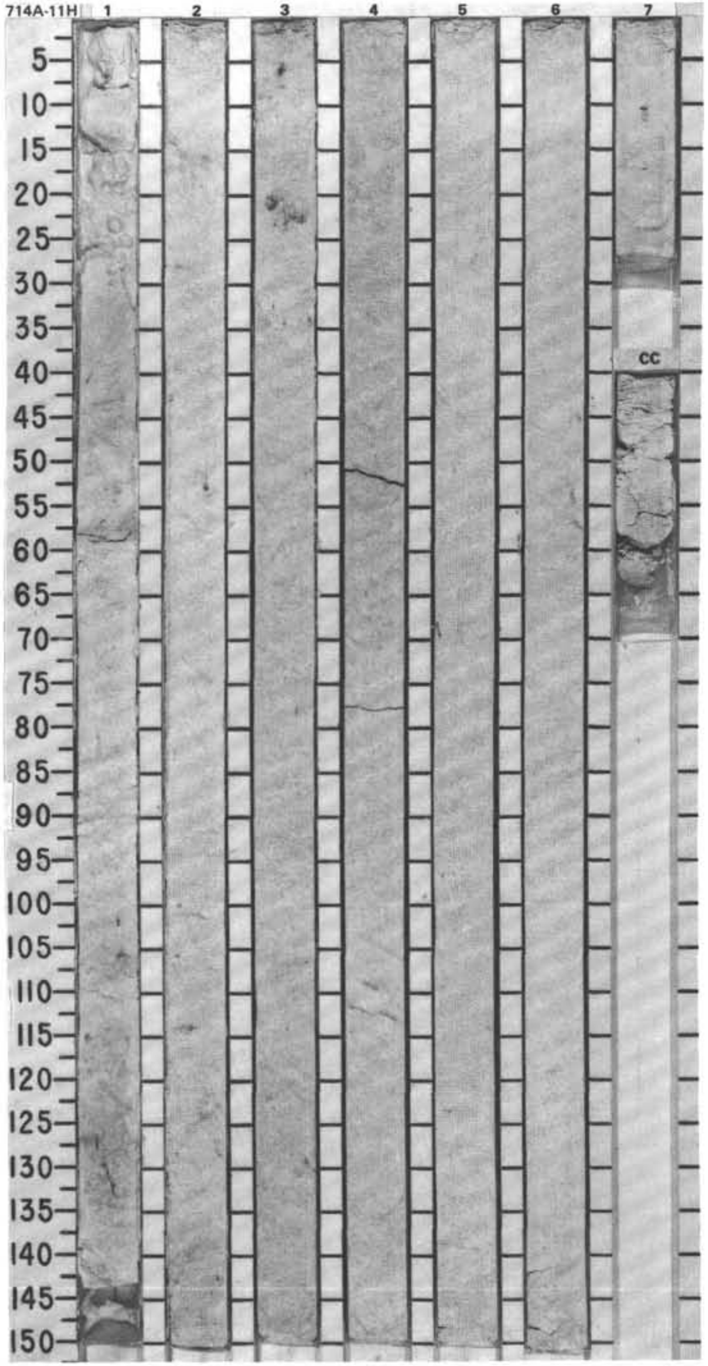

SITE 714 HOLE A CORE 12H CORED INTERVAL 2130.6-2140.2 mbsl; 99.1-108.7 mbsf

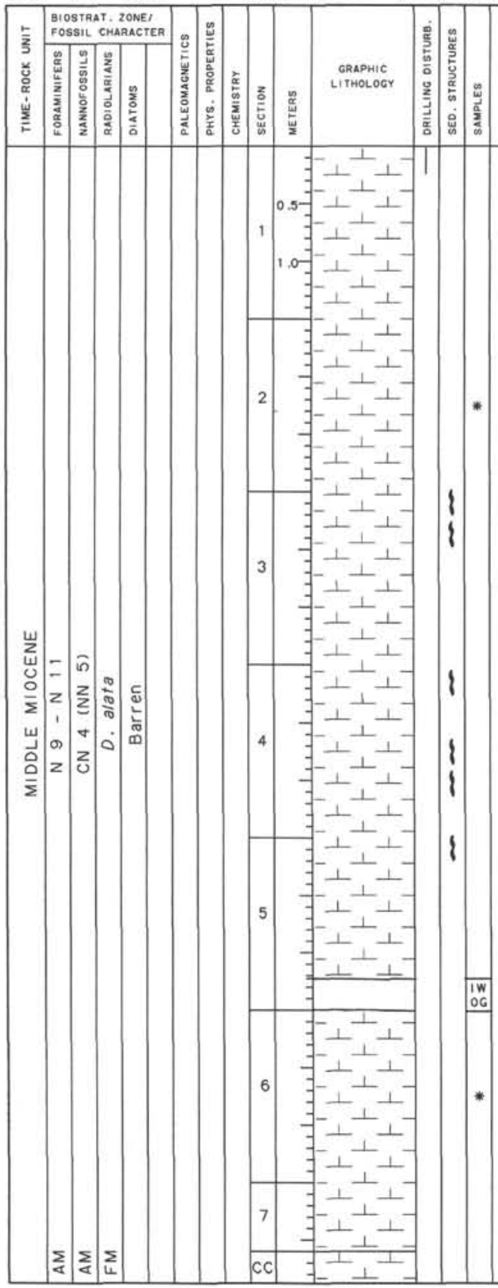

LITHOLOGIC DESCRIPTION

FORAMINIFER-BEARING NANNOFOSSIL OOZE and CLAY-BEARING FORAMINIFER-BEARING NANNOFOSSIL OOZE

Major lithologies: Foraminifer-bearing nannofossil ooze and clay-bearing foraminifer-bearing nannofossil ooze, very light greenish gray (5G 8/1). Pyritized burrows occur in Sections 2 and 4, faint thin gray (N6) horizons occur in Sections 3 and 4.

SMEAR SLIDE SUMMARY (%):

	2, 80 D	6, 80 D
TEXTURE:		
Sand	15	15
Silt	20	20
Clay	65	65
COMPOSITION:		
Clay	5	5
Volcanic glass	Tr	—
Cement	—	Tr
Foraminifers	15	18
Nannofossils	77	73
Radiolarians	Tr	1
Sponge spicules	3	3

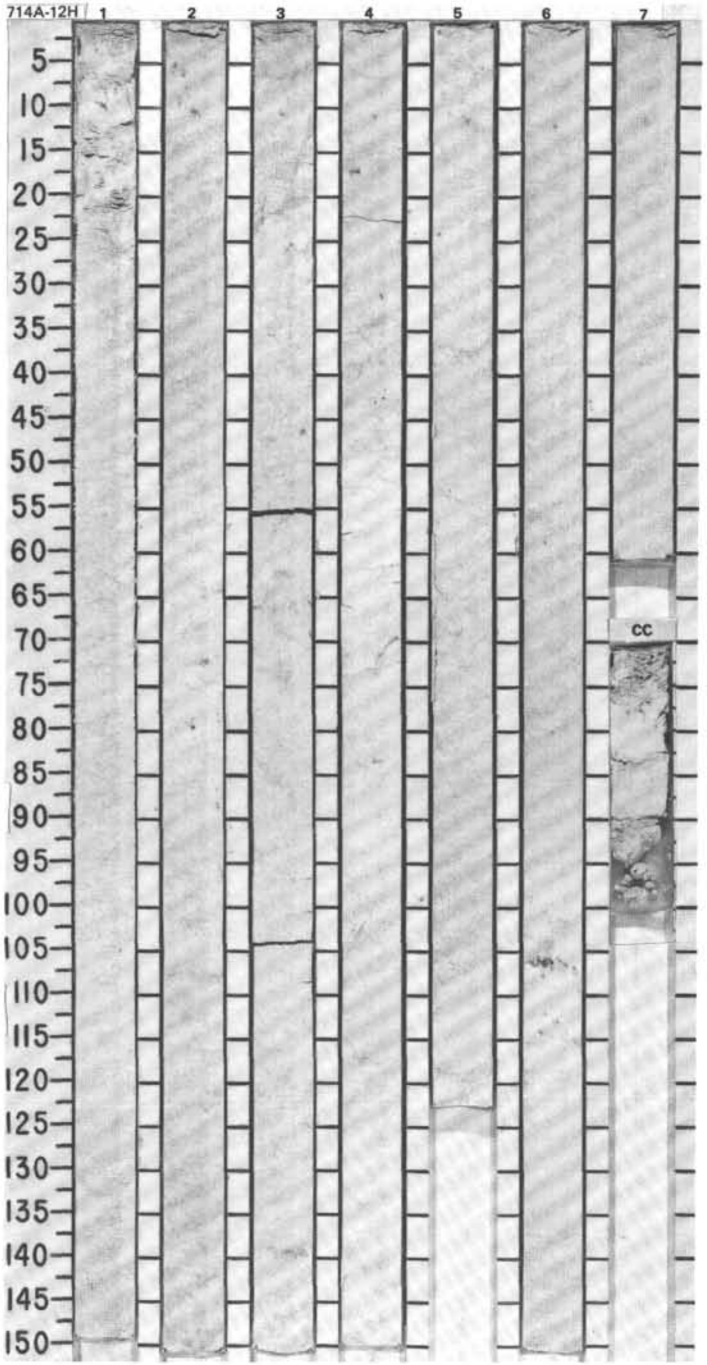

SITE 714 HOLE A CORE 13H CORED INTERVAL 2140.2-2149.9 mbsl; 108.7-118.4 mbsf

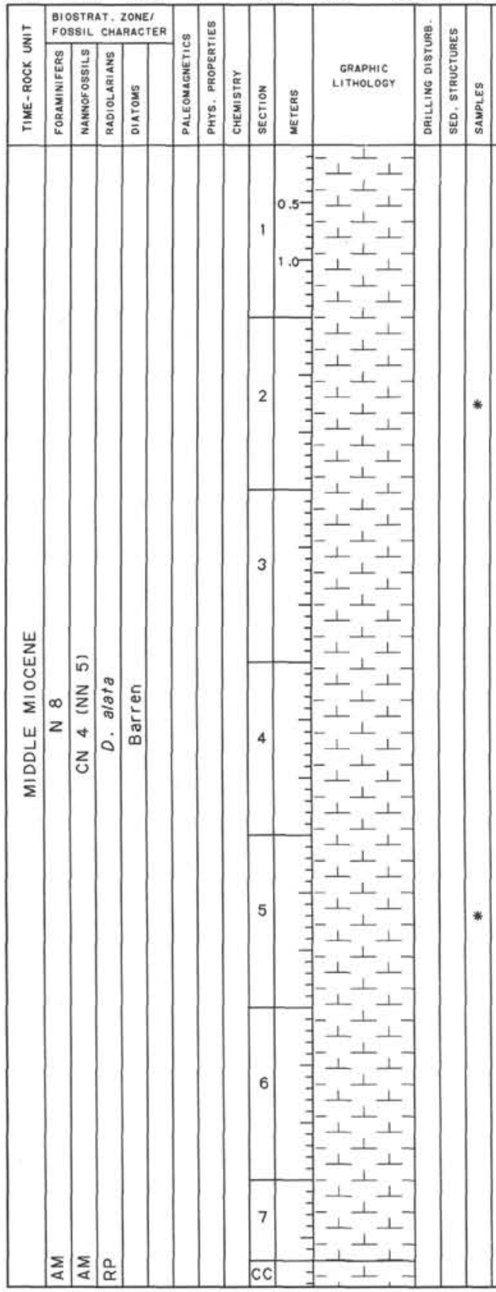

LITHOLOGIC DESCRIPTION

FORAMINIFER-BEARING NANNOFOSSIL OOZE and CLAY-BEARING FORAMINIFER-BEARING NANNOFOSSIL OOZE

Major lithologies: Foraminifer-bearing nannofossil ooze and clay-bearing foraminifer-bearing nannofossil ooze, very light greenish gray (5G 8/1), *pyrite burrows, Section 4, 45 cm, and Section 6, 43 cm;* a few thin, more firmly consolidated intervals scattered throughout core.

SMEAR SLIDE SUMMARY (%):

	2, 80 D	5, 80 D
TEXTURE:		
Sand	5	10
Silt	30	30
Clay	65	60
COMPOSITION:		
Quartz	Tr	—
Clay	5	5
Volcanic glass	—	Tr
Foraminifers	10	20
Nannofossils	84	74
Radiolarians	Tr	Tr
Sponge spicules	1	1

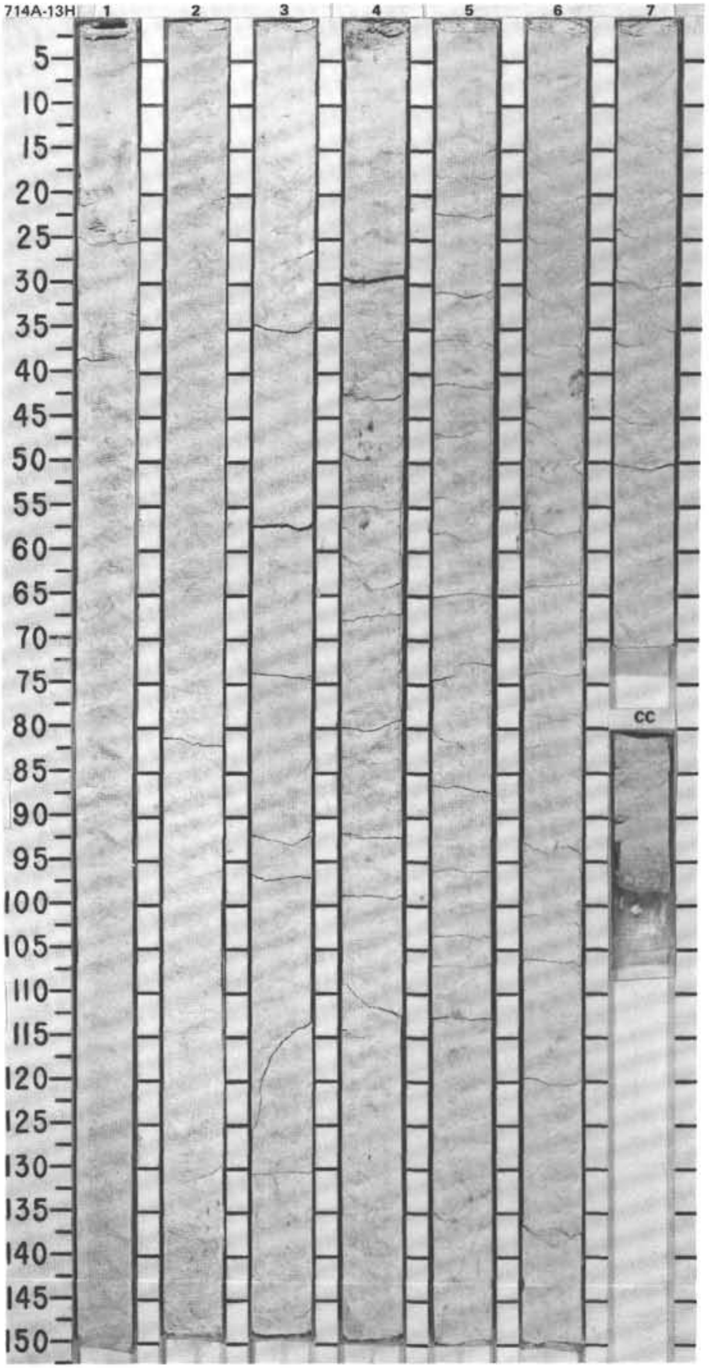

SITE 714 HOLE A CORE 14X CORED INTERVAL 2149.9-2158.3 mbsl; 118.4-126.8 mbsf

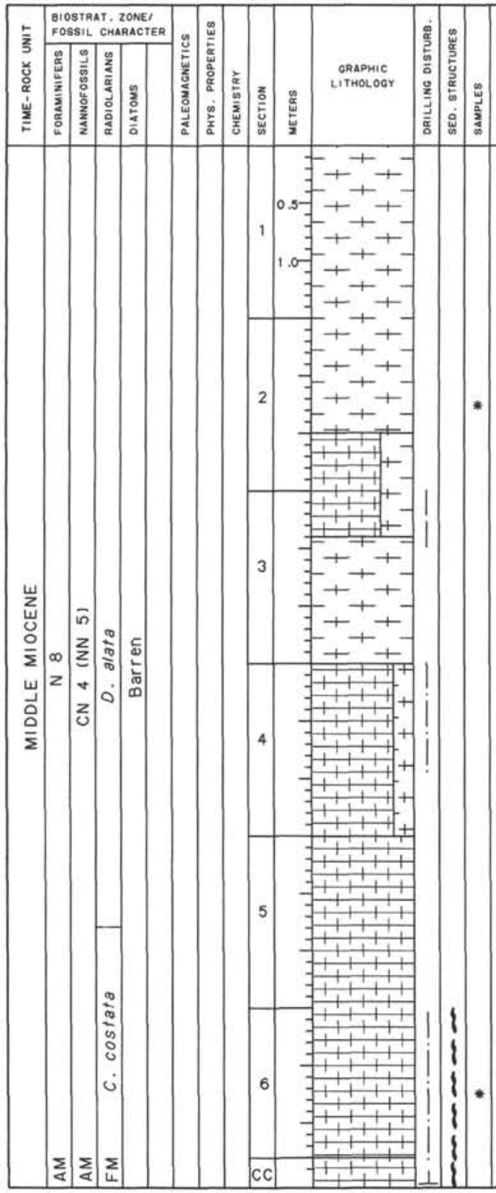

LITHOLOGIC DESCRIPTION

CLAY-BEARING FORAMINIFER-NANNOFOSSIL CHALK, alternating with CLAY-BEARING FORAMINIFER-NANNOFOSSIL OOZE

Major lithologies:

a. Clay-bearing foraminifer-nannofossil chalk, homogeneous, very light greenish gray (5G 8/1), occurs as nodules and layers.
b. Clay-bearing foraminifer-nannofossil ooze, homogeneous, very light greenish gray (5G 8/1), occurs as firm, thick layers and less firm thin layers between chalk.

SMEAR SLIDE SUMMARY (%):

	2, 76 D	6, 80 D
TEXTURE:		
Sand	15	15
Silt	30	30
Clay	55	55
COMPOSITION:		
Clay	5	5
Volcanic glass	—	Tr
Foraminifers	28	30
Nannofossils	63	60
Radiolarians	Tr	Tr
Sponge spicules	4	5

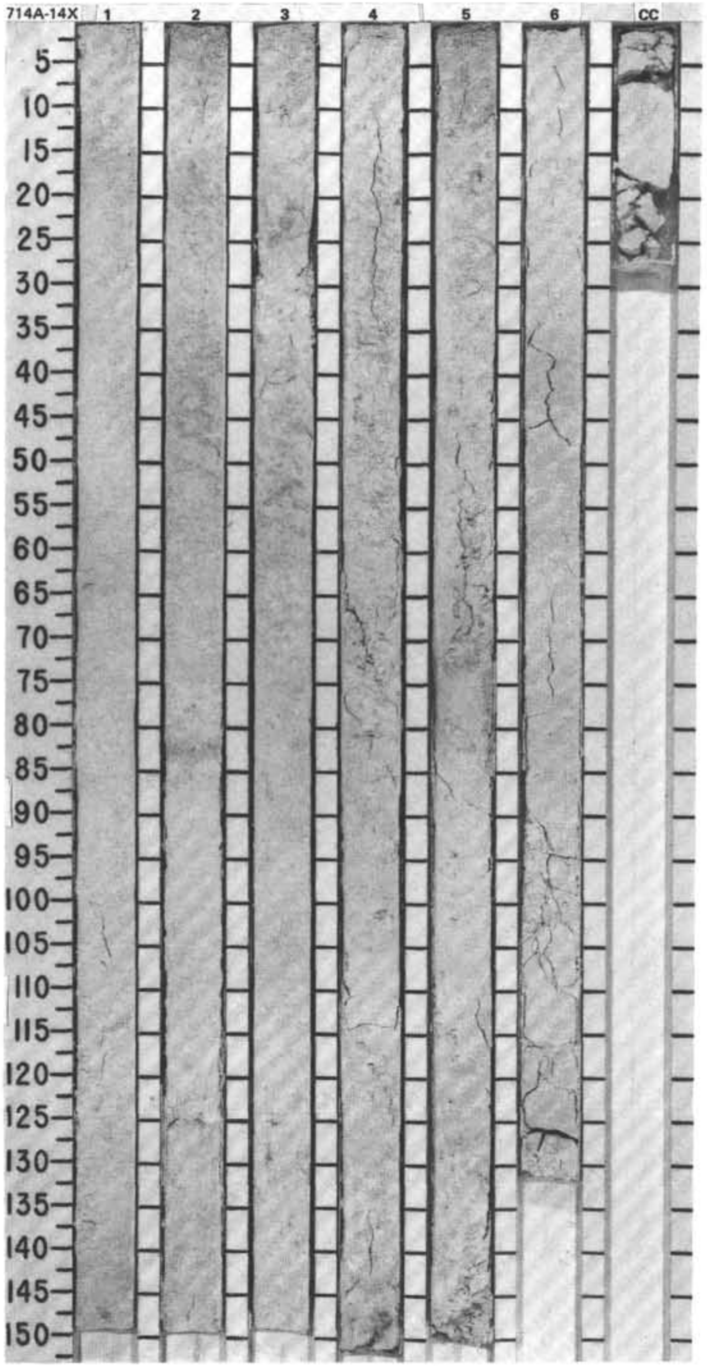

SITE 714 HOLE A CORE 15X CORED INTERVAL 2158.3-2167.9 mbsl; 126.8-136.4 mbsf

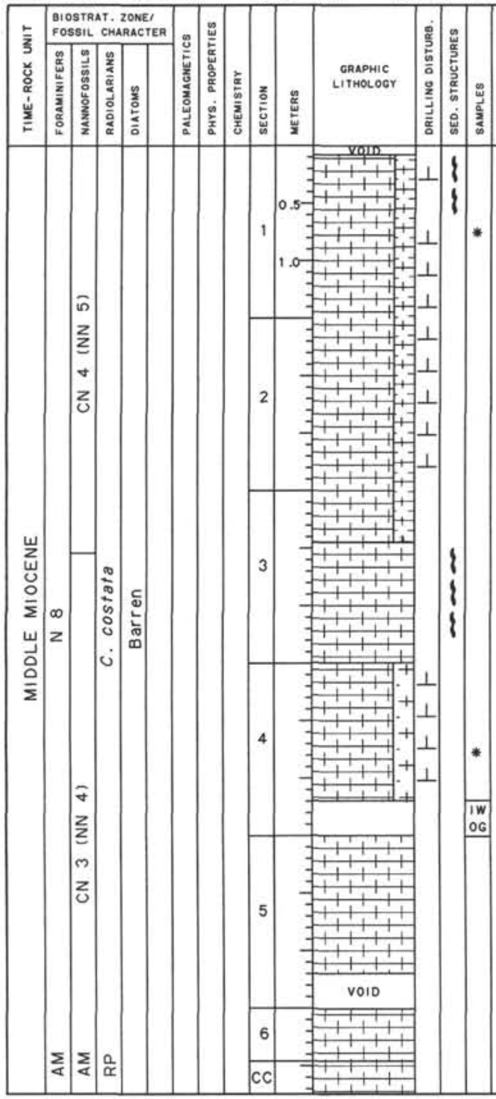

LITHOLOGIC DESCRIPTION

CLAY-BEARING FORAMINIFER-NANNOFOSSIL CHALK

Major lithology: Clay-bearing foraminifer-nannofossil chalk, homogeneous, very light greenish gray (5G 8/1) with intervals of light greenish gray (5G 7/1), occurs as continuous layers and nodules (drilling biscuits?).

Minor lithology: Clay-bearing foraminifer-nannofossil ooze, homogeneous, light greenish gray (5Y 7/1), occurs as thin layers between chalk nodules and clay (drilling paste?).

SMEAR SLIDE SUMMARY (%):

	1, 84 D	4, 80 D
TEXTURE:		
Sand	15	15
Silt	30	30
Clay	55	55
COMPOSITION:		
Clay	5	5
Volcanic glass	Tr	Tr
Foraminifers	28	30
Nannofossils	65	62
Radiolarians	—	Tr
Sponge spicules	2	3
Silicoflagellates	Tr	—

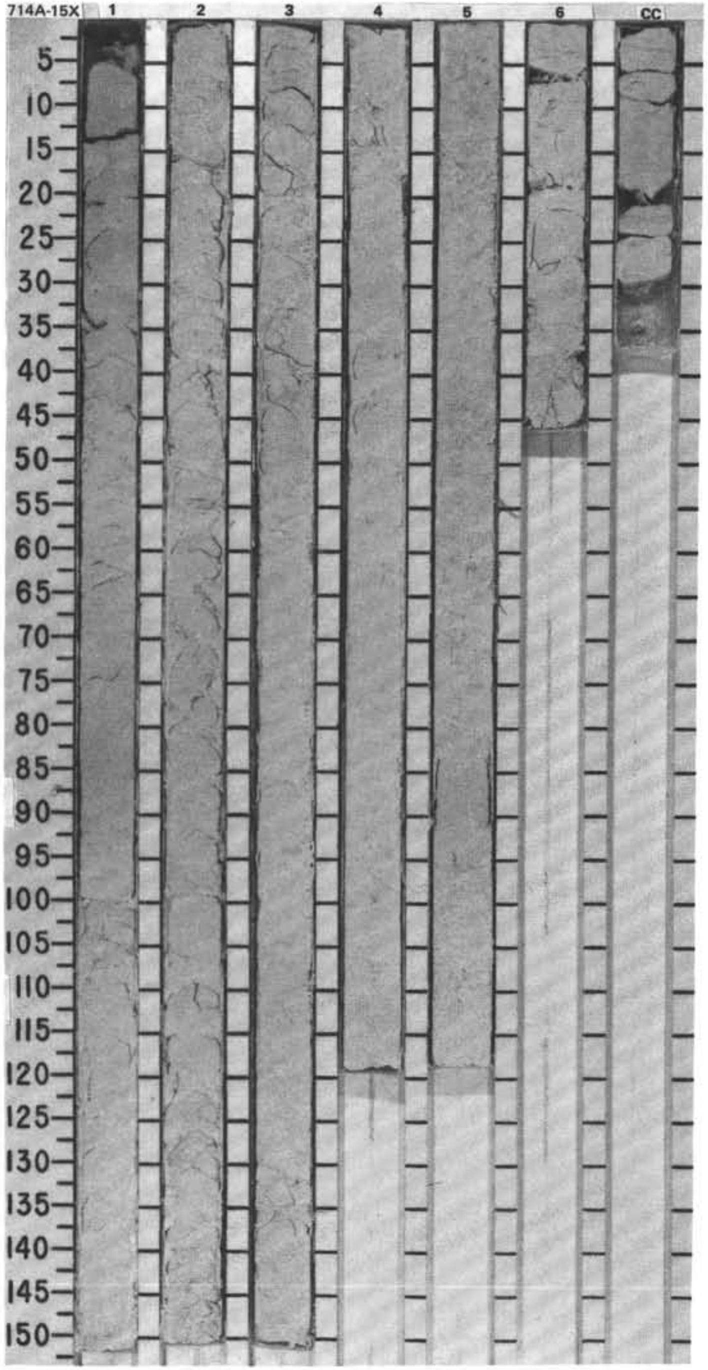

SITE 714 HOLE A CORE 16X CORED INTERVAL 2167.9-2177.6 mbsl; 136.4-146.1 mbsf

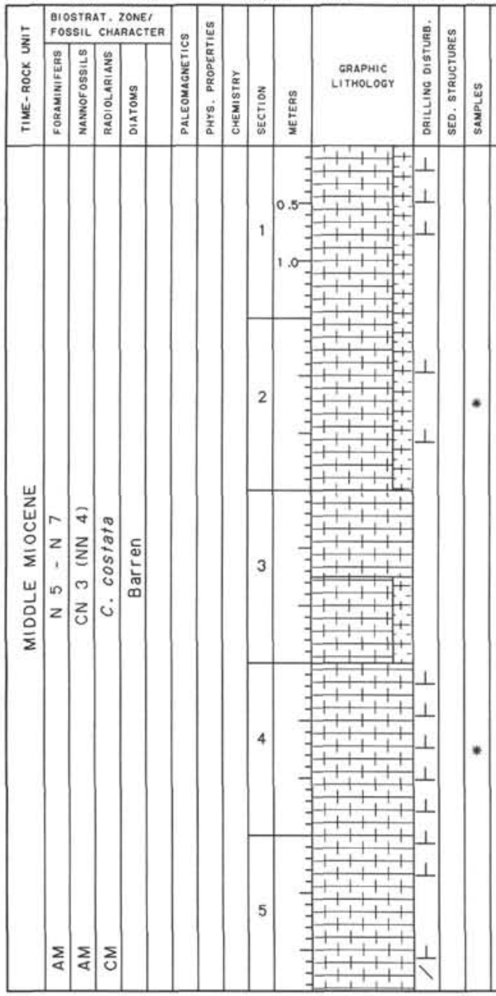

LITHOLOGIC DESCRIPTION

CLAY-BEARING FORAMINIFER-NANNOFOSSIL CHALK

Major lithology: Clay-bearing foraminifer-nannofossil chalk, homogeneous, very light greenish gray (5G 8/1), occurs as fractured layers and approximately regularly spaced nodules (drilling biscuits?) varying in size from 3-12 cm.

Minor lithology: Clay-bearing foraminifer-nannofossil ooze, homogeneous, very light greenish gray (5G 8/1), thinly distributed between chalk nodules (drilling paste?).

SMEAR SLIDE SUMMARY (%):

	2, 80 D	4, 80 D
TEXTURE:		
Sand	20	15
Silt	30	30
Clay	50	55
COMPOSITION:		
Clay	5	5
Volcanic glass	Tr	Tr
Accessory minerals:		
Pyrite	Tr	—
Foraminifers	38	38
Nannofossils	50	50
Radiolarians	2	2
Sponge spicules	5	5

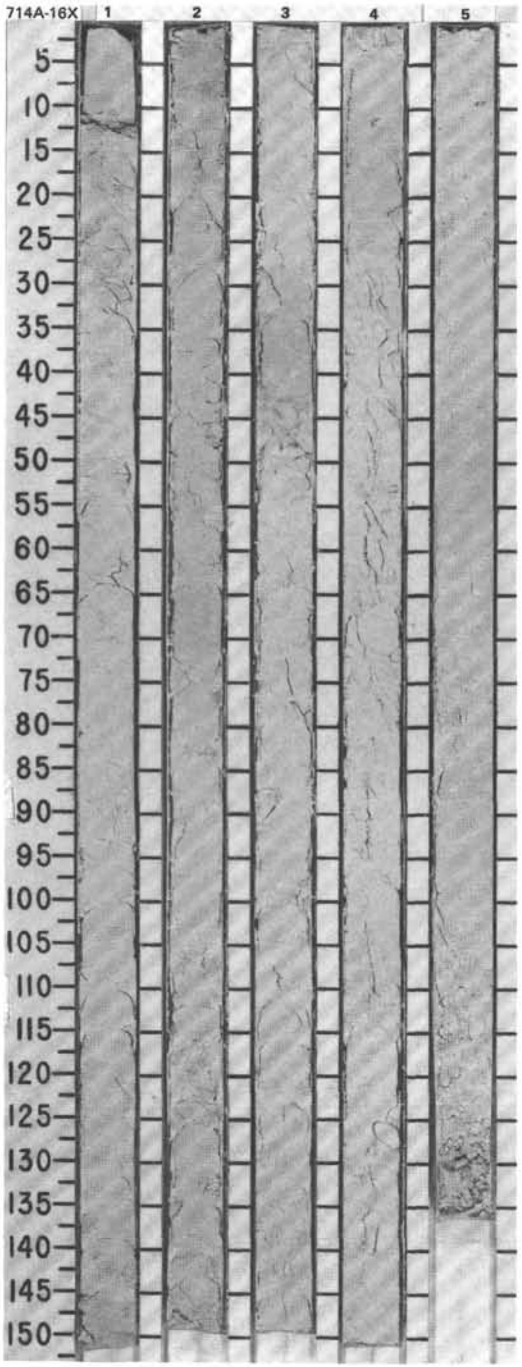

SITE 714 HOLE A CORE 17X CORED INTERVAL 2177.6-2187.2 mbsl; 146.1-155.7 mbsf

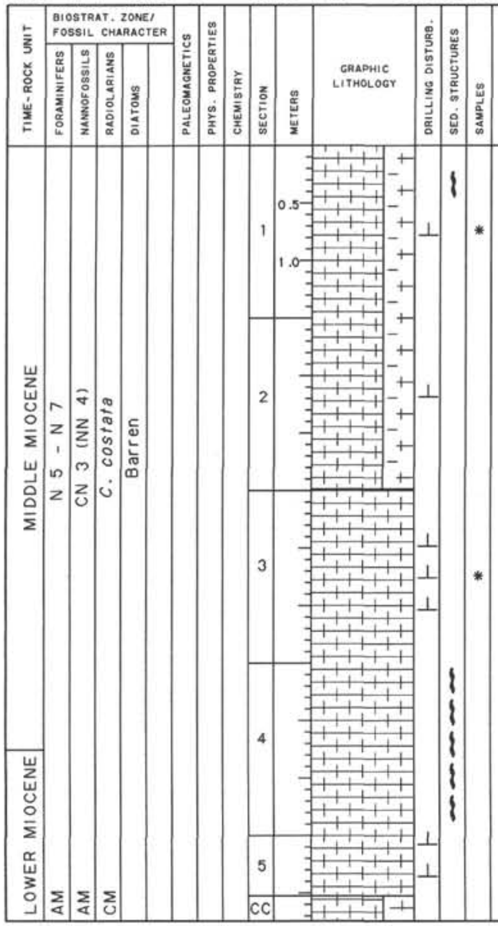

LITHOLOGIC DESCRIPTION

CLAY-BEARING FORAMINIFER-NANNOFOSSIL CHALK

Major lithology: Clay-bearing foraminifer-nannofossil chalk, very light greenish gray (5G 8/1), occurs as nodules (drilling biscuits?) and fractured layers; faintly burrow-mottled, Section 4.

Minor lithology: Clay-bearing foraminifer-nannofossil ooze, homogeneous, very light greenish gray (5Y 8/1), somewhat firm, occurs between and around nodules and layers (drilling paste?).

SMEAR SLIDE SUMMARY (%):

	1, 80 D	3, 80 D
TEXTURE:		
Sand	20	20
Silt	40	40
Clay	40	40
COMPOSITION:		
Clay	5	5
Volcanic glass	—	Tr
Foraminifers	43	43
Nannofossils	50	50
Radiolarians	Tr	—
Sponge spicules	2	2

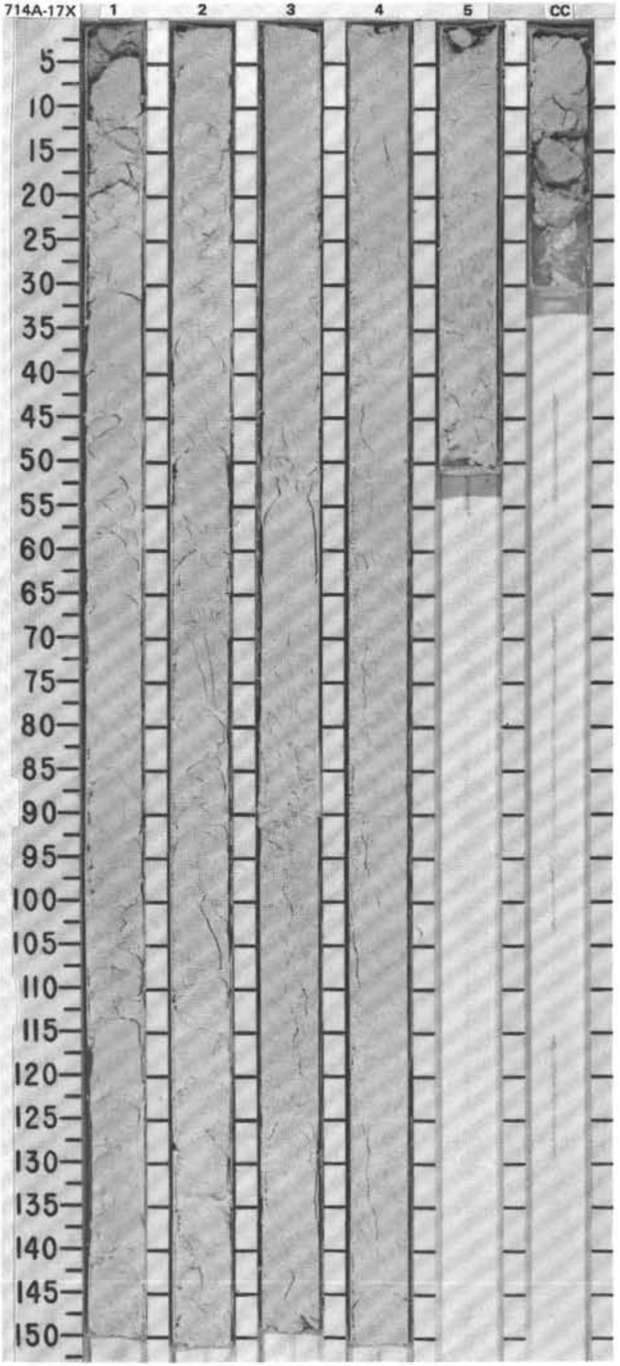

SITE 714 HOLE A CORE 18X CORED INTERVAL 2187.2-2196.8 mbsl; 155.7-165.3 mbsf

TIME-ROCK UNIT	FORAMINIFERS	NANNOFOSSILS	RADIOLARIANS	DIATOMS	PALEOMAGNETICS	PHYS. PROPERTIES	CHEMISTRY
LOWER MIOCENE	N 5 - N 7	CN 3 - NN 4 NN 3 (CN 2)	*S. wolffii*	Barren			
	AM	AM	RM				

BIOSTRAT. ZONE/ FOSSIL CHARACTER

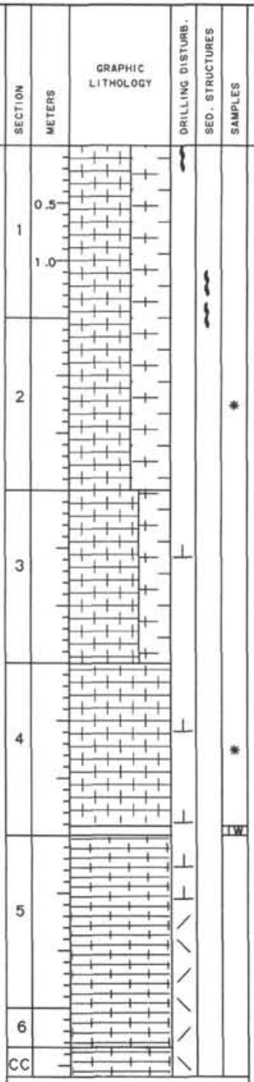

LITHOLOGIC DESCRIPTION

CLAY-BEARING FORAMINIFER-NANNOFOSSIL CHALK

Major lithology: Clay-bearing foraminifer-nannofossil chalk, fairly homogeneous, very light greenish gray (5G 8/1), occurs as somewhat regularly spaced nodules and biscuits grading into more continuous, regularly fractured layers, faintly burrow-mottled in parts of Sections 1 and 4.

Minor lithology: Clay-bearing foraminifer-nannofossil ooze, homogeneous, firm, very light greenish gray (5G 8/1), occurs around and in layers up to 4 cm thick between nodules and biscuits (drilling paste?).

SMEAR SLIDE SUMMARY (%):

	2, 82 D	4, 80 D
TEXTURE:		
Sand	15	20
Silt	40	40
Clay	45	40
COMPOSITION:		
Clay	8	8
Volcanic glass	Tr	—
Foraminifers	30	40
Nannofossils	60	50
Radiolarians	—	Tr
Sponge spicules	2	2

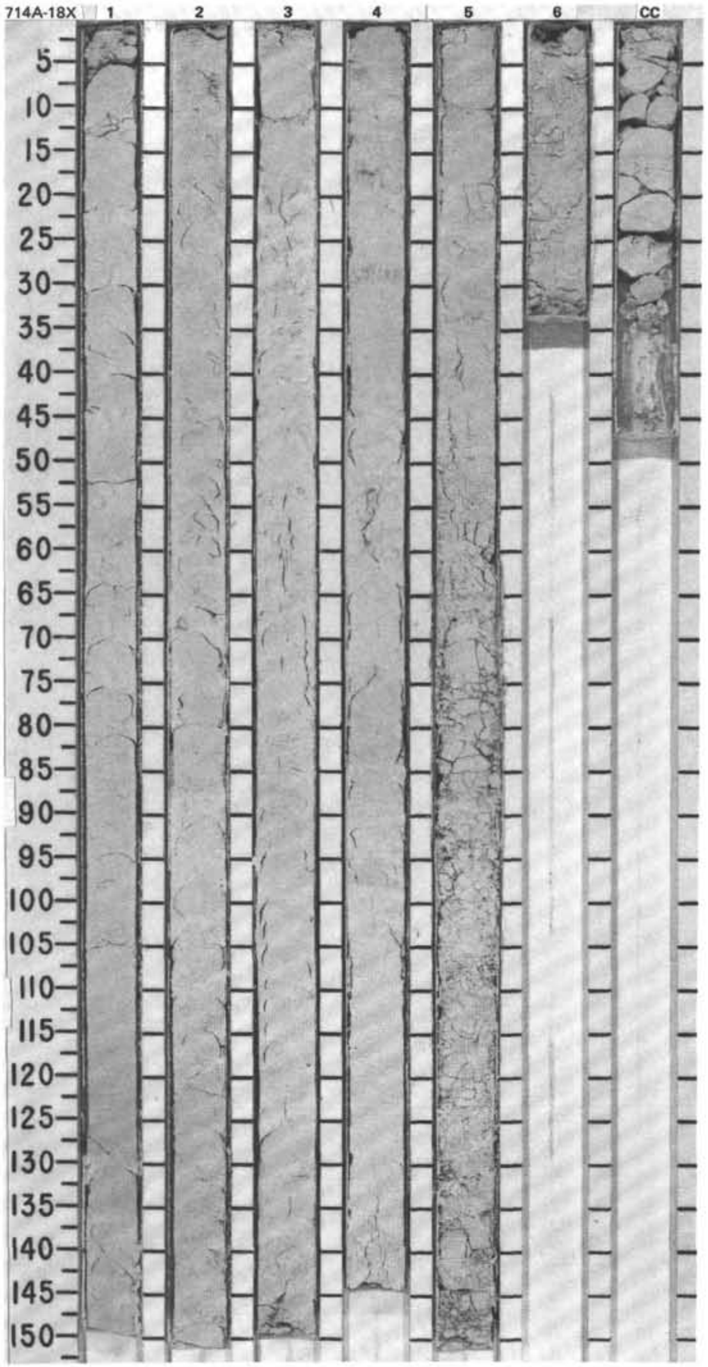

SITE 714 HOLE A CORE 19X CORED INTERVAL 2196.8-2206.5 mbsl; 165.3-175.0 mbsf

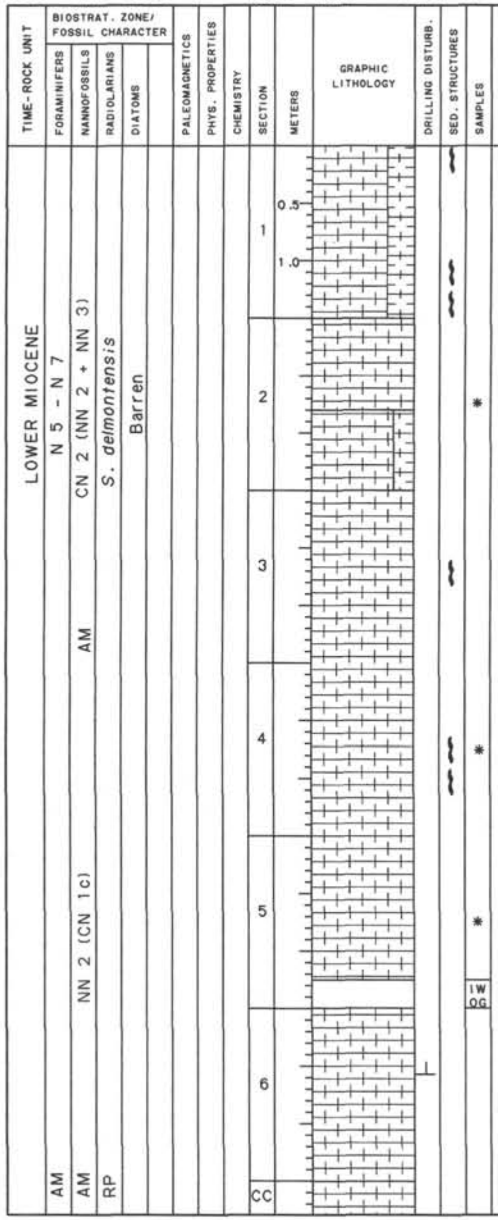

LITHOLOGIC DESCRIPTION

CLAY-BEARING FORAMINIFER-NANNOFOSSIL CHALK

Major lithology: Clay-bearing foraminifer-nannofossil chalk, very light greenish gray (5G 8/1), occurs as layers, regularly spaced 2 cm biscuits, and larger biscuits (7–10 cm), fairly homogeneous, Sections 1–3, 146 cm; numerous faint to distinct, very thin horizons of light greenish gray (5Y 7/1), occurring mainly in concentrated groups, Section 3, 146 cm, through Section 5; faint light gray (10YR 7/2) horizontal burrows sparsely distributed throughout Sections 5 and 6.

Minor lithology: Clay-bearing foraminifer-nannofossil ooze, homogeneous, very firm, very light greenish gray (5G 8/1), occurring between and around biscuits (drilling paste?).

SMEAR SLIDE SUMMARY (%):

	2, 80 D	4, 77 M	5, 80 D
TEXTURE:			
Sand	20	20	25
Silt	30	30	25
Clay	50	50	50
COMPOSITION:			
Clay	8	8	8
Volcanic glass	—	Tr	Tr
Accessory minerals:			
Pyrite	—	Tr	—
Foraminifers	40	30	40
Nannofossils	50	47	50
Diatoms	—	Tr	—
Radiolarians	—	Tr	—
Sponge spicules	2	15	2

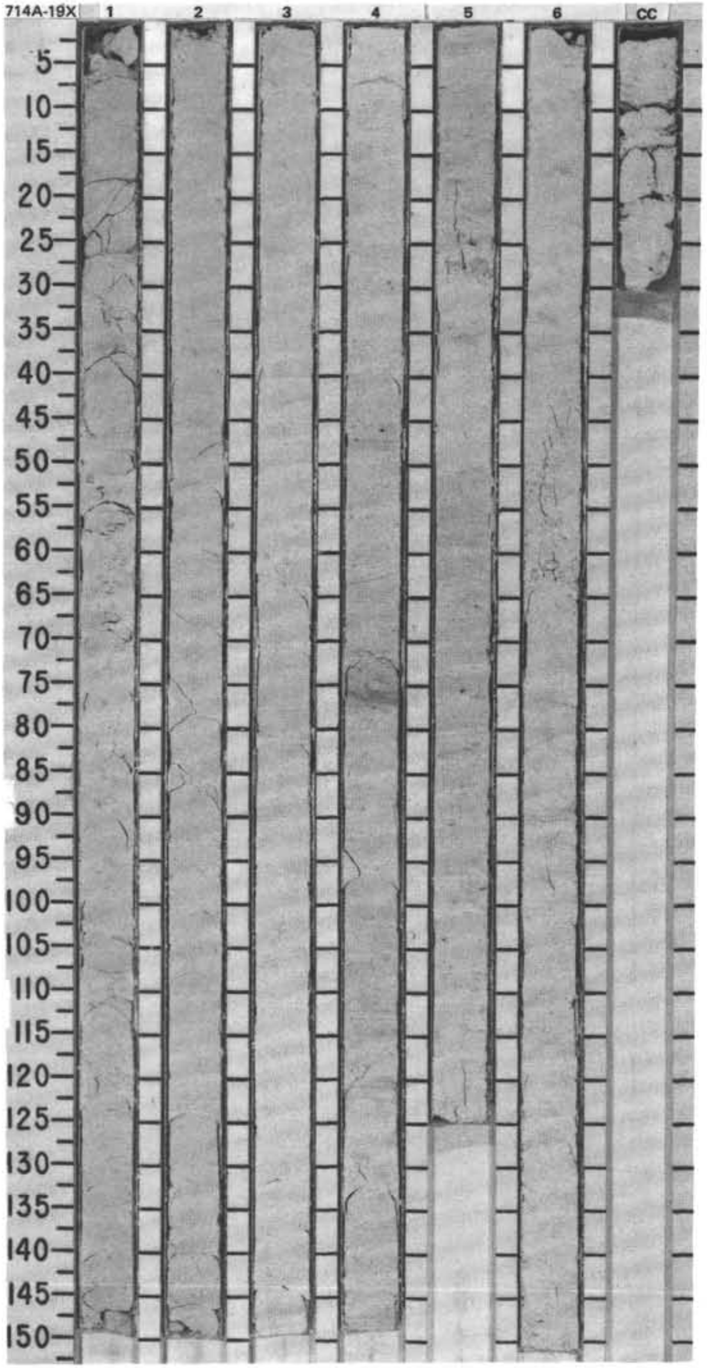

SITE 714 HOLE A CORE 20X CORED INTERVAL 2206.5-2216.2 mbsl; 175.0-184.7 mbsf

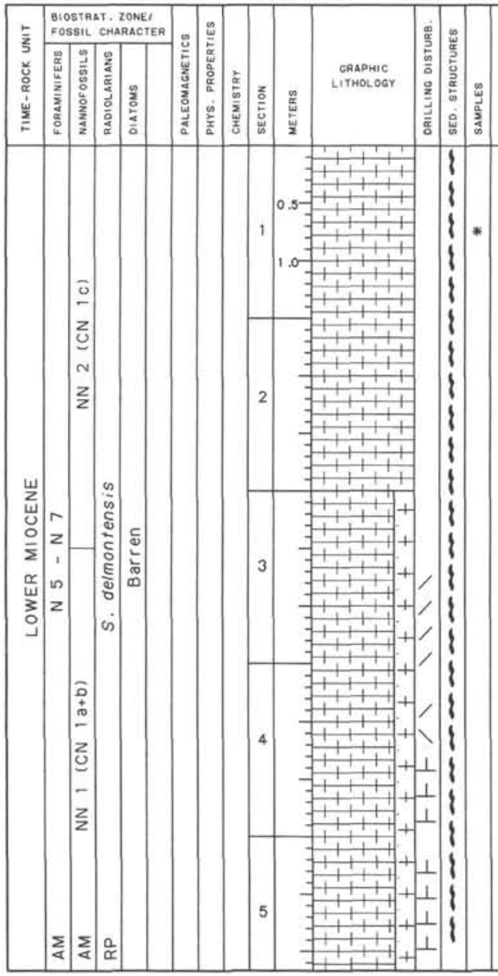

LITHOLOGIC DESCRIPTION

FORAMINIFER-NANNOFOSSIL CHALK

Major lithology: Foraminifer-nannofossil chalk, faintly burrow-mottled, very light greenish gray (5G 8/1), occurs as layers and thick biscuits; 3 zones of concentrated thin horizons of light greenish gray (5G 7/1), number of *Zoophycos* burrows, some light gray (5Y 7/1); zone of abundant benthic foraminifers, Section 3, 85–125 cm.

Minor lithology: Foraminifer-nannofossil ooze, homogeneous, very light greenish gray (5G 8/1), occurs between and around thick biscuits (drilling paste?).

SMEAR SLIDE SUMMARY (%):

	1, 80 D
TEXTURE:	
Sand	30
Silt	20
Clay	50
COMPOSITION:	
Quartz	Tr
Clay	5
Volcanic glass	Tr
Foraminifers	35
Nannofossils	50
Radiolarians	2
Sponge spicules	8
Silicoflagellates	Tr

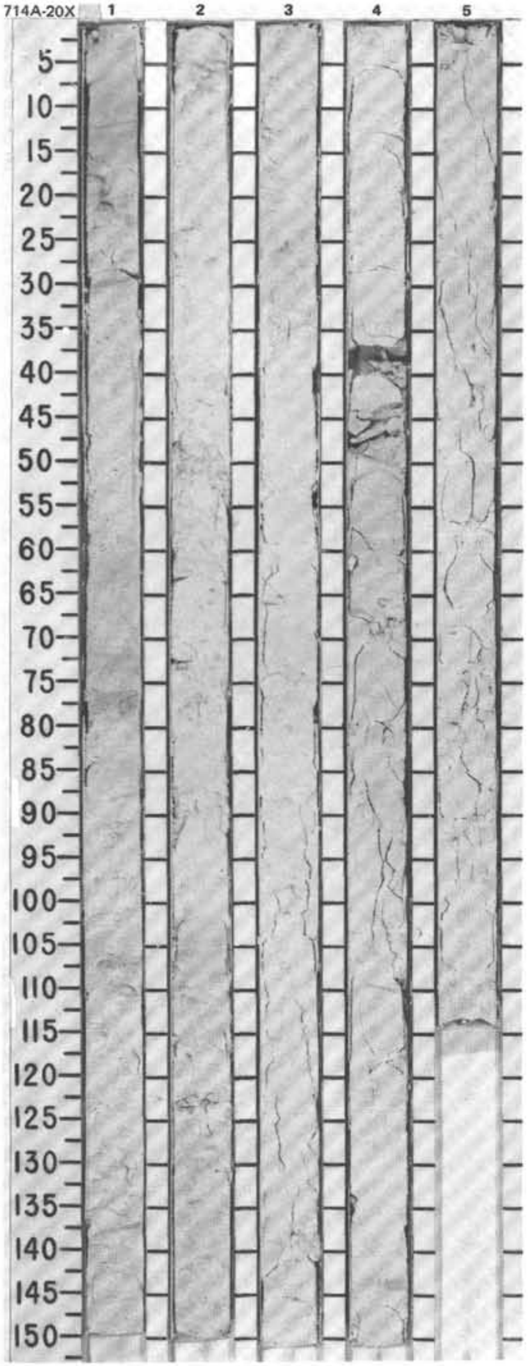

SITE 714 HOLE A CORE 21X CORED INTERVAL 2216.2-2225.9 mbsl; 184.7-194.4 mbsf

TIME-ROCK UNIT	BIOSTRAT. ZONE/ FOSSIL CHARACTER FORAMINIFERS	NANNOFOSSILS	RADIOLARIANS	DIATOMS		PALEOMAGNETICS	PHYS. PROPERTIES	CHEMISTRY	SECTION	METERS	GRAPHIC LITHOLOGY	DRILLING DISTURB.	SED. STRUCTURES	SAMPLES	LITHOLOGIC DESCRIPTION
LOWER MIOCENE	N 4 AM	CN 1 (NN 1) AM	*C. tetrapera* RP	Barren					1 CC	0.5	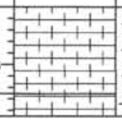				FORAMINIFER-NANNOFOSSIL CHALK Major lithology: Foraminifer-nannofossil chalk, burrow-mottled with several faint *Zoophycos* burrows, very light greenish gray (5G 8/1).

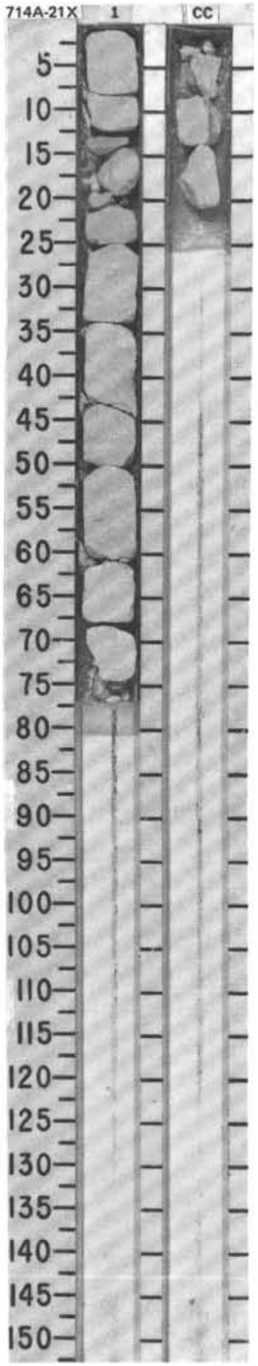

SITE 714 HOLE A CORE 22X CORED INTERVAL 2225.9-2235.6 mbsl; 194.4-204.1 mbsf

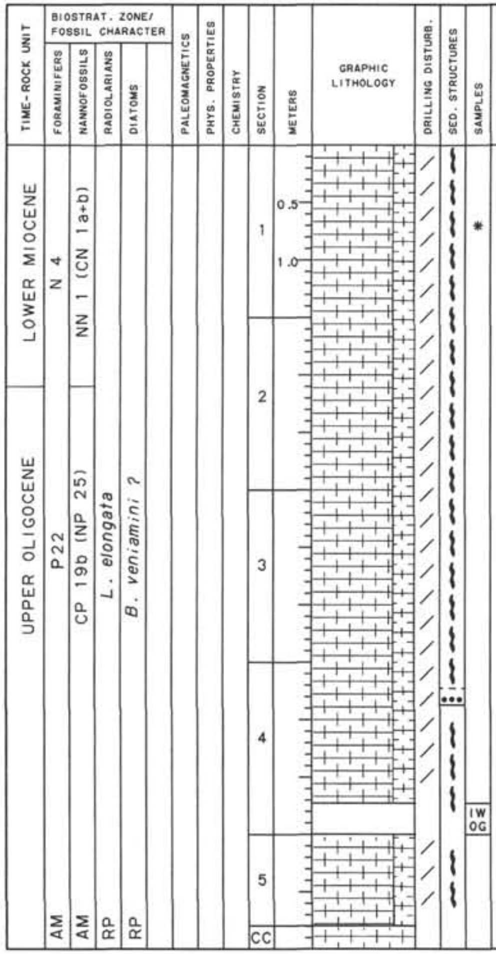

LITHOLOGIC DESCRIPTION

FORAMINIFER-NANNOFOSSIL CHALK

Major lithology: Foraminifer-nannofossil chalk, faintly burrow-mottled, very light greenish gray (5G 8/1) to light greenish gray (5G 7/1), occurs primarily as thick biscuits; two intervals (Section 2, 10 cm, and Section 5, 125–140 cm) of thin layers of large benthic foraminifers; turbidite in Section 4, 18–32 cm, with large (up to 1 cm) benthic foraminifers and limestone fragments at the base.

Minor lithology: Foraminifer-nannofossil ooze, homogeneous, very light greenish gray (5G 8/1), occurs around and between chalk biscuits (drilling paste?).

SMEAR SLIDE SUMMARY (%):

	1, 80 D
TEXTURE:	
Sand	25
Silt	20
Clay	55
COMPOSITION:	
Quartz	Tr
Clay	8
Dolomite	Tr
Foraminifers	30
Nannofossils	55
Radiolarians	2
Sponge spicules	5
Mollusk debris	Tr

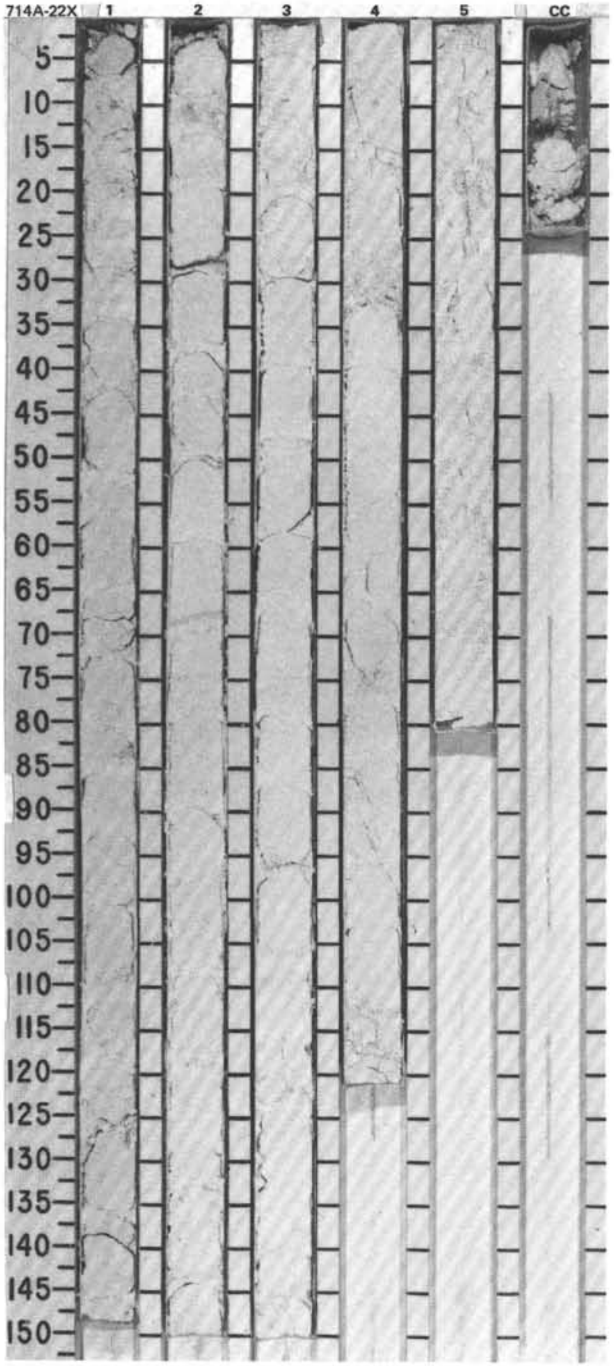

SITE 714 HOLE A CORE 23X CORED INTERVAL 2235.6-2245.3 mbsl; 204.1-213.8 mbsf

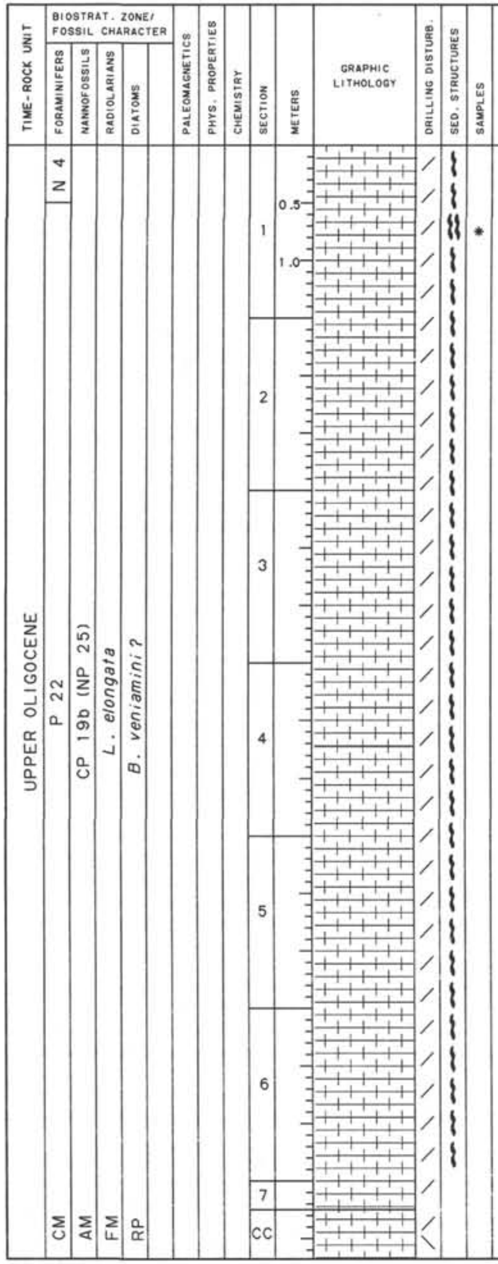

LITHOLOGIC DESCRIPTION

FORAMINIFER-NANNOFOSSIL CHALK

Major lithology: Foraminifer-nannofossil chalk, faintly burrow-mottled, very light greenish gray (5G 8/1), occurs as series of long intervals, faint thin horizons of light greenish gray (5GY 7/1) distributed throughout core; zone of abundant bioturbation, Section 1, 60–70 cm; 6 light greenish gray (5G 7/1) *Zoophycos* burrows, Section 3; exotic silicified limestone fragments along inside of liner, Section 1, 0–15 cm (from overlying strata?)

Minor lithology: Foraminifer-nannofossil ooze, homogeneous, very light greenish gray (5G 8/1), occurs around and between chalk intervals (drilling paste?).

SMEAR SLIDE SUMMARY (%):

	1, 80 D
TEXTURE:	
Sand	30
Silt	20
Clay	50
COMPOSITION:	
Quartz	Tr
Clay	5
Volcanic glass	Tr
Foraminifers	35
Nannofossils	51
Radiolarians	2
Sponge spicules	7

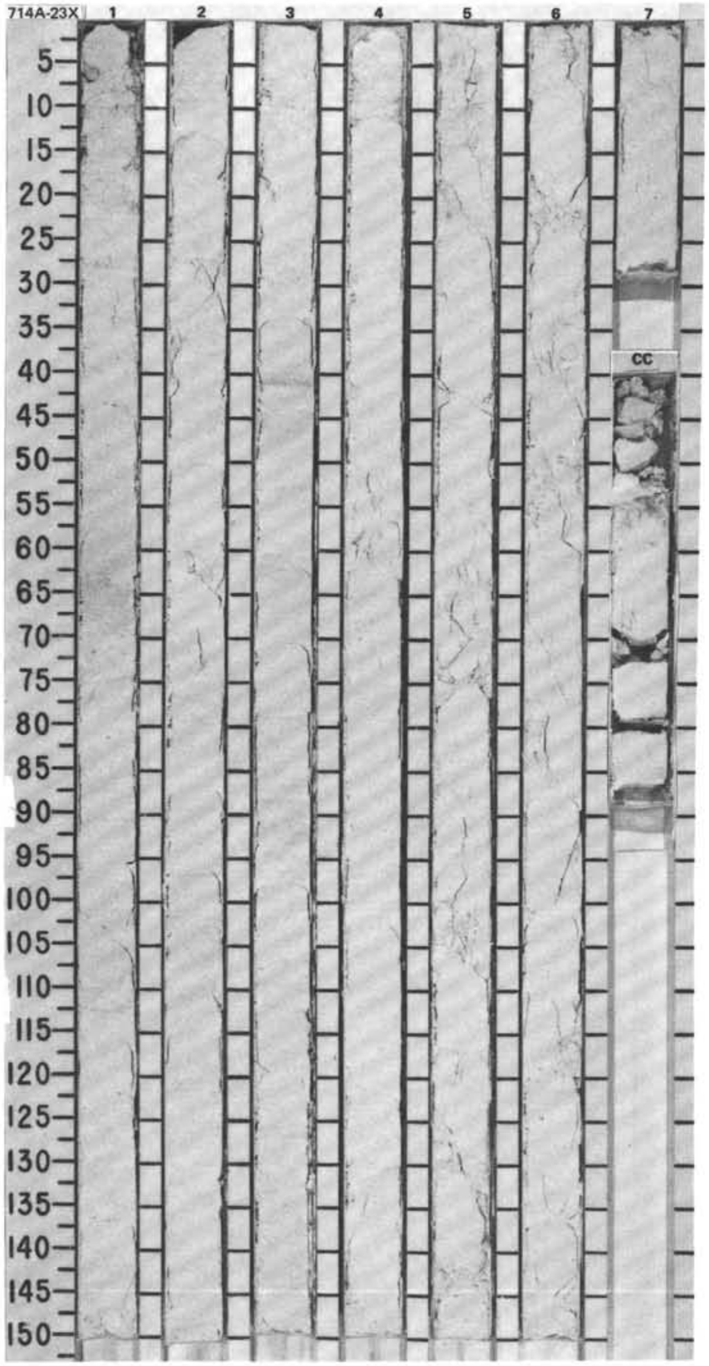

SITE 714 HOLE A CORE 24X CORED INTERVAL 2245.3-2254.6 mbsl; 213.8-223.3 mbsf

TIME-ROCK UNIT	BIOSTRAT. ZONE/ FOSSIL CHARACTER					PALEOMAGNETICS	PHYS. PROPERTIES	CHEMISTRY	SECTION	METERS	GRAPHIC LITHOLOGY	DRILLING DISTURB.	SED. STRUCTURES	SAMPLES	LITHOLOGIC DESCRIPTION
	FORAMINIFERS	NANNOFOSSILS	RADIOLARIANS	DIATOMS											
UPPER OLIGOCENE	P 20a	CP 19a (NP 24)	Barren	Barren					1	0.5 1.0	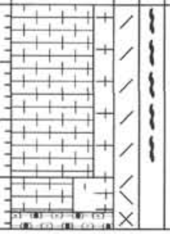			*	see below
									CC						
	CM	AM													

FORAMINIFER-NANNOFOSSIL CHALK

Major lithology: Foraminifer-nannofossil chalk, faintly burrow-mottled, very light greenish gray (5G 8/1), occurs as series of thick nodules.

Minor lithologies:
a. Foraminifer-nannofossil ooze, homogeneous, very light greenish gray (5G 8/1), occurs around and between chalk nodules.
b. Wackestone, very pale brown (10YR 7/3), silicified with benthic foraminifer grains (drilling breccia?).

SMEAR SLIDE SUMMARY (%):

	1, 80 D
TEXTURE:	
Sand	30
Silt	15
Clay	55
COMPOSITION:	
Clay	5
Volcanic glass	Tr
Dolomite	Tr
Foraminifers	35
Nannofossils	52
Diatoms	Tr
Radiolarians	2
Sponge spicules	6

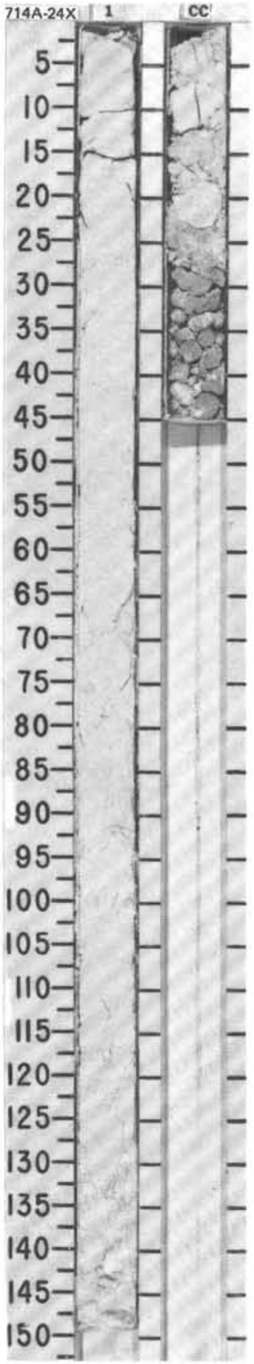

SITE 714 HOLE A CORE 25X CORED INTERVAL 2254.8-2264.5 mbsl; 223.3-233.0 mbsf

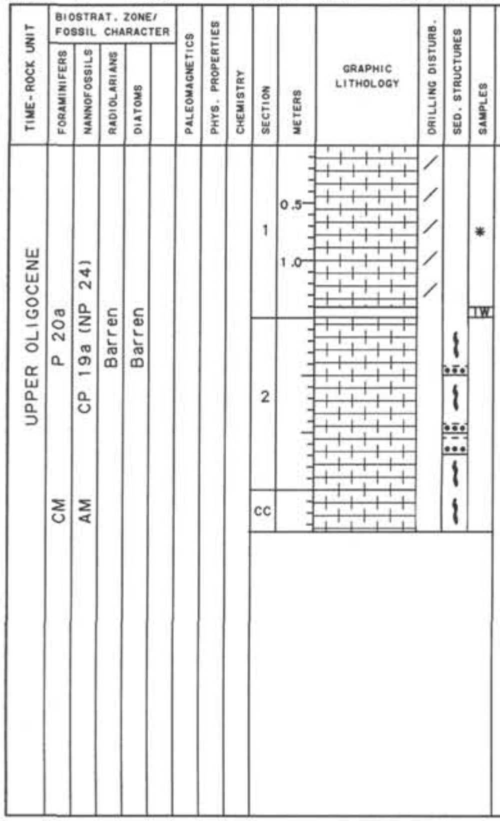

LITHOLOGIC DESCRIPTION

FORAMINIFER-NANNOFOSSIL CHALK

Major lithology: Foraminifer-nannofossil chalk, very light greenish gray (5G 8/1), occurs predominantly as long intervals, abundant large benthic foraminifers scattered throughout core. Several ungraded turbidites in Section 2, boundaries indistinct, most particles in turbidites are limestone fragments and benthic foraminifers, up to 0.5 cm in diameter and down to coarse sand size, particles are white (N9) in background of very pale brown (10YR 7/3).

Minor lithology: Foraminifer-nannofossil ooze, very light greenish gray (5G 8/1), occurs around and between chalk intervals.

SMEAR SLIDE SUMMARY (%):

	1, 80 D
TEXTURE:	
Sand	30
Silt	20
Clay	50
COMPOSITION:	
Quartz	Tr
Clay	5
Volcanic glass	1
Foraminifers	30
Nannofossils	54
Diatoms	Tr
Radiolarians	2
Sponge spicules	8
Fish remains	Tr
Mollusk debris	Tr

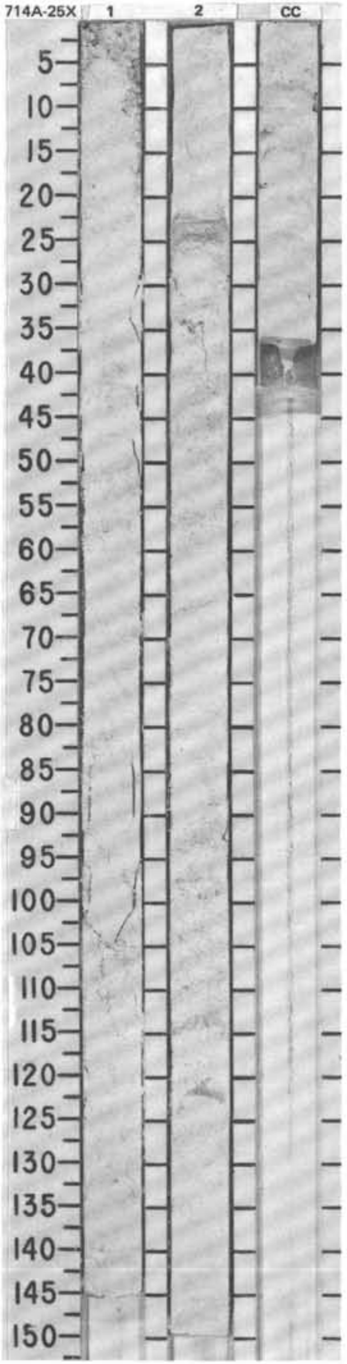

SITE 714 HOLE B CORE 1H CORED INTERVAL 2031.5-2038.3 mbsl; 0.0-6.8 mbsf

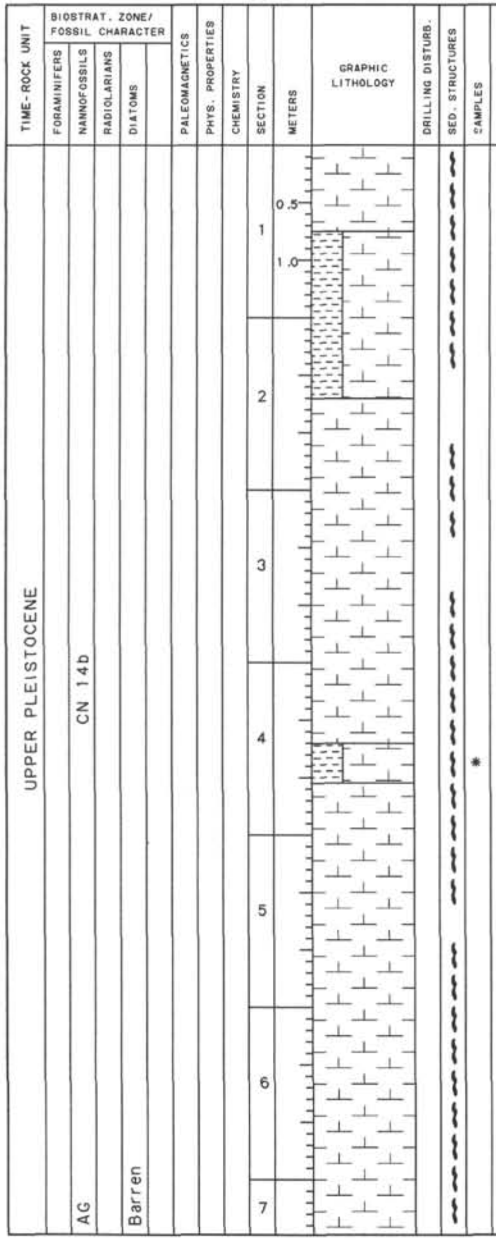

LITHOLOGIC DESCRIPTION

FORAMINIFER-BEARING CLAY-BEARING NANNOFOSSIL OOZE and FORAMINIFER-BEARING CLAYEY NANNOFOSSIL OOZE

Major lithologies: Foraminifer-bearing clay-bearing nannofossil ooze and foraminifer-bearing clayey nannofossil ooze, slightly burrow-mottled, alternating colors of dark gray (5Y 4/1) and gray (5Y 5/1) with greenish gray (5GY 5/1), color changes are gradational due to bioturbation; oxidized light yellowish brown (10YR 6/4) interval in Section 1, 0–7 cm.

SMEAR SLIDE SUMMARY (%):

	4, 90 D
TEXTURE:	
Sand	25
Silt	25
Clay	50
COMPOSITION:	
Clay	20
Volcanic glass	Tr
Dolomite	Tr
Accessory minerals	1
Foraminifers	25
Nannofossils	46
Radiolarians	Tr
Sponge spicules	1
Fish remains	1
Aragonite needles	2
Calcispheres	4

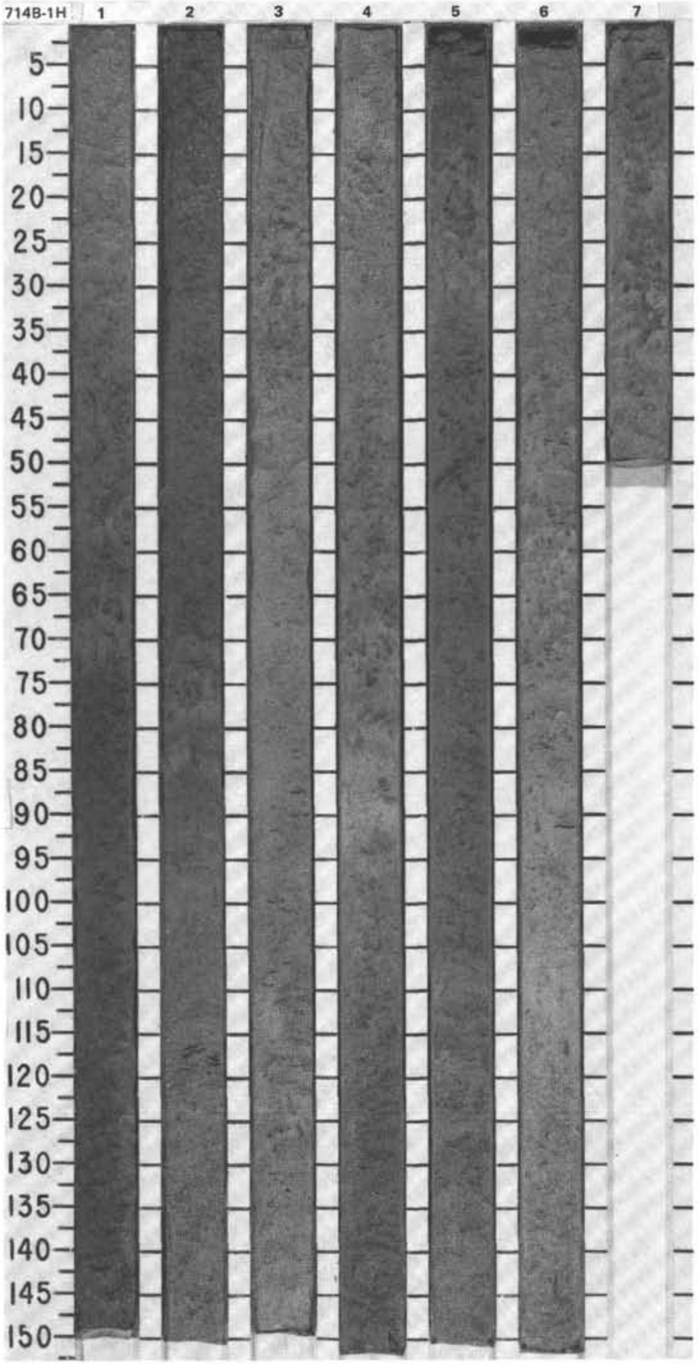

714 B 2H NO RECOVERY

SITE 714 HOLE B CORE 3H CORED INTERVAL 2047.9-2057.5 mbsl; 16.4-26.0 mbsf

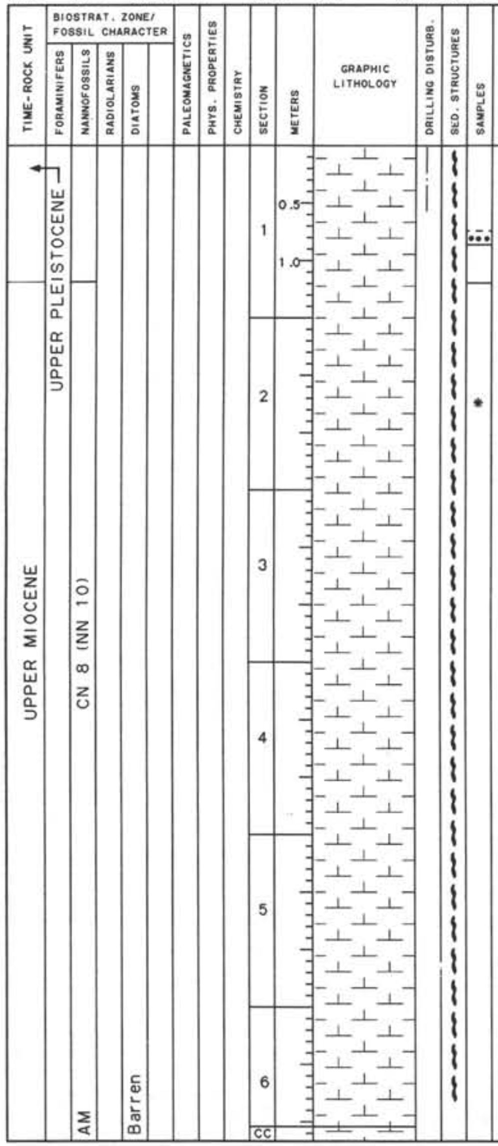

LITHOLOGIC DESCRIPTION

FORAMINIFER-BEARING CLAY-BEARING NANNOFOSSIL OOZE

Major lithology: Foraminifer-bearing clay-bearing nannofossil ooze, burrow-mottled, gray (5Y 5/1, 6/1) changing to light gray (5Y 7/1) alternating with light brownish gray (2.5Y 6/2) to light greenish gray (5GY 7/1), contacts gradational due to bioturbation, intermittent pyrite staining throughout core; 3 thin horizons of light greenish gray (5G 7/1) in Sections 2 and 4; thin turbidite, Section 1, 82–87 cm.

Sharp color change from gray (5Y 5/1) to light gray (5Y 7/1), Section 1, 125 cm, unconformity separating Pleistocene sediments above from Miocene sediments below.

SMEAR SLIDE SUMMARY (%):

	2, 80 D
TEXTURE:	
Sand	25
Silt	6
Clay	69
COMPOSITION:	
Volcanic glass	Tr
Foraminifers	25
Nannofossils	69
Diatoms	Tr
Radiolarians	3
Sponge spicules	3
Silicoflagellates	Tr.
Fish remains	Tr

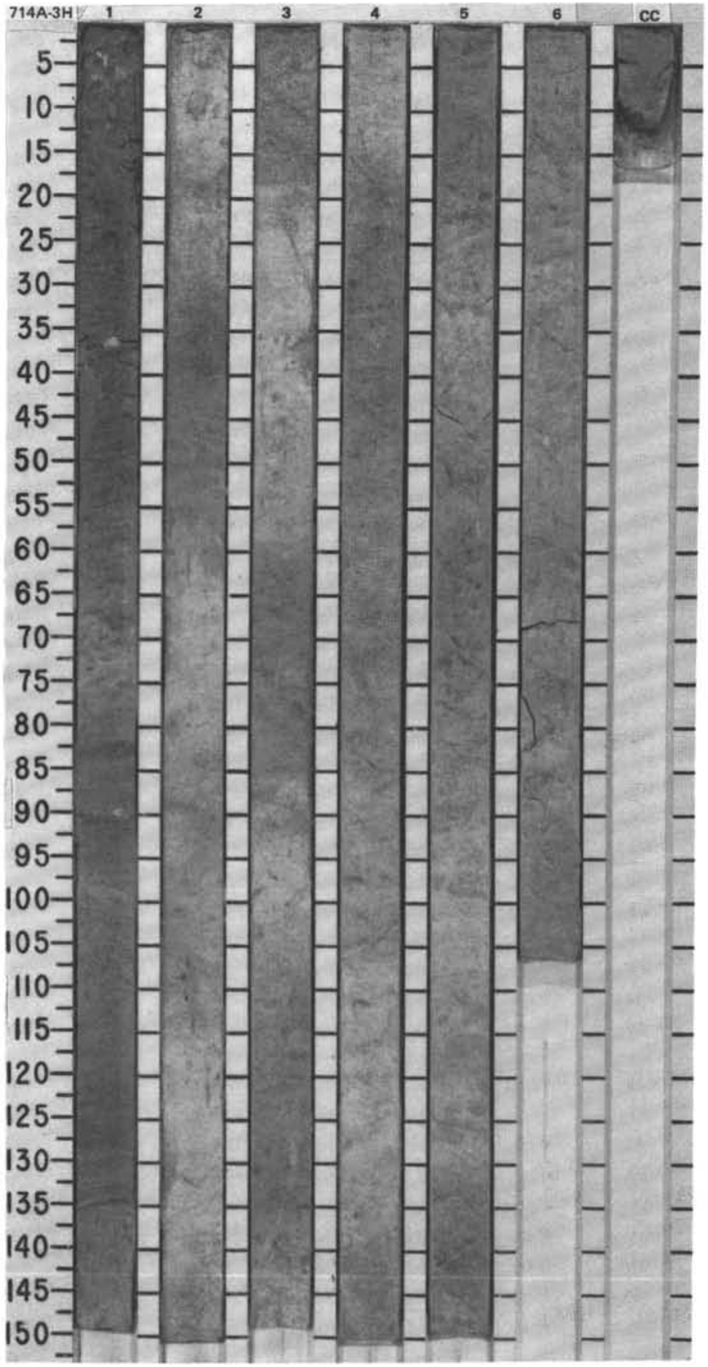

SITE 714 HOLE B CORE 4H CORED INTERVAL 2057.5-2067.2 mbsl; 26.0-35.7 mbsf

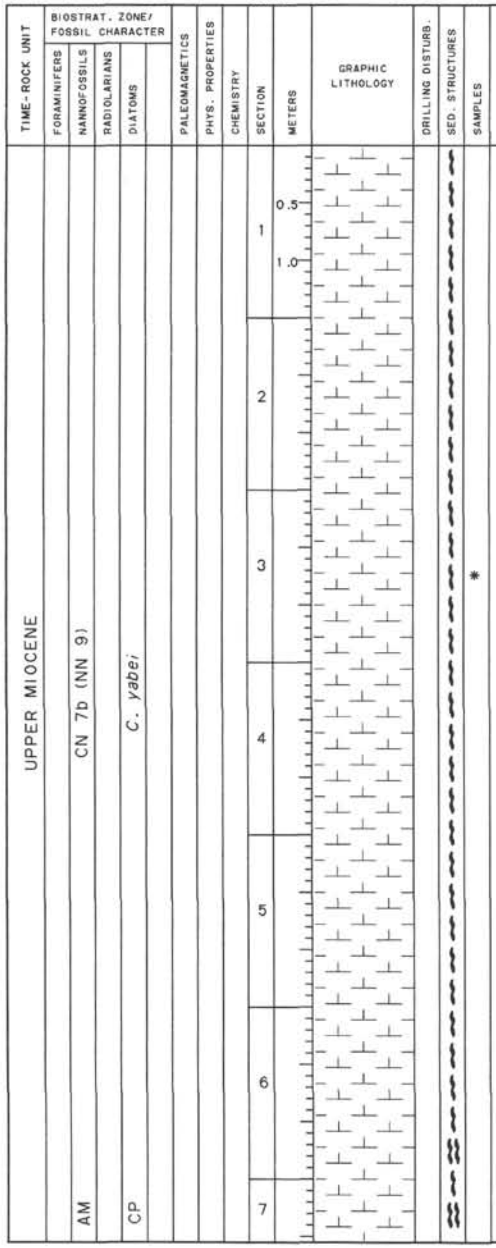

LITHOLOGIC DESCRIPTION

FORAMINIFER-BEARING CLAY-BEARING NANNOFOSSIL OOZE

Major lithology: Foraminifer-bearing clay-bearing nannofossil ooze, burrow-mottled, alternating intervals of light gray (5Y 7/1), light greenish gray (5GY 7/1, 7/2), light brownish gray (2.5Y 6/2), and light yellowish brown (2.5Y 6/4), contacts gradational; scattered pockets of pyrite staining occur throughout core, 6 thin horizons of light greenish gray (5G 7/2) in Sections 4 and 5.

SMEAR SLIDE SUMMARY (%):

	3, 70 D
TEXTURE:	
Sand	15
Silt	10
Clay	75
COMPOSITION:	
Foraminifers	15
Nannofossils	75
Diatoms	Tr
Radiolarians	4
Sponge spicules	5
Silicoflagellates	Tr
Fish remains	1

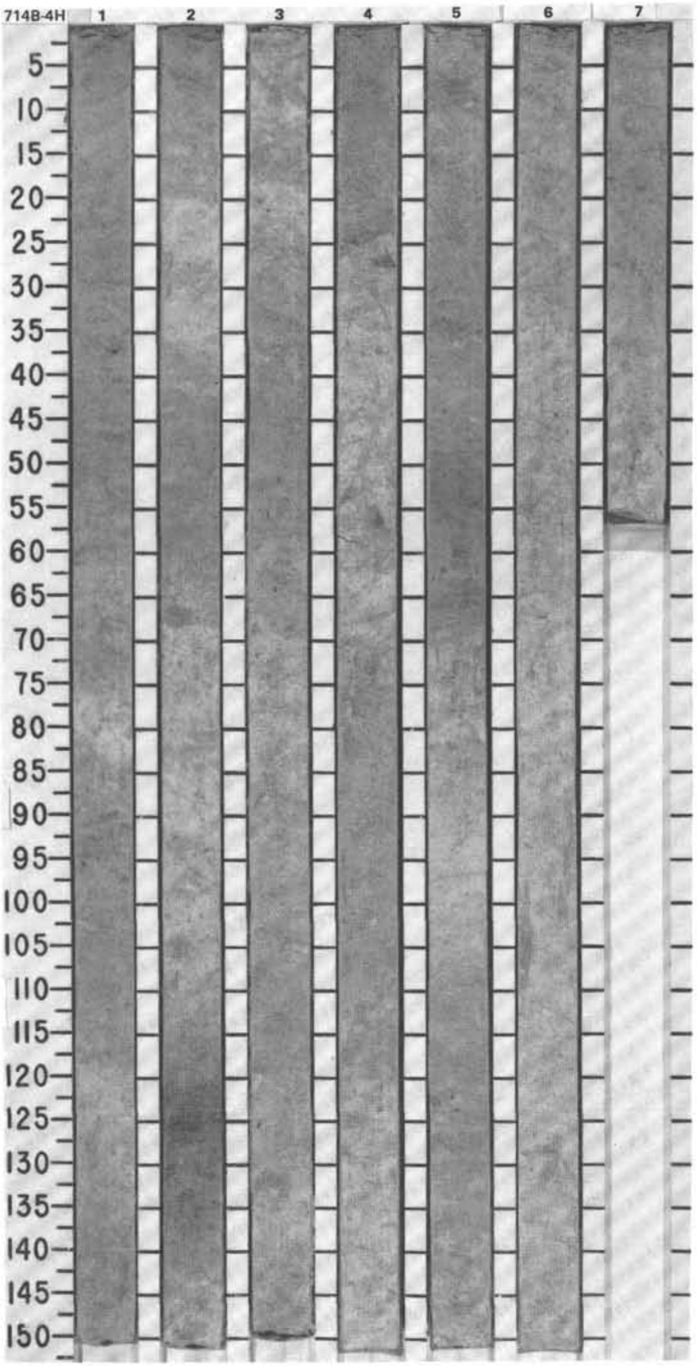

SITE 714 HOLE B CORE 5H CORED INTERVAL 2067.2-2076.9 mbsl; 35.7-45.4 mbsf

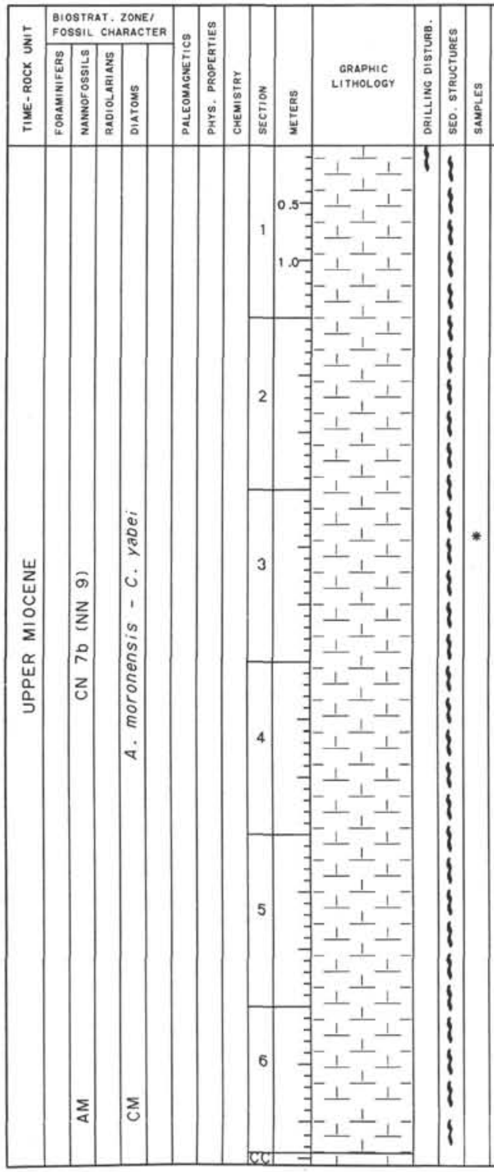

LITHOLOGIC DESCRIPTION

FORAMINIFER-BEARING CLAY-BEARING NANNOFOSSIL OOZE

Major lithology: Foraminifer-bearing clay-bearing nannofossil ooze, burrow-mottled, alternating intervals of light gray (5Y 7/1, 7/2) and light greenish gray (5GY 7/1), minor pyrite staining, Sections 3 and 5; slight hydrogen sulfide odor detectable over freshly cut sections.

SMEAR SLIDE SUMMARY (%):

	3, 44 M
TEXTURE:	
Sand	20
Silt	10
Clay	70
COMPOSITION:	
Clay	15
Volcanic glass	Tr
Foraminifers	20
Nannofossils	59
Diatoms	1
Sponge spicules	5
Silicoflagellates	Tr

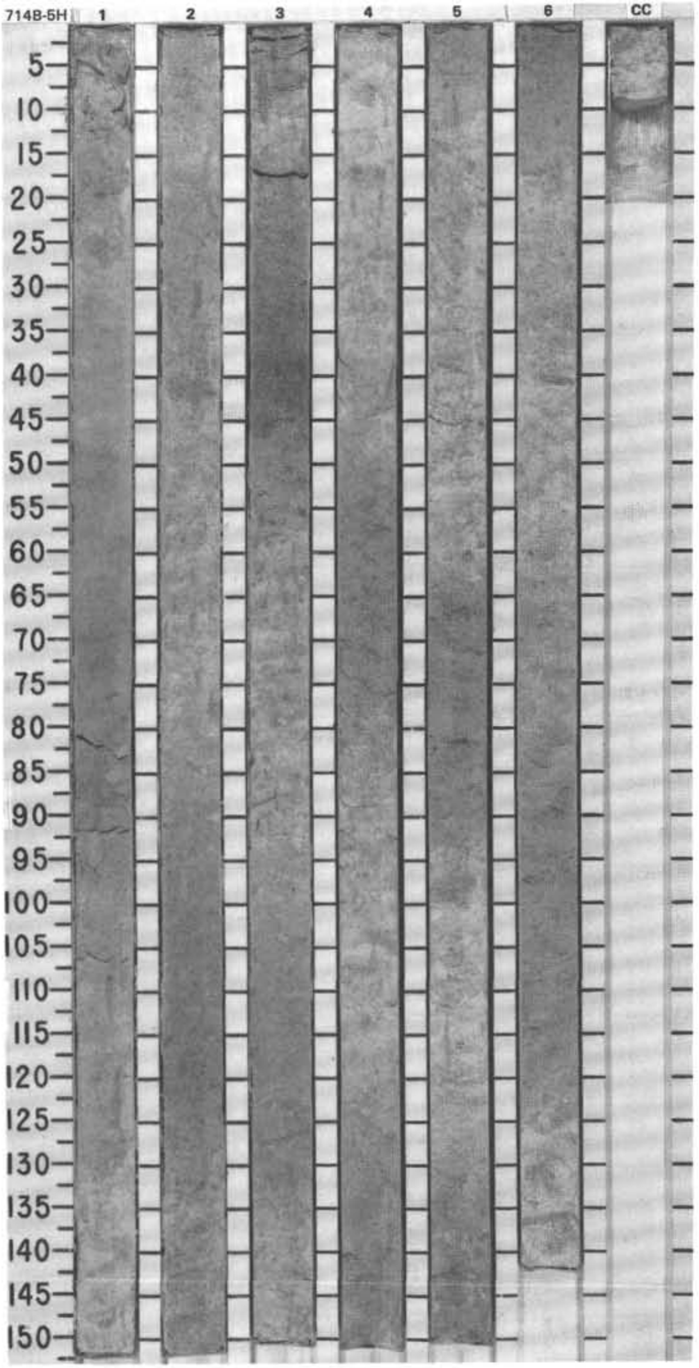

SITE 714 HOLE B CORE 6H CORED INTERVAL 2076.9-2086.5 mbsl; 45.4-55.0 mbsf

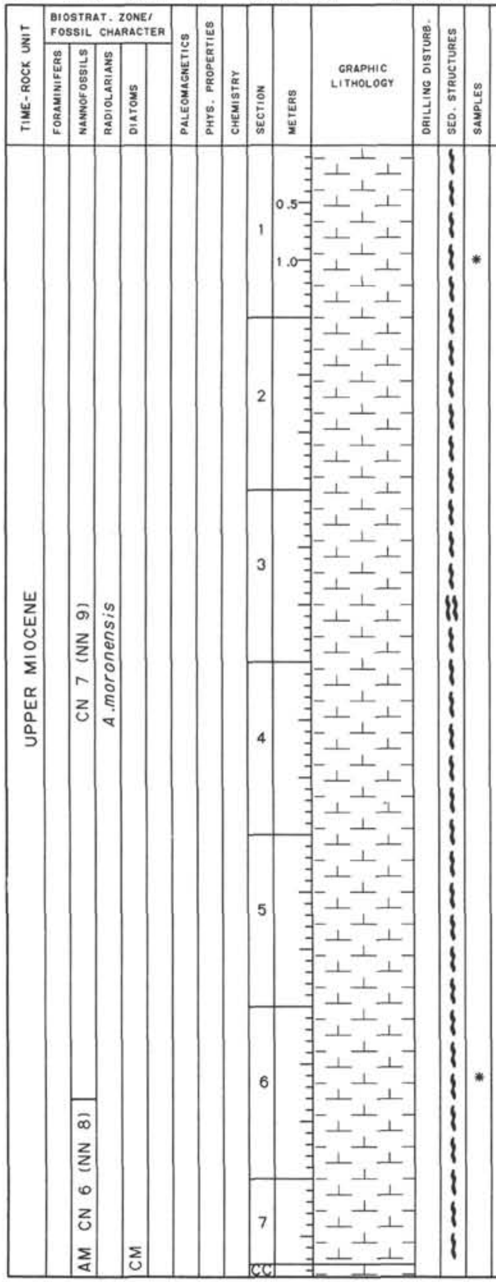

LITHOLOGIC DESCRIPTION

FORAMINIFER-BEARING CLAY-BEARING NANNOFOSSIL OOZE

Major lithology: Foraminifer-bearing clay-bearing nannofossil ooze, burrow-mottled, alternating intervals of light gray (5Y 7/2) and light greenish gray (5GY 7/1), pyrite staining common, particularly in light greenish (5GY 7/1) intervals; 6 thin horizons of gray (N6) and light greenish gray (5G 7/1) occur in Sections 1-5.

SMEAR SLIDE SUMMARY (%):

	1, 100 D	6, 56 M
TEXTURE:		
Sand	25	20
Silt	6	25
Clay	69	55
COMPOSITION:		
Clay	—	15
Accessory minerals:		
Pyrite	—	10
Foraminifers	25	20
Nannofossils	69	39
Diatoms	Tr	1
Radiolarians	1	10
Sponge spicules	5	5
Fish remains	Tr	—

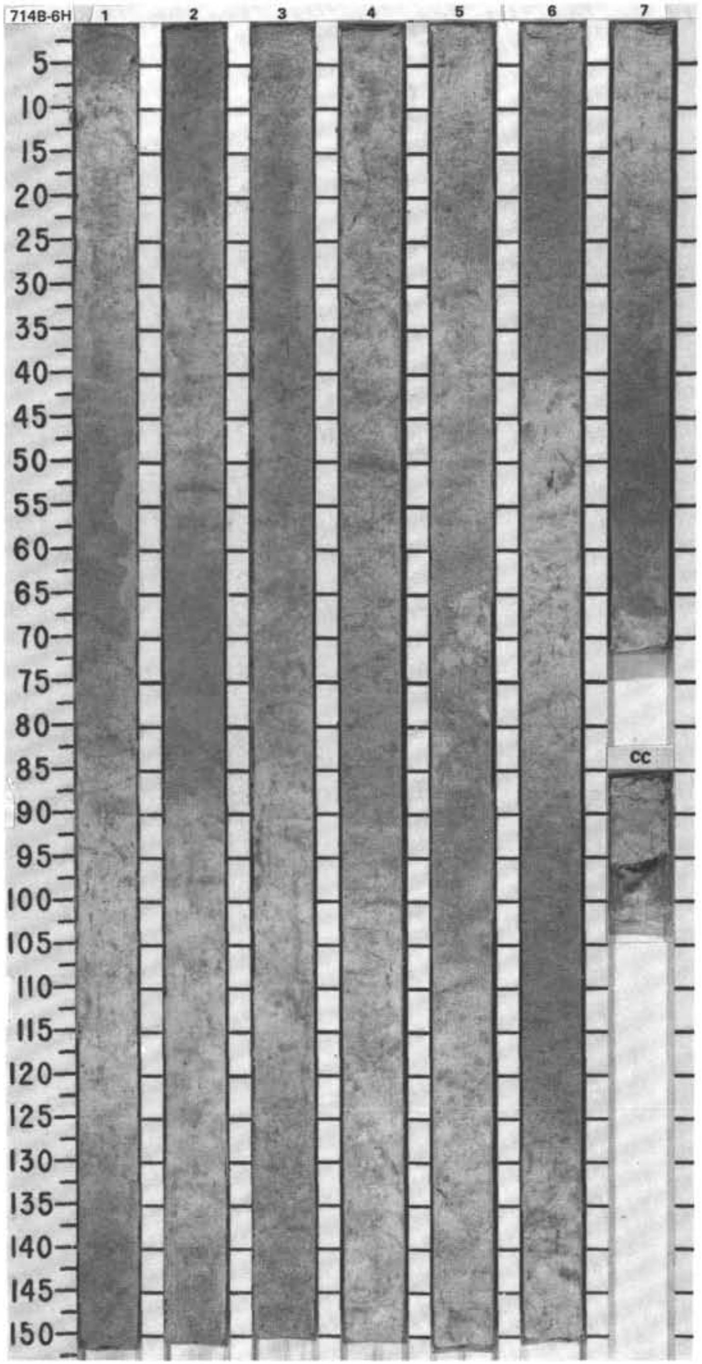

SITE 714 HOLE B CORE 7H CORED INTERVAL 2086.5-2096.1 mbsl; 55.0-64.6 mbsf

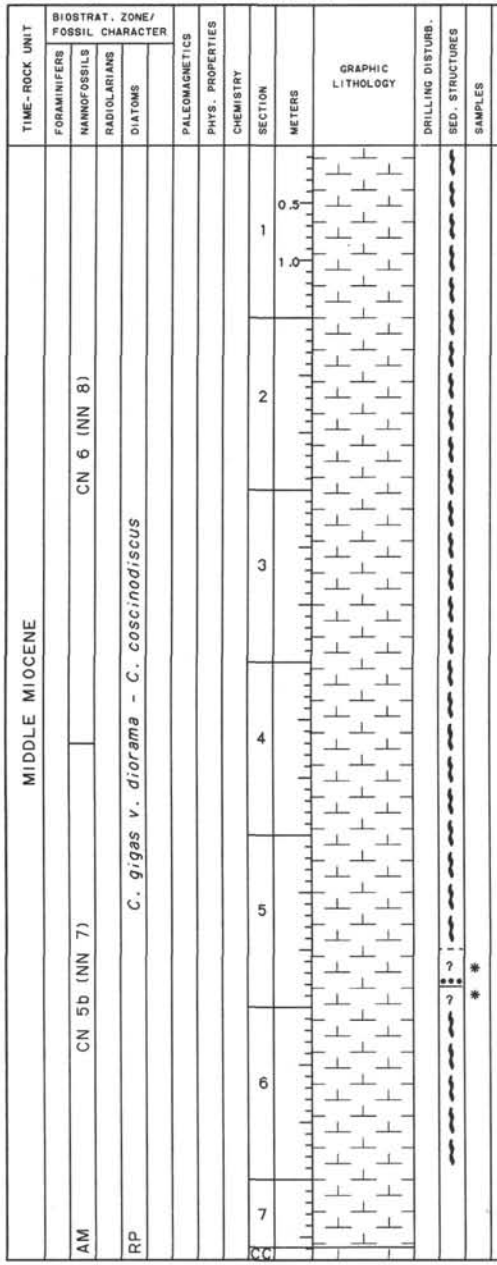

LITHOLOGIC DESCRIPTION

FORAMINIFER-BEARING NANNOFOSSIL OOZE and CLAY-BEARING FORAMINIFER-BEARING NANNOFOSSIL OOZE

Major lithologies: Foraminifer-bearing nannofossil ooze and clay-bearing foraminifer-bearing nannofossil ooze, burrow-mottled, alternating intervals of light gray (5Y 7/2) and light olive gray (5Y 6/2) with light gray (5GY 7/1), very light gray (5Y 8/2), and light greenish gray (5GY 7/2), scattered pyrite staining throughout core; possible turbidite or slump, Section 5, 100–130 cm.

SMEAR SLIDE SUMMARY (%):

	5, 120 M	5, 140 D
TEXTURE:		
Sand	40	20
Silt	9	3
Clay	51	77
COMPOSITION:		
Foraminifers	40	20
Nannofossils	51	77
Diatoms	—	Tr
Radiolarians	1	1
Sponge spicules	8	2

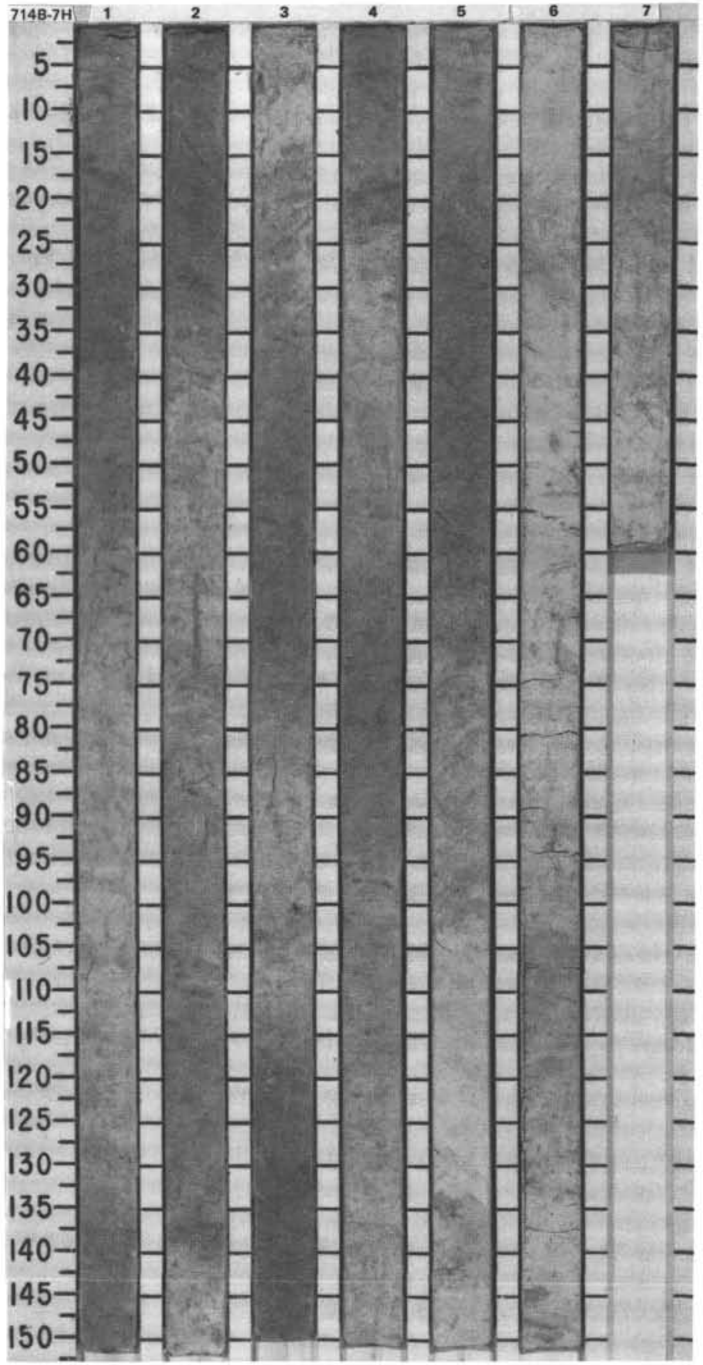

SITE 714 HOLE B CORE 8H CORED INTERVAL 2096.1-2105.8 mbsl; 64.6-74.3 mbsf

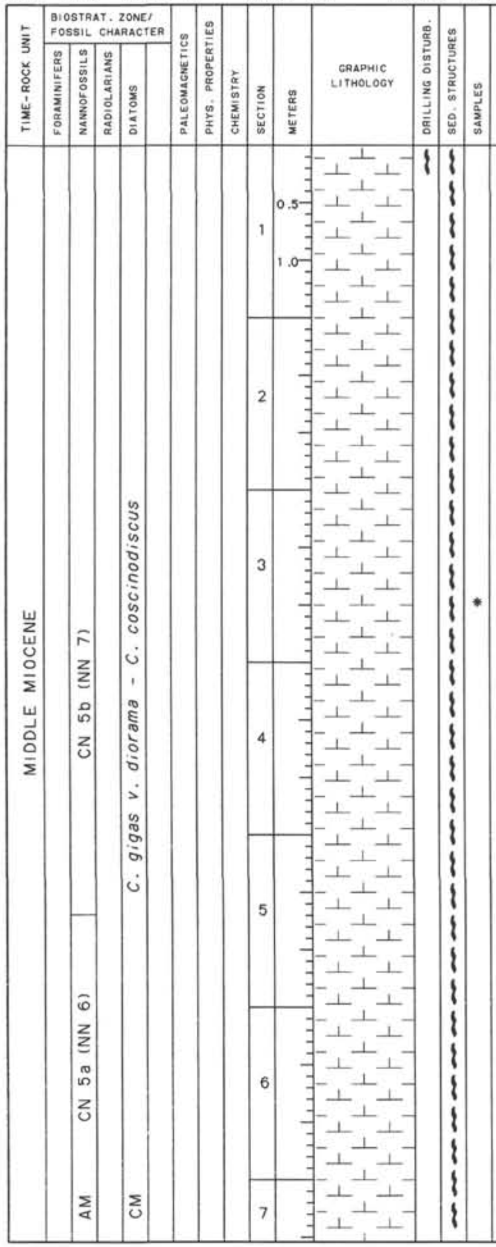

LITHOLOGIC DESCRIPTION

FORAMINIFER-BEARING NANNOFOSSIL OOZE

Major lithology: Foraminifer-bearing nannofossil ooze, burrow-mottled, alternating intervals of very light greenish gray (5G 8/1, 8/2) and light gray (5Y 7/2), pyrite-stained burrow traces scattered throughout core, pale olive (5Y 6/3) interval in Section 3, 82-102 cm, with a sharp basal (erosive?) contact.

SMEAR SLIDE SUMMARY (%):

	3, 102 M
TEXTURE:	
Sand	20
Silt	10
Clay	70
COMPOSITION:	
Volcanic glass	Tr
Foraminifers	20
Nannofossils	71
Radiolarians	2
Sponge spicules	5
Fish remains	2

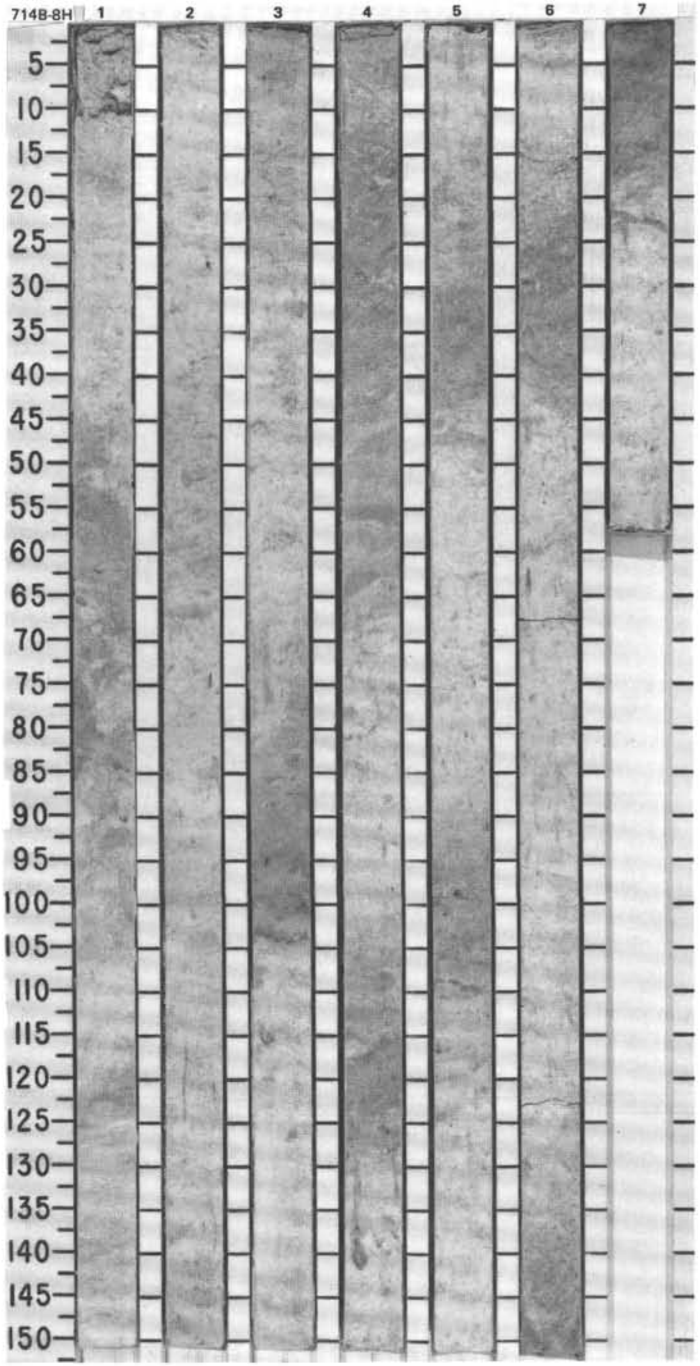

SITE 714 HOLE B CORE 9H CORED INTERVAL 2105.8-2115.4 mbsl; 74.3-83.9 mbsf

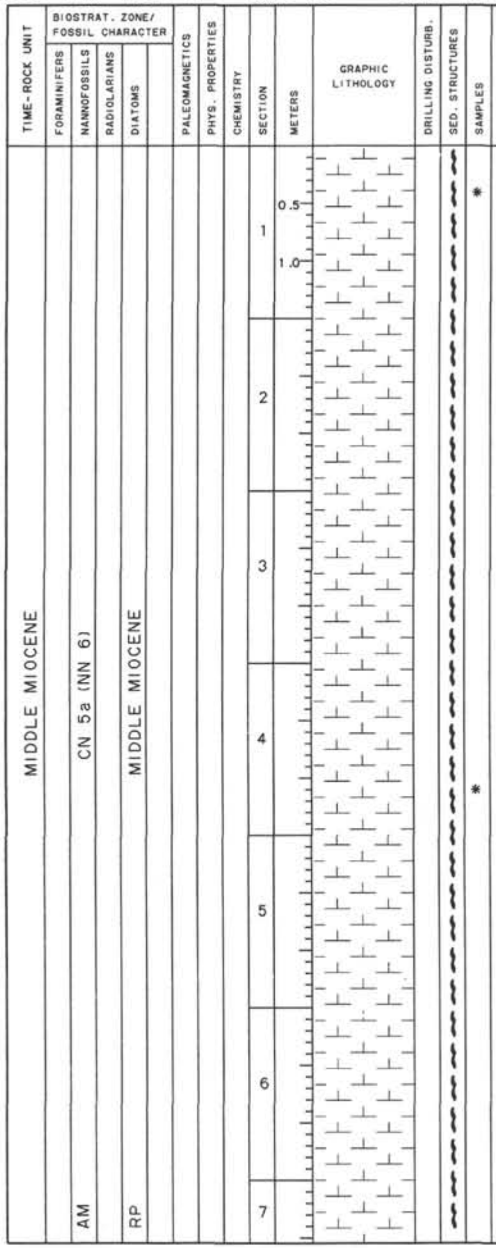

LITHOLOGIC DESCRIPTION

FORAMINIFER-BEARING NANNOFOSSIL OOZE

Major lithology: Foraminifer-bearing nannofossil ooze, burrow-mottled, alternating intervals of very light greenish gray (5G 8/1) and light greenish gray (5G 7/1) with gradational transitions, scattered pyritic burrows throughout core, faint thin horizons of light greenish gray (5G 7/1) distributed throughout core.

SMEAR SLIDE SUMMARY (%):

	1, 48 D	4, 110 D
TEXTURE:		
Sand	10	10
Silt	15	15
Clay	75	75
COMPOSITION:		
Volcanic glass	Tr	Tr
Foraminifers	15	15
Nannofossils	80	80
Radiolarians	Tr	Tr
Sponge spicules	5	5
Silicoflagellates	Tr	—
Opaques	Tr	—

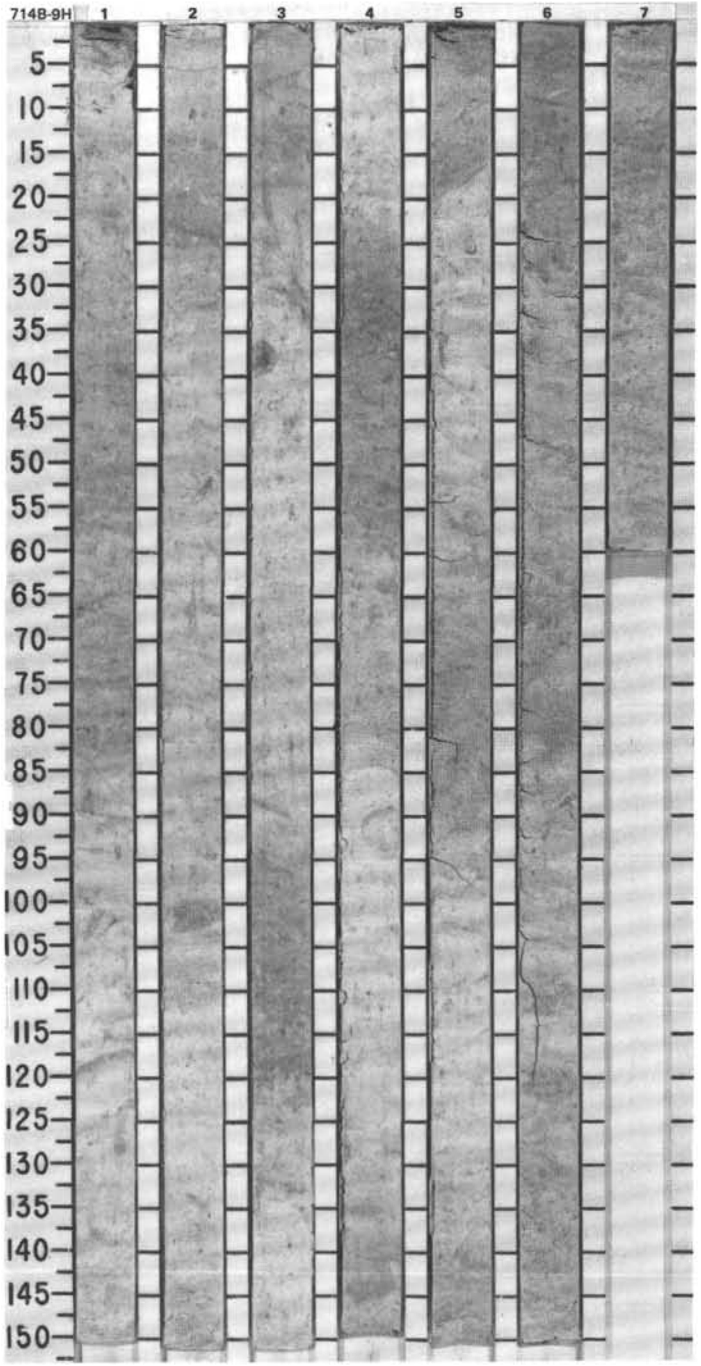

SITE 714 HOLE B CORE 10H CORED INTERVAL 2115.4-2125.1 mbsl; 83.9-93.6 mbsf

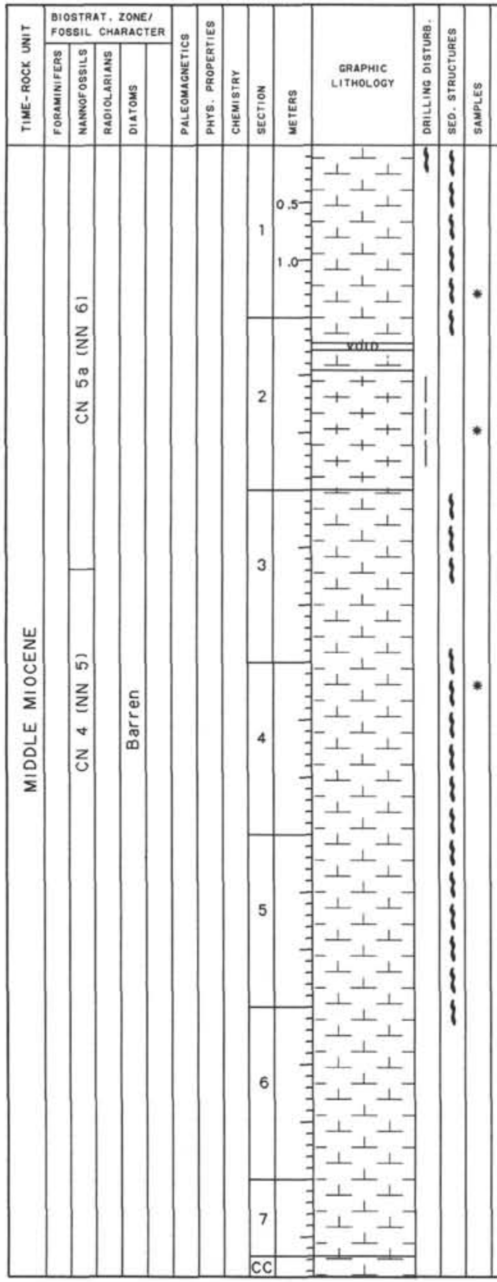

LITHOLOGIC DESCRIPTION

FORAMINIFER-BEARING NANNOFOSSIL OOZE and CLAY-BEARING FORAMINIFER-BEARING NANNOFOSSIL OOZE

Major lithologies: Foraminifer-bearing nannofossil ooze and clay-bearing foraminifer-bearing nannofossil ooze, patchy burrow-mottling, alternating very light greenish gray (5G 8/1) and light greenish gray (5G 7/1).

Minor lithology: Foraminifer-nannofossil ooze, Section 2, 45 cm, and Section 3, 70 cm, possible turbidite with evidence of reworking at base, light greenish gray (5G 7/1), "watery".

SMEAR SLIDE SUMMARY (%):

	1, 135 D	2, 100 D	4, 17 D
TEXTURE:			
Sand	8	40	10
Silt	12	10	15
Clay	80	40	75
COMPOSITION:			
Foraminifers	12	45	17
Nannofossils	85	52	80
Radiolarians	Tr	—	Tr
Sponge spicules	3	3	3
Fish remains	—	—	Tr

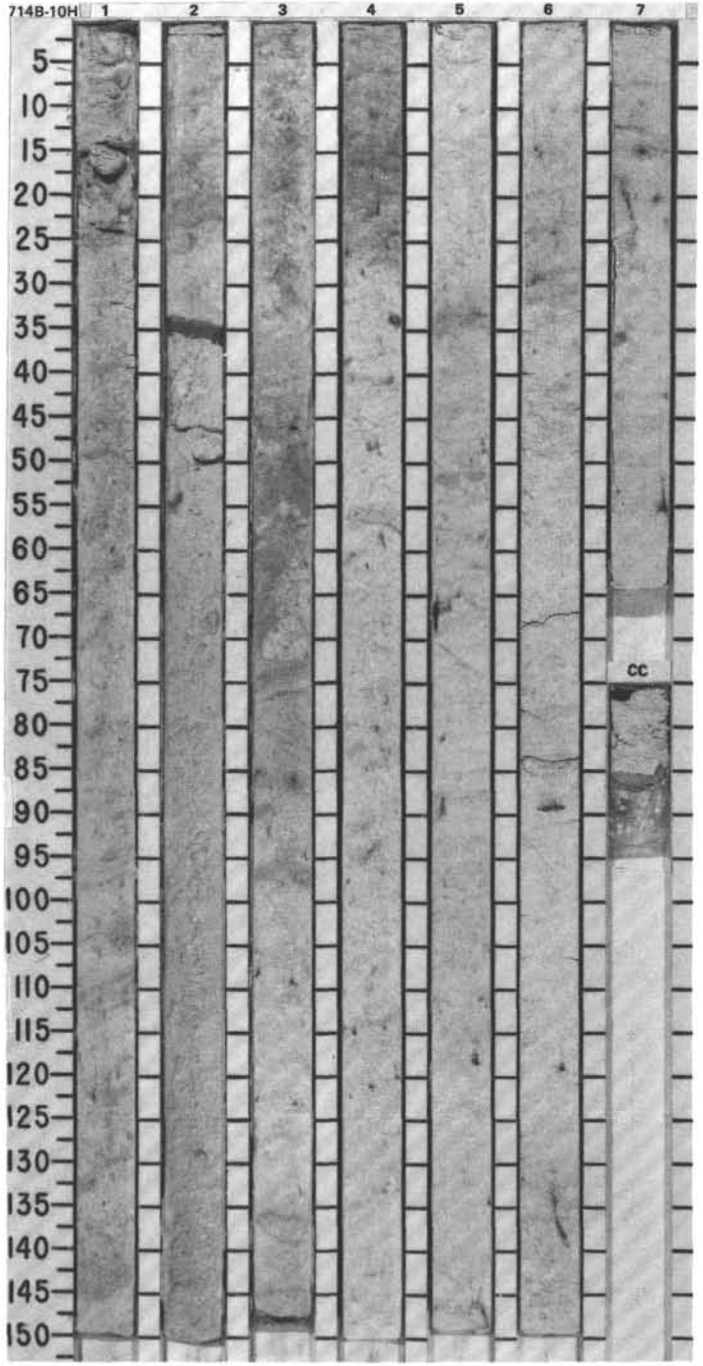

SITE 714 HOLE B CORE 11H CORED INTERVAL 2125.1-2134.7 mbsl; 93.6-103.2 mbsf

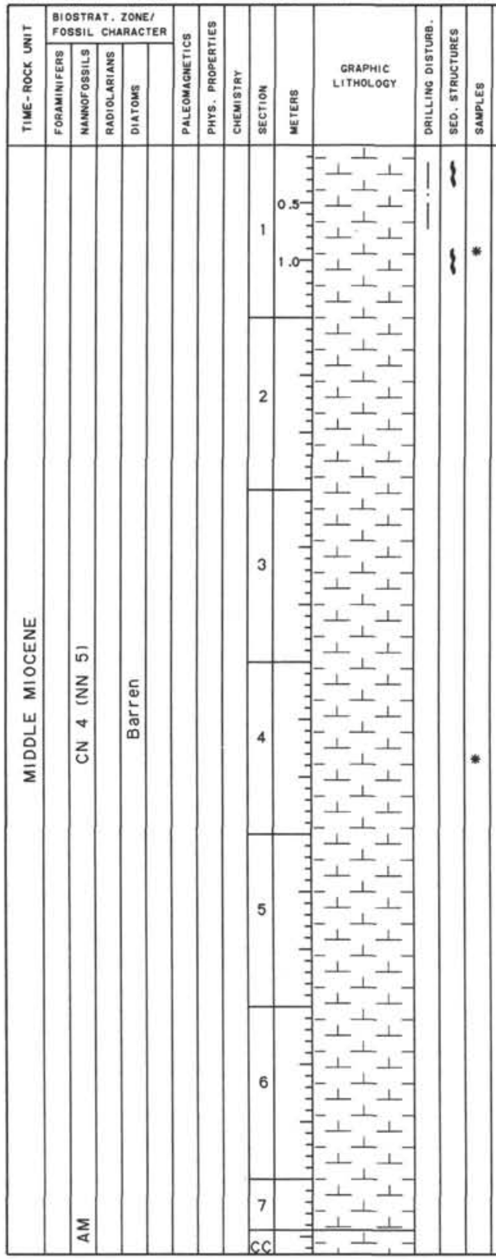

LITHOLOGIC DESCRIPTION

FORAMINIFER-BEARING NANNOFOSSIL OOZE and CLAY-BEARING FORAMINIFER-BEARING NANNOFOSSIL OOZE

Major lithologies: Foraminifer-bearing nannofossil ooze and clay-bearing foraminifer-nannofossil ooze, homogeneous, except for scattered faint burrow-mottling, very light greenish gray (5G 8/1); minor pyritized burrows scattered throughout the core, 2 to 4 per section.

SMEAR SLIDE SUMMARY (%):

	1, 90 D	4, 90 D
TEXTURE:		
Sand	10	10
Silt	30	20
Clay	60	70
COMPOSITION:		
Volcanic glass	Tr	Tr
Foraminifers	20	18
Nannofossils	76	80
Radiolarians	2	1
Sponge spicules	2	1

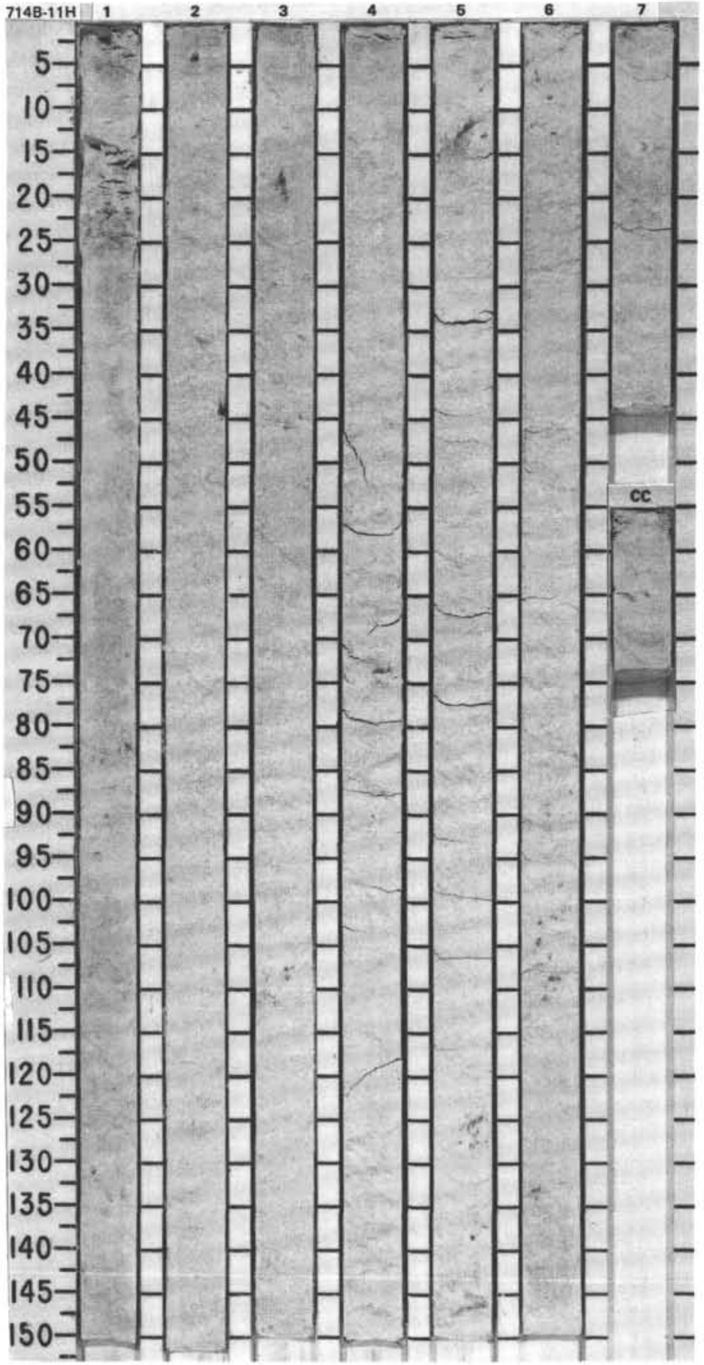

SITE 714 HOLE B CORE 12H CORED INTERVAL 2134.7-2144.4 mbsl; 103.2-112.9 mbsf

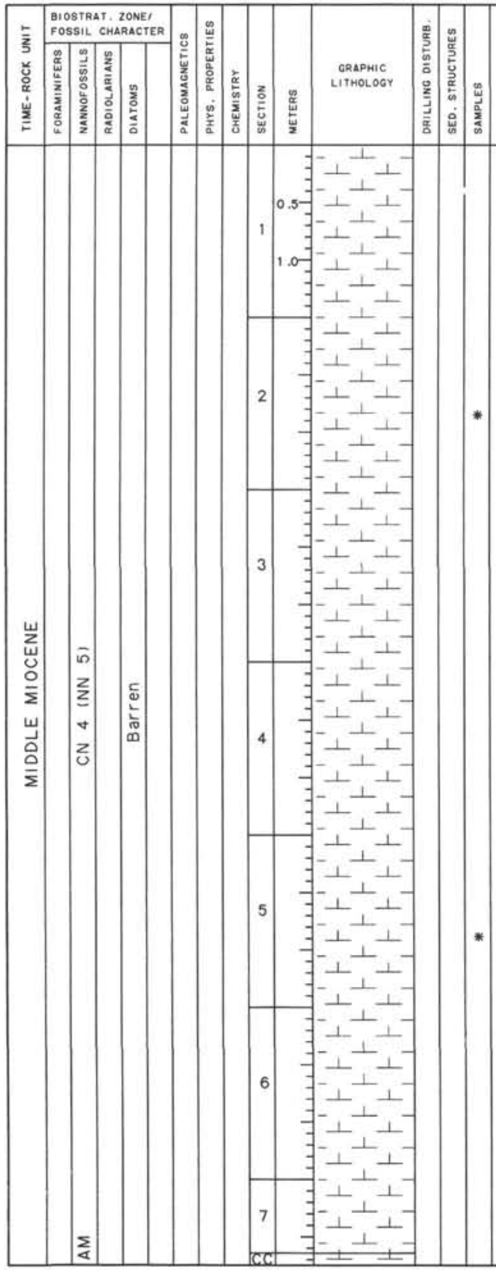

LITHOLOGIC DESCRIPTION

FORAMINIFER-BEARING NANNOFOSSIL OOZE and CLAY-BEARING FORAMINIFER-BEARING NANNOFOSSIL OOZE

Major lithologies: Foraminifer-bearing nannofossil ooze and clay-bearing foraminifer-bearing nannofossil ooze, homogeneous, firm, very light greenish gray (5G 8/1); minor pyrite staining.

SMEAR SLIDE SUMMARY (%):

	2, 90 D	5, 90 D
TEXTURE:		
Sand	10	10
Silt	40	40
Clay	50	50
COMPOSITION:		
Volcanic glass	Tr	—
Foraminifers	20	22
Nannofossils	79	78
Radiolarians	Tr	Tr
Sponge spicules	1	Tr

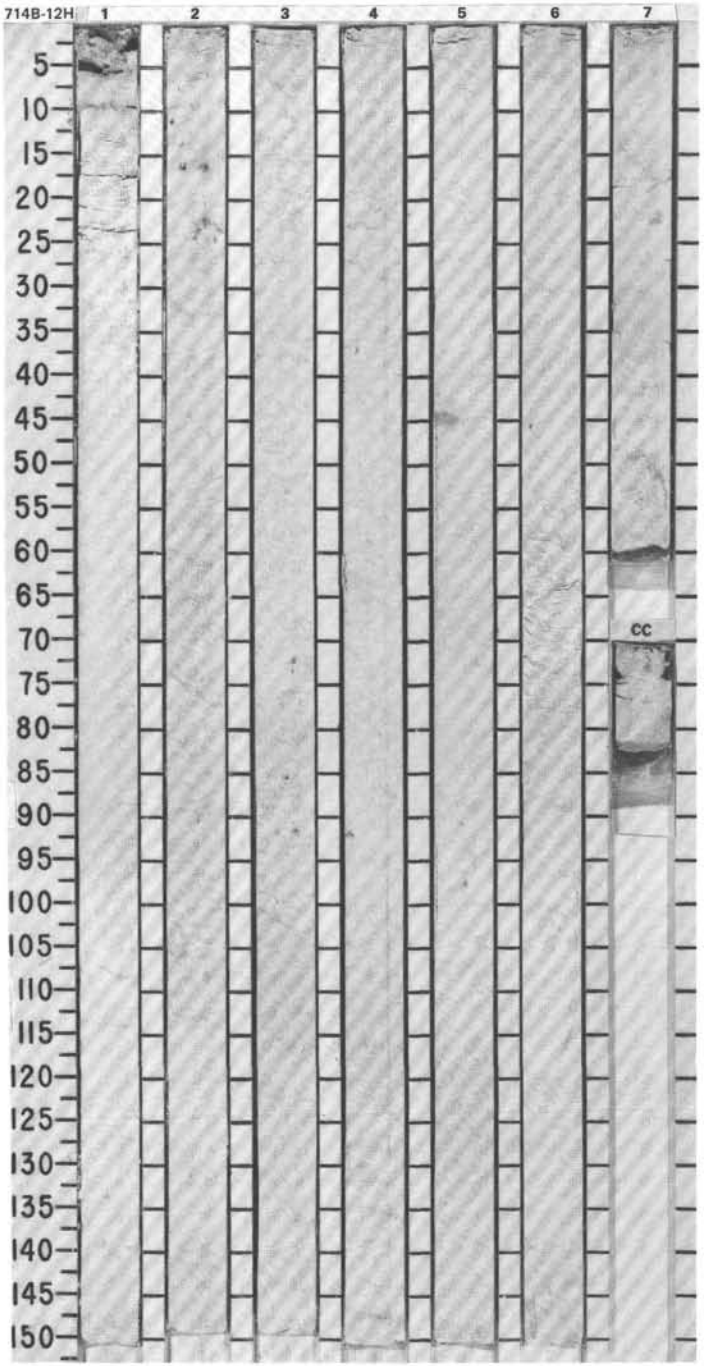

SITE 714 HOLE B CORE 13H CORED INTERVAL 2144.4-2154.1 mbsl; 112.9-122.6 mbsf

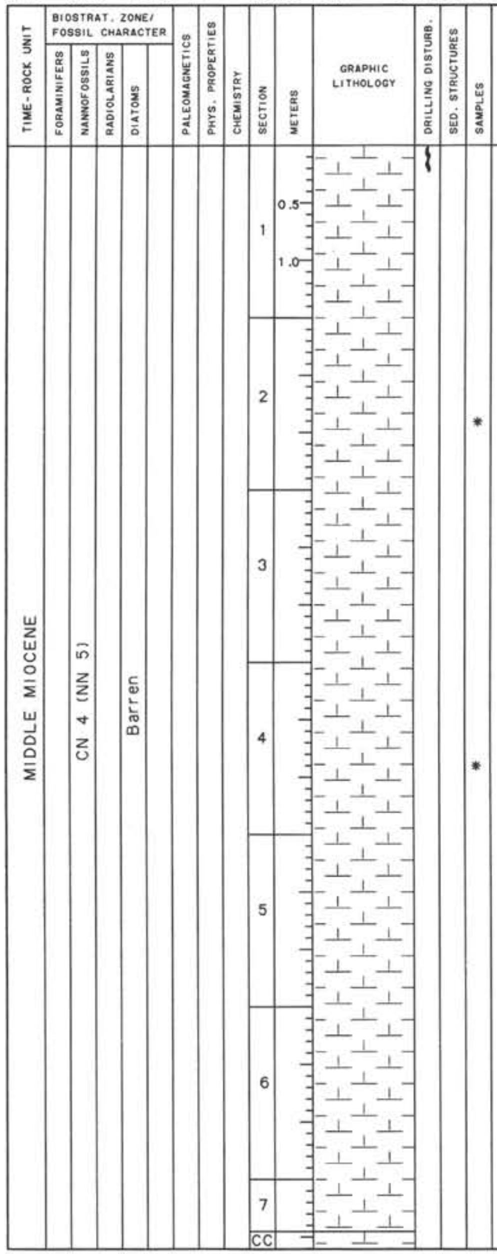

LITHOLOGIC DESCRIPTION

FORAMINIFER-BEARING NANNOFOSSIL OOZE and CLAY-BEARING FORAMINIFER-BEARING NANNOFOSSIL OOZE

Major lithologies: Foraminifer-bearing nannofossil ooze and clay-bearing foraminifer-bearing nannofossil ooze, homogeneous, firm, very light greenish gray (5G 8/1), scattered pyrite staining present throughout the core.

Minor lithology: Foraminifer-bearing nannofossil chalk and foraminifer-bearing clay-bearing nannofossil chalk, homogeneous, very light greenish gray (5G 8/1), occurs as thin nodules in Section 4, 110 cm, through Section 7.

SMEAR SLIDE SUMMARY (%):

	2, 90 D	4, 90 D
TEXTURE:		
Sand	10	10
Silt	40	40
Clay	50	50
COMPOSITION:		
Volcanic glass	Tr	Tr
Foraminifers	16	18
Nannofossils	82	81
Radiolarians	Tr	Tr
Sponge spicules	2	1